UFRRJ

INSTITUTO DE GEOCIÊNCIAS

CURSO DE PÓS-GRADUAÇÃO EM MODELAGEM E EVOLUÇÃO GEOLÓGICA

DISSERTAÇÃO

Petrogênese do magmatismo drifte na região do Alto de Cabo Frio, Bacia de Campos, Brasil

Tatiele Marques Jatobá de Barros

2024

UNIVERSIDADE FEDERAL RURAL DO RIO DE JANEIRO INSTITUTO DE GEOCIÊNCIAS
CURSO DE PÓS-GRADUAÇÃO EM MODELAGEM E EVOLUÇÃO GEOLÓGICA

TATIELE MARQUES JATOBÁ DE BARROS

Dissertação submetida como requisito parcial para obtenção do grau de Mestre em Geociências, no Curso de Pós-Graduação em Modelagem e Evolução Geológica, área de Concentração em Modelagem de Processos Geológicos e Geodinâmicos.

DISSERTAÇÃO APROVADA EM: 15/04/2024

Documento assinado digitalmente
ARTUR CORVAL VIEIRA
Data: 25/04/2024 11:15:15-0300
Verifique em https://validar.iti.gov.br

Artur Corval Vieira. Dr. UFRRJ (Orientador)

Documento assinado digitalmente
ALAN WANDERLEY ALBUQUERQUE MIRANDA
Data: 10/06/2024 08:44:45-0300
Verifique em https://validar.iti.gov.br

(Membro Interno) ...da – Dr. UFRRJ

Documento assinado digitalmente
FABIO BRAZ MACHADO
Data: 25/04/2024 14:45:34-0300
Verifique em https://validar.iti.gov.br

Fábio Braz Machado. Dr. UFPR

(Membro Externo)

Universidade Federal Rural do Rio de Janeiro
Biblioteca Central / Seção de Processamento Técnico

Ficha catalográfica elaborada
com os dados fornecidos pelo(a) autor(a)

B277p

Barros, Tatiele Marques Jatobá de, 1996-
Petrogênese do magmatismo drifte na região do Alto de Cabo Frio, Bacia de Campos, Brasil / Tatiele Marques Jatobá de Barros. - Nova Era, 2024.
109 f.: il.

Orientador: Artur Corval Vieira.
Dissertação(Mestrado). -- Universidade Federal Rural do Rio de Janeiro, Programa de Pós-Graduação em Modelagem e Evolução Geológica, 2024.

1. Magmatismo. 2. Alto de Cabo Frio. 3. Litogeoquímica. 4. Geoquímica Isotópica. I. Corval Vieira, Artur, 1977-, orient. II Universidade Federal Rural do Rio de Janeiro. Programa de Pós-Graduação em Modelagem e Evolução Geológica III. Título.

AGRADECIMENTOS

Agradeço aos meus pais Jozélia e Marivaldo, e à minha irmã Sabrina por todo o amor, apoio e suporte que me deram, não somente durante o mestrado, mas por toda a minha vida. Obrigada por estarem sempre comigo, mesmo que a distância. E obrigada pela paciência, nos momentos mais difíceis. Agradeço também à minha sobrinha de quatro patas: Kiki, a gatinha mais fofa, que tem me acompanhado desde o início do processo seletivo. E à toda a minha família e amigos pelo apoio e amizade.

Agradeço ao meu orientador Prof. Dr. Artur Corval Vieira, por tudo o que tem me ensinado, pela dedicação e pela paciência comigo durante todos estes anos. Também a todos os colegas e docentes do Labmeg e do Programa de Pós-Graduação em Modelagem e Evolução Geológica, em especial o Prof. Dr. Sérgio Valente e à Natália por todo o suporte.

Agradeço à FAPUR e à EQUINOR por meio do apoio financeiro no projeto de pesquisa *Magmatismo e Processos Tectônicos das Fases Rifte, Pós-Rifte e Drifte nas áreas central e norte da Bacia de Santos* (Projeto EQUIMAG - FAPUR 07/19, ANP 21110-2). E à ANP pela disponibilidade das amostras e demais dados dos poços estudados.

À Universidade Federal Rural do Rio de Janeiro e ao Programa de Pós-graduação em Modelagem e Evolução Geológica, por toda a infraestrutura, recursos e oportunidade de realizar este trabalho.

O presente trabalho foi realizado com apoio da Coordenação de Aperfeiçoamento de Pessoal de Nível Superior - Brasil (CAPES) - Código de Financiamento 001.

Por fim, agradeço à geologia e a todos que de alguma forma me contribuíram e estiveram comigo durante esta jornada.

RESUMO

DE BARROS, Tatiele Marques Jatobá. **Petrogênese do magmatismo drifte na região do Alto de Cabo Frio, Bacia de Campos, Brasil.** 2024. 109p Dissertação (Mestrado em Modelagem e Evolução Geológica). Instituto de Geociências, Departamento de Petrologia e Geotectônica, Universidade Federal Rural do Rio de Janeiro, Seropédica, RJ, 2024.

A região do Alto de Cabo Frio, localizada entre as bacias de Campos e Santos na margem sudeste brasileira, é caracterizada por um intenso magmatismo que exibe dois picos, durante o Santoniano-Campaniano e durante o Eoceno. A presente dissertação estudou rochas magmáticas de três poços localizados nesta região e que estão associados aos eventos que datam do Santoniano-Campaniano. Perfis dos poços foram analisados e amostras de seções magmáticas foram selecionadas para análises petrográficas e geoquímicas. Elas consistem em amostras laterais e amostras de calhas que foram classificadas, baseado em dados petrográficos, como cinzas piroclásticas, lapilli tufos, basaltos, escórias e diabásios, todas consideravelmente alteradas. Resultados litogeoquímicos indicaram que estas rochas são predominantemente alcalinas e associadas com processos de fusões mantélicos rasos que envolveram a mistura de uma fonte depletada e o manto litosférico subcontinental loca. Dados isotópicos de Sr-Nd-Pb-Hf indicam que processos envolvendo assimilação e cristalização fracionada foram os principais processos que poderiam estar associados às rochas estudadas. Modelagens mais aprofundadas utilizando razões isotópicas indicaram a contribuição de uma fonte mantélica depletada, como DM/MORB ou HIMU combinada com uma fonte enriquecida, como EMI e EMII, que teria dado origem a este magmatismo. A contribuição de uma fonte fértil do tipo OIB é uma questão principal ainda a ser considerada e, baseando-se no contexto geodinâmico, a pluma de Trindade seria uma possível opção.

Palavras-chave: Magmatismo. Alto de Cabo Frio. Litogeoquímica. Geoquímica isotópica.

ABSTRACT

DE BARROS, Tatiele Marques Jatobá. **Petrogenesis of drift magmatism in Cabo Frio High Region, Campos Basin, Brazil.** 2024. 109p Dissertation (Master of Science in Modeling and Geological Evolution) Geosciences Institute, Department of Petrology and Geotectonics, Federal Rural University of Rio de Janeiro, Seropédica, RJ, 2024.

The Cabo Frio High area, located between the Campos and Santos basins in the Brazilian Southeastern margin is characterized by an intense magmatism that exhibits two peaks, during the Santonian-Campanian and Eocene. The present dissertation studied magmatic rocks from three wells located in this region and associated to the Santonian-Campanian events. Well profiles were analyzed and samples from magmatic sections were selected to petrographic analysis. They consisted in sidewall core samples and drill cutting samples that were classified as considerably altered pyroclastic ash, lapilli tuffs, basalts, scorias, and diabases based on petrographic data. Lithogeochemical results indicated these rocks were predominantly alkaline and associated to shallow mantle processes that involved mixing between a depleted source and the local subcontinental lithospheric mantle. Sr-Nd-Pb-Hf isotopic data indicate that processes involving assimilation and fractional crystallization were the main evolutive processes that could be related to studied rocks. Further modeling using isotope ratios pointed out to the contribution of a depleted mantle source, such as DM/MORB or HIMU combined with an enriched source, such as EMI or EMII, to have given origin to this magmatism. The contribution of a fertile OIB-like source is a key feature to be considered and based on the geodynamic context, the Trindade plume would be a possible candidate.

Keywords: Magmatism. Cabo Frio High. Lithogeochemistry. Isotopic geochemistry.

LISTA DE TABELAS

LISTA DE FIGURAS

SUMÁRIO

1 INTRODUÇÃO

1.1 Apresentação

A presente dissertação de mestrado visa estudar o magmatismo associado à fase drifte na área do Alto de Cabo Frio, região limítrofe entre as bacias de Campos e Santos, margem sudeste brasileira. A realização do mesmo envolveu análises petrográficas, litogeoquímicas e isotópicas de amostras laterais e de calha oriundas de três poços de exploração e produção situados na localidade de interesse. Por meio destes dados, foram elaborados modelos petrogenéticos e geodinâmicos que permitiram melhor compreensão a respeito do contexto de formação do respectivo magmatismo, seus processos evolutivos e fontes mantélicas associadas.

Os resultados obtidos por meio dos dados e modelos gerados a partir das rochas ígneas estudadas foram parcialmente publicados na revista Comunicações Geológicas (B1), sendo o artigo referente ao Capítulo 4 da presente dissertação de mestrado. Os demais resultados e discussões serão publicados em revista ainda a ser definida, sendo o artigo referente ao Capítulo 5 da presente dissertação.

A área de estudo constitui de grande importância geológica e econômica, em especial no que se refere à exploração de hidrocarbonetos. Ambas as bacias de Santos e Campos são caracterizadas e têm sua evolução tectonossedimentar associada à ruptura do supercontinente Gondwana, posterior abertura do Oceano Atlântico e estágio de margem passiva. Durante a fase drifte, estas bacias foram afetadas por dois importantes eventos tectonomagmáticos durante o Santoniano-Campaniano e Eoceno, gerando o magmatismo observado em especial na área do Alto de Cabo Frio. Este magmatismo teve uma grande influência na evolução sedimentar das Bacias de Santos e Campos, bem como na qualidade dos reservatórios de óleo e gás destas bacias (**Moreira *et al.*, 2006; Castro e Picolini, 2014**).

Eventos magmáticos, sejam eles intrusivos ou extrusivos, são importantes agentes atuantes em diversos aspectos da evolução de bacias sedimentares, incluindo nos processos associados à geração, migração e acumulação de hidrocarbonetos (**Thomaz Filho *et al.*, 2008**). Tais episódios magmáticos envolvem uma grande liberação de energia durante um curto espaço de tempo geológico, modificando química e fisicamente os ambientes deposicionais, afetando a diagênese, atuando como uma nova fonte de sedimentos, e alterando a paleotopografia da região, processos observados na área do Alto Estrutural de Cabo Frio (**Oreiro, 2006**).

Apesar da relevância geológica e econômica da região, ainda existe uma carência de dados e de conhecimento detalhado do cenário petrogenético e geodinâmico associado aos eventos magmáticos pós-fragmentação na região do Alto de Cabo Frio, em especial quando comparado à porção *onshore* da bacia. O presente trabalho faz-se necessário e visa, portanto, contribuir para a melhor compreensão destes aspectos magmáticos da área por meio de estudos petrográficos e geoquímicos. Por meio deste estudo, buscou-se o enriquecendo os dados bibliográficos acerca dos eventos magmáticos que afetaram as bacias de Campos e Santos durante sua fase drifte, elucidando o contexto geodinâmico ao qual tais eventos estão associados e contribuindo para a indústria de exploração e produção de hidrocarbonetos, dado a relevância destes eventos para o desenvolvimento dos sistemas petrolíferos.

1.2 Objetivos

O principal objetivo desta dissertação de mestrado é obter uma maior compreensão do magmatismo e cenário geodinâmico associados a fase drifte da porção noroeste da Bacia de Santos.

Os objetivos específicos incluem:

a) Elaboração de um modelo petrogenético, incluindo a identificação de processos evolutivos e possíveis fontes magmáticas;

b) Auxiliar na elucidação do contexto geodinâmico ao qual estas rochas estão associadas;

c) Fornecer novos dados e enriquecer o conhecimento a respeito do magmatismo na região.

1.3 Justificativa

O magmatismo constitui um dos elementos chaves na evolução e consolidação de bacias sedimentares. Tal fator contribui, por exemplo, para um incremento térmico nos ambientes deposicionais afetados por estes eventos. Além disso, essas rochas podem gerar alterações morfológicas e estruturais durante a consolidação das bacias (**Thomaz Filho *et al.*, 2008**) ou até mesmo atuar como importantes reservatórios de hidrocarbonetos, como por exemplo no caso dos campos de Badejo e Linguado na Bacia de Campos (**Marins *et al.*, 2020**).

A área de estudo é de grande importância geológica e econômica, em especial no que se refere à exploração de hidrocarbonetos no Brasil. Entretanto, apesar da importância dos eventos magmáticos que afetaram a região, ainda existe uma carência de conhecimento detalhado do cenário petrogenético e geodinâmico associado ao seu magmatismo, em especial quando comparado à porção *onshore* da bacia. Os episódios magmáticos da fase drifte, mais especificamente, ainda carecem de estudos mais aprofundados a respeito da sua caracterização petrográfica e litogeoquímica, e do contexto geodinâmico em que eles ocorreram.

O presente trabalho faz-se necessário e visa, portanto, contribuir para a melhor compreensão destes aspectos da área estudada por meio de estudos petrográficos e geoquímicos, enriquecendo os dados bibliográficos e elucidando ainda mais quais foram e como se deram os eventos magmáticos que afetaram das bacias de Campos e Santos durante sua fase drifte.

1.4 Área de Estudo

O Alto de Cabo Frio está localizado entre as Bacias sedimentares de Campos e Santos, na margem sudeste do Brasil. Os poços estudados (EG1, EG2 e EG3) estão localizados na área demarcada em azul na **Figura 4**.

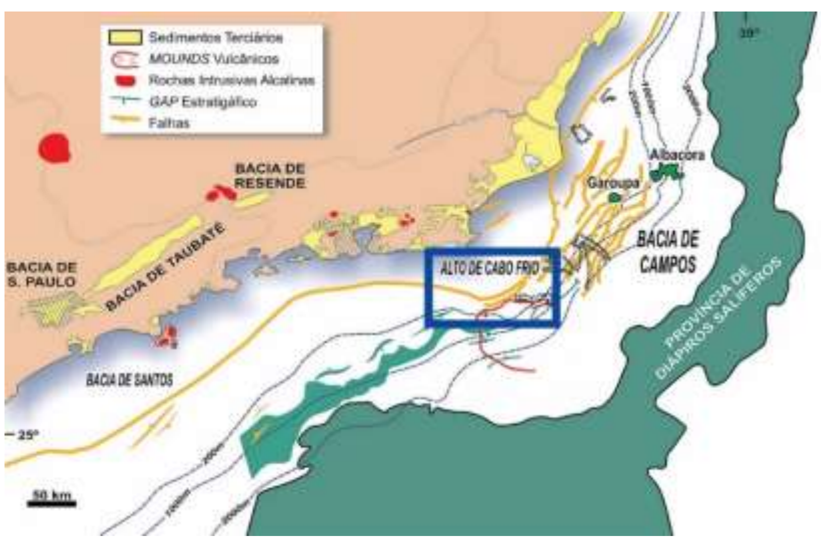

Figura 4. Mapa esquemático da área entre as bacias de Campos e Santos. Área de estudo destacada no quadrado azul. Modificado de **Oreiro (2006).**

Em função de cláusulas de confidencialidade do projeto ao qual o presente mestrado está associado, não é possível revelar a exata localização e nomenclatura dos referidos poços.

2 REVISÃO DE LITERATURA

2.1 Bacia de Campos: Estratigrafia e Contexto Tectônico

A Bacia de Campos possui uma área de cerca de 100.000 km^2 e está localizada entre o litoral norte do Rio de Janeiro e o litoral sul do Espírito Santos, sendo limitada a norte pelo Arco de Vitória e a sul pelo Arco de Cabo Frio (**Winter *et al.*, 2007**). Sua evolução tectonossedimentar seguiu três estágios: Rifte ou continental, associado aos falhamentos e processos de extensão crustal da separação do Gondwana; fase intermediária ou Pós-Rifte, associado a atividades tectônicas extensionais e vulcânicas; e por último o estágio marinho ou Drifte, caracterizado pelo afastamento contínuo da margem Atlântica em relação a cadeia meso-oceânica, pela deposição de sedimentos carbonáticos, e por eventos de halocinese, eustasia e vulcanismo (**Lopes, 2004**).

Definidas como bacias de margem divergente passiva, a evolução estrutural da região está atrelada a processos extensivos oriundos da separação das placas tectônicas da América do Sul e África. No que se refere ao padrão tectonoestratigráfico de evolução, os mecanismos de formação das bacias da margem brasileira são semelhantes. Os processos de geração das bacia de Campos e Santos tiveram início no rifteamento resultante da ruptura do Supercontinente Gondwana e Abertura do Atlântico Sul no Mesojurássico (**Moreira *et al.*, 2007; Winter *et al.*, 2007**). Como resultado, o embasamento Pré-Cambriano da bacia foi definido por estruturas significantemente marcadas, tais como uma série de falhas normais e zonas de acomodação que dominam os horsts e grabens (**Chang *et.al*, 1992**). O rifteamento afetou a Bacia de Campos no Eocretáceo, sobretudo durante a deposição da Formação Cabiúnas. A subsidência térmica crustal e a movimentação halocinética foram os fatores da Sequência de Margem Passiva / Drifte da Bacia, resultando em grandes domínios estruturais: distencional (águas rasas), translacional (em águas profundas) e compressional (em águas ultraprofundas) (**Guardado *et al.*, 1989; Castro e Picolini, 2014**).

A evolução estratigráfica e tectonossedimentar da Bacia de Campos é compartimentada em três supersequências: Rifte, Pós-Rifte e Drifte (**Winter *et al.*, 2007; Castro e Picolini, 2014**).

O embasamento cristalino da bacia é constituído por granitos e gnaisses pré-cambrianos pertencentes à Faixa Ribeira (**Castro e Picolini, 2014**). A deposição da Supersequência Rifte se inicia em um contato discordante entre o embasamento cristalino e o denominado embasamento econômico (derrames ígneos da Formação Cabiúnas) (**Winter *et al.*, 2007**). Esta formação é caracterizada por diabásios e basaltos subalcalinos subaéreos e subaquosos que apresentam espessura máxima perfurada de 650 metros. Arenitos siltitos e conglomerados ocorrem intercalados localmente com estes derrames (*intertraps*) (**Winter *et al.*, 2007**). Datado de 134 a 122 Ma, este evento magmático toleítico constitui uma extensão do vulcanismo intracontinental existente na bacia do Paraná (**Mizusaki *et al.*, 1992**).

Acima da Formação Cabiúnas foram depositados sedimentos caracterizados por um ambiente continental lacustre, ainda na Supersequência Rifte (**Dias *et al.*, 1988**). Esta sedimentação se decorreu entre o Barremiano e Aptiano, e compreende a porção inferior a intermediária do Grupo Lagoa Feia (formações Itabapoana, Atafona e Coqueiros). A Formação Itabapoana é caracterizada por conglomerados, arenitos, siltitos e folhelhos avermelhados, sendo associada a porções proximais de borda de bacia e borda de falha (**Winter *et al.*, 2007**). A Formação Atafona é representada principalmente por arenitos, siltitos e folhelhos depositados em um meio alcalino, o que resultou na deposição de minerais de talco e estevensita (**Winter *et al.*, 2007**). Os folhelhos desta formação são denominados Buracica e constituem importantes rochas geradoras de hidrocarbonetos (**Castro e Picolini, 2014**). A Formação Coqueiros, também é de grande importância para a indústria de óleo e gás, uma vez que é caracterizada pela intercalação de folhelhos ricos em matéria orgânica (folhelhos Jiquiá, principais rochas geradoras da bacia) e carbonatos lacustres porosos (coquinas, principais reservatórios da bacia) (**Winter *et al.*, 2007**).

A Supersequência Pós-Rifte representa a transição entre um ambiente continental lacustre e um ambiente marinho restrito, sendo correspondente à porção superior do Grupo Lagoa Feia. Esta sedimentação consiste em uma etapa de expansão da bacia e se decorreu durante o Aptiano, compreendendo as formações Itabapoana, Gargaú, Macabu e Retiro (**Winter *et al.*, 2007**). A Formação Itabapoana é marcada por intensa progradação e apresenta fácies associadas a leques aluviais nas bordas da bacia (conglomerados e arenitos) (**Dias *et al.*, 1988**). A deposição destes sedimentos terrígenos é contemporânea à sedimentação carbonática distal que compreende as formações Gargaú e Macabu (**Dias *et al.*, 1988; Winter *et al.*, 2007**). Tais formações são compostas por carbonatos, margas e arenitos depositados em um ambiente de mar raso. A exposição subaérea desta sedimentação pode ser evidenciada pela presença de calcários estromatolíticos nas porções mais distais da Formação Macabu (**Winter *et al.*, 2007**). Acima desta unidade caracterizada por rochas siliciclásticas e carbonáticas encontra-se a Formação Retiro, constituída essencialmente por evaporitos. Tais rochas indicam um ambiente marinho/lagunar associado a planícies de *sabkha*, no qual processos de sedimentação e precipitação química propiciaram a deposição de sais (**Castro e Picolini, 2014; Winter *et al.*, 2007**). Estima-se que estas rochas foram depositadas em um intervalo entre 0,7 e 1 Ma, sendo observada a seguinte sequência mineral da porção mais proximal à distal: anidrita, anidrita + halita, anidrita + halita + carnalita/silvinita Macabu (**Winter *et al.*, 2007**). Na porção proximal também pode ser observada a presença de calcário, ainda que o mesmo ocorra apenas localmente (**Dias *et al.*, 1988**). Este sal representa um importante papel no sistema petrolífero da Bacia de Campos, uma vez que atua como rocha selante e como caminho de migração para depósitos sedimentares sobrejacentes, por meio de sua própria movimentação (**Riccomini *et al.*, 2012**).

A Supersequência Drifte é dividida em duas grandes sequências: Marinha Transgressiva e Regressiva. Esta supersequência é constituída pelos Grupos Macaé e Campos que apresentam sedimentos marinhos de idades que variam do Albiano ao Holoceno. A fase Drifte é um registro da subsidência térmica da bacia, sendo caracterizada também por eventos de halocinese restritos ao Albiano (**Dias *et al.*, 1990**).

O Grupo Campos posiciona-se sobreposto às rochas do Grupo Macaé e inclui as formações Emborê, Ubatuba, Carapebus e Barreiras, além dos membros Tamoios, Geribá, Grussaí, Siri e São Tomé. As rochas desse grupo são depositadas em ambientes proximais, marinhos distais e depósitos turbidíticos (**Castro e Picolini, 2014**). A Formação Emborê possui conglomerados polimíticos e arenitos grosseiros típicos de depósitos de leques aluviais. Na paleoborda formou-se o Membro Siri, que é caracterizado por uma plataforma carbonática com bancos de algas vermelhas (**Castro e Picolini, 2014**). As rochas do Membro Siri são predominantemente calcirruditos e calcarenitos (**Winter *et al.*, 2007**). Alguns membros da Formação Emborê foram definidos para identificar fácies, sendo eles: Membro São Tomé, caracterizado por clásticos avermelhados e Membro Grussaí (Mioceno ao Recente) constituído por calcarenito bioclástico de plataforma (**Rangel *et al.*, 1994; Lopes, 2004**). A base da Formação Emborê corresponde ao Membro São Tomé, que representa depósitos arenosos mal selecionados e avermelhados (**Lopes, 2004**). A Formação Ubatuba do Cretáceo Superior possui depósitos de sedimentação hemipelágica, com folhelhos e margas depositados em ambiente marinho aberto batial e abissal (**Castro e Picolini, 2014**). A Formação Ubatuba ocorre interdigitada lateralmente com os sedimentos clásticos e carbonáticos da Formação Emborê, sendo possível observar essa configuração em regiões mais proximais da bacia (Rangel *et al.*, 1994 *in* Lopes, 2004). Na parte inferior da formação está localizado o Membro Tamoios, depositado no Turoniano Superior/ Maastrichtiano (**Lopes, 2004**).

Os sedimentos arenosos da Formação Carapebus foram depositados a partir de fluxos gravitacionais sedimentares caracterizados por um pacote siliciclástico fino com corpos arenosos, originados por fluxos hiperpicnais de sistemas turbidíticos depositados em ambiente marinho profundo. Essa formação abrange os principais reservatórios de hidrocarbonetos da bacia (**Castro e Picolini, 2014; Winter *et al.*, 2007**). Depósitos conglomeráticos, arenosos, siliciclásticos ferruginosos, lamosos de alta energia e de fluxos gravitacionais (leques aluviais) caracterizam a Formação Barreiras (**Winter *et al.*, 2007**). A porção basal do Grupo Campos compreende as formações: Ubatuba (Membro Tamoios), Carapebus e Emborê (Membro São Tomé), onde foram depositados folhelhos turonianos, além de arenitos de ambiente batial superior produzidos em fluxos hiperclinais. Nas regiões distais dessa porção é observada uma grande deposição de evaporitos e pacotes arenosos do Coniaciano/Santoniano. Nesse mesmo sistema arenoso há evidências de atividade vulcânica intensa, com a presença de basaltos, hialoclastitos, diabásios e gabros. No topo ocorrem cinzas vulcânicas (Campaniano). Outra atividade vulcânica na Bacia é evidenciada por basaltos datados de 65,5 Ma (Evento Magmático Cretáceo-Paleógeno) e 62 Ma (Evento Magmático Paleoceno) (**Winter *et al.*, 2007**).

É possível definir grandes eventos magmáticos que influenciaram de maneira direta no contexto de evolução tectônica, na sedimentação e na estratigrafia da Bacia de Campos (**Dani *et al.*, 2017**). Na fase Rifte o vulcanismo intenso é evidenciado na formação Cabiúnas. Na fase Pós-Rifte, por sua vez, podemos observar o magmatismo Alagoas, enquanto na fase Drifte os eventos relevantes ocorrem no Santoniano-Campaniano, Cretáceo-Paleógeno, Eoceno Inferior e Eoceno Médio (**Bastos *et.al.*, 2017**). No intervalo entre o Neoconiaciano até o Maastrichtiano (25 Ma) a influência desse magmatismo se deu pelo aporte de vulcanoclastos intercalados e pela ação de terremotos e sismos. A deposição destes originou dois marcos estratigráficos de composição traquítica. O primeiro marco é chamado Marco 3-Dedos que exibe camadas interdigitadas com rochas pelíticas consideradas representativas da seção marinha hemipelágica (**Alves, 2005**). Esse marco datado do Santoniano está inserido na Formação Ubatuba, acima dos reservatórios turbidíticos cretácicos (Formação Carapebus) (**Caddah *et al.*,1994**). O marco é constituído por vidro vulcânico e representa a litofácie mais fina deste vulcanismo com afinidade traquítica. Tal característica o diferencia das rochas encontradas na Formação Cabiúnas. O segundo marco é chamado arco 3B e está localizado na porção norte da bacia. Ele é caracterizado por um longo intervalo de rochas pelíticas e depósitos de turbiditos interdigitados, possui litofácie mais híbrida contendo vulcanoclastos retrabalhados. Apesar dos diferentes tipos de litofácies dos marcos, a correlação genética de ambos está atrelada à uma fonte vulcânica comum (**Alves, 2005**).

2.2 O Magmatismo no Alto de Cabo Frio

A região do Alto Estrutural de Cabo Frio apresenta características estruturais e estratigráficas diferentes daquelas observadas nas demais áreas das bacias associadas, inclusive no que se refere aos eventos magmáticos do Santoniano e Eoceno (**Oreiro, 2006**). Este magmatismo teve uma grande influência na evolução sedimentar das Bacias de Santos e Campos (**Figura 5**), bem como na qualidade dos reservatórios de óleo e gás destas bacias (**Mohriak et al., 2005; Oreiro, 2006; Moreira *et al.*, 2006**).

Estudos geofísicos na região revelam a presença de várias feições magmáticas, incluindo diques, soleiras, inundações, cones vulcânicos e sequências vulcaniclásticas espessas associadas a episódios distintos (***e. g.*** **Moreira et al., 2006; Oreiro, 2006; Oreiro *et al.*, 2008; Gordon *et al.*, 2023a**). As composições destas rochas consistem predominantemente em tufos, hialoclastitos, brechas e basaltos, com um carácter globalmente alcalino (***e. g.*** **Moreira *et al.*, 2006; Oreiro, 2006; Rangel, 2006; Frank e Valente, 2023**). Possíveis fontes férteis do manto profundo são identificadas como elementos potenciais na origem dos magmas de deriva da Bacia de Santos, com uma pequena contribuição de componentes do manto EMI e EMII (**Gordon *et al.*, 2023b**).

Segundo **Oreiro (2006)**, as rochas magmáticas do Santoniano-Campaniano e Eoceno ocorrem sob a forma de derrames, edifícios vulcânicos, diques e soleiras, sendo predominantes as manifestações extrusivas. Além disso, estes materiais magmáticos encontram-se associados a sedimentos gerando uma espessa sequência vulcanoclástica.

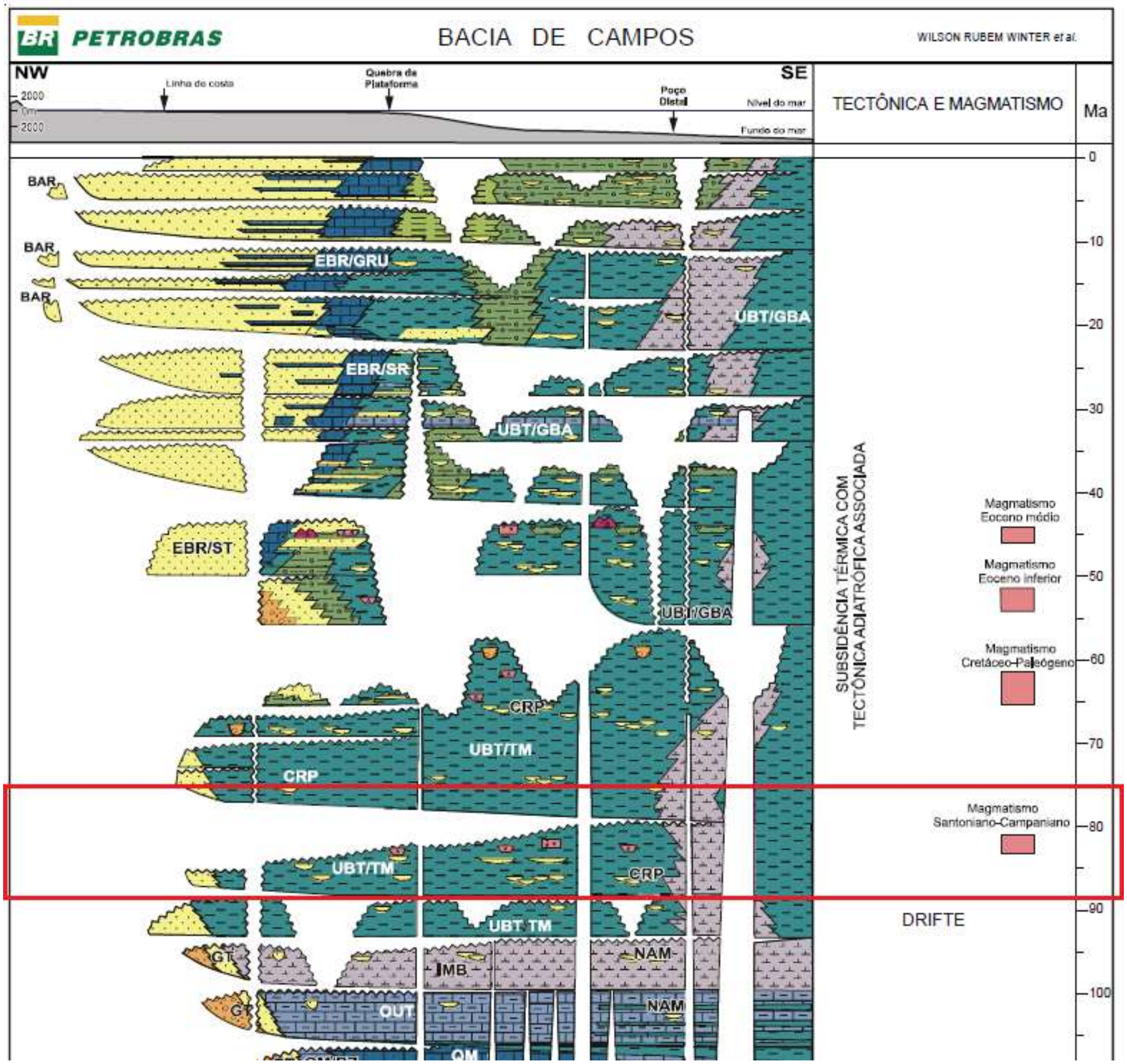

Figura 5. Carta estratigráfica da Bacia de Campos, com destaque para o evento Magmático Santoniano-Campaniano, bastante expressivo no Alto de Cabo Frio (área de estudo). Adaptado de **Winter *et al.*, 2007**.

3 MATERIAIS E MÉTODOS

Os materiais usados neste estudo consistem em perfis de poço, amostras laterais e amostras de calha organizadas em seções magmáticas de três poços localizados na área do Alto de Cabo Frio, entre as bacias de Campos e Santos.

A execução da presente dissertação de mestrado envolveu cinco etapas metodológicas principais: a) revisão temática; b) preparação e obtenção de dados petrográficos; c) preparação e obtenção de dados litogeoquímicos e isotópicos; d) análise e interpretação de dados; e) elaboração dos modelos e textos finais.

As etapas metodológicas são detalhadas abaixo:

a) Revisão Temática

Trata-se de um estudo do material bibliográfico a respeito da área de estudo e das Bacias de Santos e Campos. Esta etapa incluiu a obtenção de informações a respeito da geologia regional e local, cronoestratigrafia e, em especial, da influência e caracterização do magmatismo atuante na região. Também envolveu pesquisa específica a respeito do magmatismo alcalino no sudeste do Brasil cogenético às rochas estudadas, em especial aqueles observados no Alinhamento Magmático Poços de Caldas-Cabo Frio e na Cadeia Vitória Trindade.

Nesta etapa também foram analisados os perfis compostos dos poços estudados e, com base nisto, foram escolhidas as seções compostas por rochas vulcânicas e vulcanoclásticas a fim de serem utilizadas no estudo.

Além disso, foi realizada uma compilação de dados isotópicos e membros finais pertencentes aos seguintes reservatórios do manto: DM/MORB, HIMU, EMI e EMII, e dados para os magmas de Poços de Caldas-Cabo Frio e Vitória-Trindade. Esses dados foram empregados na formulação de modelos petrológicos, contribuindo para o avanço das discussões geodinâmicas sobre o magmatismo Santoniano-Campaniano na área estudada. As informações compiladas foram obtidas dos bancos de dados GEOROC (https://georoc.eu/georoc/new-start.asp) e EarthRef (https://earthref.org/).

b) Preparação e Obtenção dos Dados Petrográficos

A fase inicial desta etapa consistiu na limpeza das amostras laterais e de calha. Quando extraídas de poços de petróleo, as rochas são expostas à fluidos de perfuração, que podem deixar resíduos e, consequentemente, são suscetíveis a afetar a composição química das rochas analisadas se não forem removidos. As amostras laterais e de calha foram então lavadas em água corrente com o auxílio de uma escova macia para melhor remoção das impurezas.

Depois de secas, as amostras de calha foram peneiradas para verificar a perda de finos com peneiras de duas partículas, nº 48 e nº 100. O material retido na peneira nº 100 foi armazenado em sacos ziplock de 4x4 cm, com o intervalo de profundidade correspondente a cada amostra. O material retido na peneira nº 48 foi dividido em duas alíquotas: amostras magnéticas e não magnéticas. Ambas as alíquotas foram agrupadas por tipo textural de acordo com a cor e a textura (como "cinza fanerítico" e "preto afanítico") (**Figura 6**). Essa separação foi realizada para classificar diferentes litologias magmáticas e sua profundidade estimada nas seções estudadas. Cada grupo de amostras foi armazenado em um saco ziplock de 4x4 cm identificado com o código correspondente e o intervalo de profundidade.

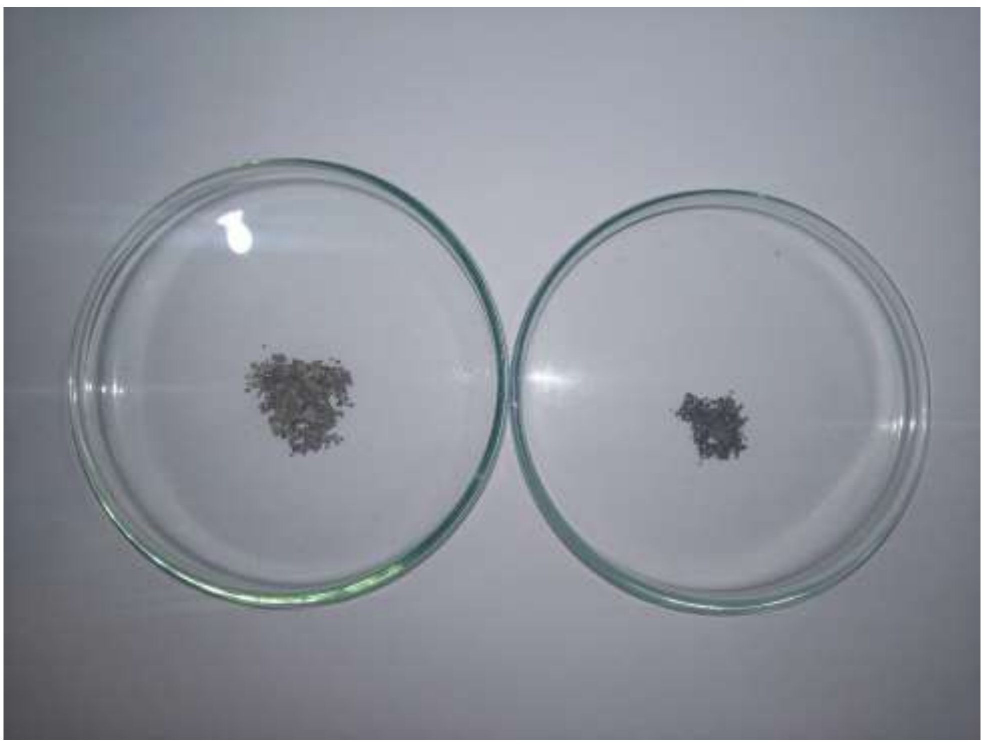

Figura 6. Separação inicial das amostras de calha com base em suas propriedades magnéticas. As frações magnéticas e não magnéticas foram dispostas em diferentes placas de Petri a fim de serem analisadas separadamente em etapa posterior.

Estas amostras, bem como as amostras laterais, foram analisadas sob lupa petrográfica a fim de serem caracterizadas com base em suas características macroscópicas (propriedade magnética, cor, brilho, estado de alteração, texturas e estruturas). As amostras foram selecionadas e preparadas para a confecção de 36 lâminas petrográficas (15 laterais e 21 calhas). As análises microscópicas e as fotomicrografias foram realizadas sob microscópio de luz transmitida Axio Zeiss Imager A2 nas dependências do Departamento de Petrologia e Geotectônica da Universidade Federal Rural do Rio de Janeiro.

c) Preparação e Obtenção dos Dados Litogeoquímicos e Isotópicos

Com base na etapa anterior, foram selecionadas 15 amostras laterais para análises litogeoquímicas (elementos maiores, traços e terras-raras). A preparação das amostras para análises litogeoquímicas envolveu moagem, lixiviação e peneiramento das amostras. Tais análises foram realizadas no laboratório Actlabs (https://actlabs.com/) utilizando os métodos de espectrometria de indução atômica por plasma indutivamente acoplado (*ICP-AES*) para elementos maiores (SiO2, TiO2, Al2O3, Fe2O3t, MnO, MgO, CaO, Na2O, K2O, P2O5, e espectrometria de massa por plasma indutivamente acoplado (*ICP-MS*) para elementos traços e terras-raras (Ba, Rb, Sr, Zr, Y, Nb, Ni, Cr, V, Co, U, Th, Hf, Ta and Pb, La, Ce, Pr, Nd, Sm, Eu, Gd, Tb, Dy, Ho, Er, Tm, Yb e Lu). A perda ao fogo (LOI) foi medida pelas diferenças de peso entre as amostras inflamadas e não inflamadas. O ferro foi medido como ferro total e ferro férrico (Fe_2O_{3t}). A precisão analítica para os elementos principais medidos com base em duplicatas ficou entre 0,3% e 1,7%, enquanto para os elementos de traço selecionados ficou entre 0,3% e 2,7% e entre 0,5% e 7,9% para os elementos de terras raras (REE). A precisão analítica dos elementos principais foi calculada com base nas concentrações de elementos dos padrões internacionais e ficou entre 0,6% e 6,9%. Para os elementos-traço, a precisão ficou entre 1,0% e 3,39% e entre 1,5% e 12,5% para o REE.

Os dados isotópicos de Sr-Nd-Pb-Hf foram adquiridos no Johnson Mass Spectrometer Laboratory da New Mexico State University (https://geofaculty.nmsu.edu/ramos/services.html), nos Estados Unidos. As análises foram conduzidas com o uso do Espectrômetro de Massa de Plasma Acoplado Indutivamente e Multicoletor Thermo Scientific Neptune Plus (MC - ICPMS). O material de referência padrão, NBS 987, produziu os seguintes resultados: 87Sr/86Sr = 0,710284 ± 0,000011; 143Nd/144Nd = 0,512099 ± 0,000008; 206Pb/204Pb = 18,898 ± 0,001; 207Pb/204Pb = 15,485 ± 0,001; 208Pb/204Pb = 38,678 ± 0,002; 176Hf/177Hf = 0,282161 ± 0,000007.

d) Análise e Interpretação de Dados

Após a obtenção dos dados petrográficos, litogeoquímicos das amostras de calha e laterais, foi realizada uma análise e integração dos mesmos. Tal feito permitiu a classificação e discriminação de séries destas rochas estudadas, além de uma melhor compreensão das fontes magmáticas e dos processos evolutivos geradores do magmatismo na área estudada. Complementando estas informações, foram utilizados os dados isotópicos das amostras laterais permitindo que haja um maior aprofundamento na compreensão do contexto petrogenético e geodinâmico associado ao magmatismo drifte da região estudada.

e) Elaboração dos Modelos e Textos Finais

A última etapa compreendeu a elaboração de modelos petrológicos e geodinâmicos com base nas interpretações previamente descritas, resultando também na elaboração de dois artigos científicos (um especificamente utilizando os dados de petrografia e litogeoquímica e o outro utilizando os dados isotópicos) e do texto final de dissertação de mestrado.

O material suplementar dos respectivos artigos está inserido nos anexos da presente dissertação de mestrado e incluem a tabela de dados geoquímicos das amostras estudadas e os dados isotópicos compilados para os reservatórios mantélicos DM, EMI, EMII, e HIMU, e para rochas magmáticas do Alinhamento Magmático Poços de Caldas – Cabo Frio e Cadeia Vitória – Trindade.

O presente trabalho de dissertação de mestrado foi elaborado em formato híbrido, sendo os resultados apresentados na forma de artigos científicos. Tal procedimento está conforme o regimento da Pró-Reitoria de Pesquisa e Pós-Graduação (PROPPG) da Universidade Federal Rural do Rio de Janeiro.

O primeiro artigo apresentado nos resultados (Capítulo 4) foi publicado na Revista Comunicações Geológicas com o título: The post-breakup magmatism in Cabo Frio High, Campos Basin, Brazil: implications to a thinned lithosphere contribution in magma formation. DOI: https://doi.org/10.34637/h145-3n13. O segundo artigo elaborado (Capítulo 5) ainda será submetido.

4 ARTIGO CIENTÍFICO 1: The post-breakup magmatism in Cabo Frio High, Campos Basin, Brazil: implications to a thinned lithosphere contribution in magma formation

4.1 Abstract

The Cabo Frio High, limit between Campos and Santos basins, consists of an elevated structure characterized by intense magmatism. Through new petrographic and geochemical data, this paper brings new highlights on sources and evolutionary processes associated with volcanic events that affected this area during Santonian-Campanian drifting stage. Samples from three studied wells are pyroclastic ash, lapilli tuffs, basalts, scoria and diabases associated with subaerial explosive volcanism. Geochemically, they are alkaline rocks classified as basalts, alkaline basalts, foidites and tephriphonolites. The evolution of these rocks derives from geodynamic processes that occurred in shallow mantle depths (35 – 80 km) and involved mixing between a depleted, relatively shallow asthenospheric source (N-MORB) and the local subcontinental lithospheric mantle represented by the average composition of the lamprophyres at the Cabo Frio Structural High.

4.2 Introduction

The southeastern Brazilian continental margin basins are important areas of oil and gas exploration. Hydrocarbon systems are intrinsically associated with their tectonic, stratigraphic and magmatic development. Igneous events can provide a thermal increment in source rocks that leads to organic matter maturation. Furthermore, magmatic rocks might be important seals, reservoirs or paths to oil and gas occurrences (**Thomaz Filho *et al.*, 2008**).

The tectonic evolution of sedimentary basins in southeastern Brazil is related to the opening of the South Atlantic Ocean. This event started in the Upper Cretaceous and evolved to the Gondwana breakup. The consequent African and South American continents separation produced all sedimentary basins on the east Brazilian margin, such as Espírito Santos, Campos, and Santos basins (**Moreira, 2007**).

Magmatic events in such rifted to passive margins are commonly referred to as associated with different tectonic evolutionary processes: lithosphere stretching efforts (***e.g.* Franke, 2013**), reactivation of major structures (**Almeida, 1983; Oreiro *et al.*, 2008**) and plume-related magmatism (**Thompson *et al.*, 1998; Thomaz Filho and Rodrigues, 1999; Thomaz Filho *et al.*,**

2005). Still, limited petrological studies comprising especially drift stage magmatism in Santos and Campos basins turned difficult to determine possible geotectonic processes and sources involved in such events.

The Cabo Frio High, an elevated structure between these two basins, encompasses important occurrences of the magmatism that affected the sedimentary evolution of Campos and Santos basins (**Oreiro, 2006; Moreira, 2007; Winter, 2007; Oreiro *et al.*, 2008**). The study of the magmatism that occurred in this area represents a key element to understand how tectonomagmatic processes can influence such marginal basin development and even how they can modify petroliferous systems, so important to the exploration of oil and gas in these basins.

Therefore, this paper aims to contribute with the generation of new data by characterizing petrographically volcanic and volcaniclastic rocks sampled in the Cabo Frio High area (**Figure 4**). Additionally, petrogenetic and geodynamic models proposed enlighten different processes and possible sources associated with this mafic magmatism.

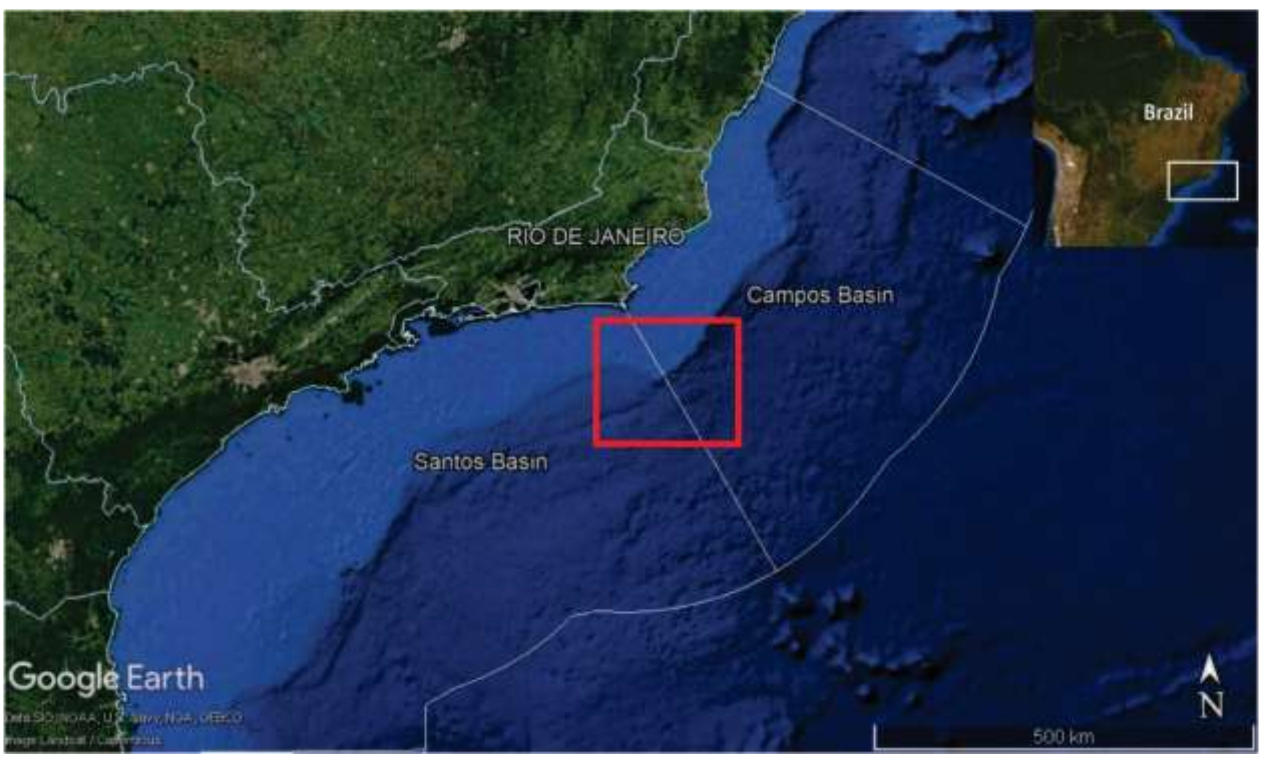

Figure 4. Schematic map showing the Cabo Frio High region and the limit between the Santos and Campos basins. The study area is highlighted by the red rectangle on the map.

4.3 Geological Setting

The Santos and Campos basins are located in the southeastern Brazilin margin. Their tectonic evolution is associated with rifting and lithospheric stretching processes that led to a Late Aptian break-up between the South America and Africa lithosphere. As a result of these extensional events, normal faults systems and accommodation zones (horsts and grabens) were created in the Pre-Cambrian basement and controlled uppermost posterior sedimentation. Subsequent opening of the South Atlantic Ocean and continuous extensional efforts led to an evolution from rift to passive continental margin basin (**Chang *et al*., 1992, Cainelli and Mohriak, 1999**).

Santos and Campos crystalline basement consists of the Cabo Frio and Oriental terrains from the Neoproterozoic Ribeira Orogen. These terrains related to the Braziliano orogenic collage, are characterized by compressional, metamorphic and magmatic episodes. This orogeny generated metasedimentary and metavolcano-sedimentary association, besides pre-to-pos collisional granitoid (**e.g., Heilbron *et al*., 2000; Schmitt *et al*., 2004; Tupinamba *et al*., 2007; Schmitt *et al*., 2008**).

These basins stratigraphic and sedimentary evolution comprises three main phases: rift, post-rift and drift supersequences (**Moreira *et al*., 2007; Winter *et al*., 2007**), also denominated continental, transitional evaporitic/shallow carbonate and open-marine, or continental, transitional and marine megasequences, respectively (**Chang *et al*, 1992, Cainelli and Mohriak, 1999**).

Both basins were affected by important magmatic events during their evolution. The first event recorded consists of the pre-to-synrift-related floods of the Cabiúnas (Campos Basin) and Camboriú (Santos Basin) formations (**Moreira *et al*., 2007; Winter *et al*., 2007**). Dating from 137 to 122 (Ar-Ar), these rocks are mainly subereous and subaqueous tholeiitic basalt, occasionally diabase and volcaniclastics rocks (**Mohriak *et al.*, 2021; Mizusaki *et al.*, 1988; De Luca *et al.*, 2015**).

The two subsequent magmatic events are characterized by basaltic floods and intrusions that occur during the syn-to-post rift phase and are associated with salt and pre-salt layers. These rocks are classified as basalts and originate from magmas with sub-alkaline tholeiitic to transitional composition (**Moreira *et al*., 2007; Winter *et al.*, 2007; Mohriak *et al.*, 2021**). Low TiO2 and high MgO2 content in these basalts indicate a possible interaction between volcanism and water, as well assimilation of contaminants from the local lower crust (**Lobo, 2007; Dani *et al*., 2017**).

The limited studies and geochronological data might suggest that these two magmatic occurrences are possibly related and part of one major event (**Gordon *et al.*, 2013**).

The drift phase in Campos and Santos basins exhibits two main magmatic pulses between the Santonian-Campanian (around 85 - 75 Ma) and the Lower Eocene (around 50 Ma). Both are characterized by intrusive and extrusive alkaline rocks including basalts, diabases trachyte, syenite, phonolite, nepheline syenite. Volcaniclastic material is also present, as well as the ones observed in the "3-Fingers" and the "3B" marks in Campos Basins (**Almeida *et al.*, 1996; Alves, 2006; De Luca *et al.*, 2015**).

Although adjacent to the Campos and Santos Basins, the Cabo Frio High shows significant differences in its structural and stratigraphic styles from the surrounding area (**Mohriak *et al.*, 1995**). It comprises an elevated structure of the basement that separates the Campos and Santos basin. This high extends across the continental shelf and by the São Paulo Plateau serving as a barrier to sedimentation between the two basins (**Pedro, 2005**).

Another difference between the Cabo Frio High and the adjacent regions is its large volume of magmatism. The magmatic rocks are both extrusive and intrusive in different stratigraphic levels. They occur as floods, sills, dikes, and mostly as volcanic cones identified in seismic sections (**Figure 5**) (**Mizusaki and Mohriak, 1992; Oreiro, 2006; Moreira *et al.*, 2005, Rangel, 2006**). Associated with this volcanism there is a record of a thick volcanoclastic sequence that sometimes has a slope that plunges towards the continent (**Oreiro, 2006**). The rocks aforementioned occur in water depths greater than 500 meters (**Misuzaki and Mohriak, 1992; Mohriak *et al.*, 2003**).

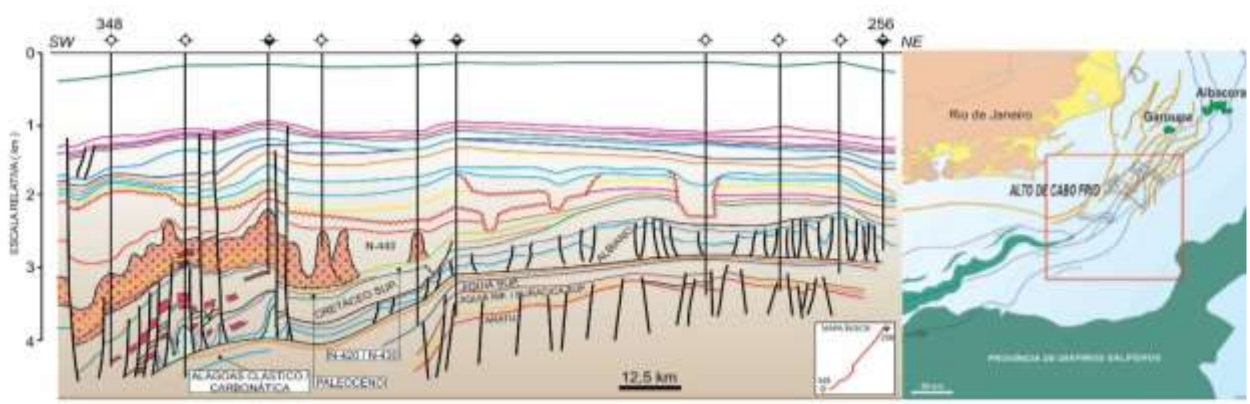

Figure 5. South Campos Basin geological section. Volcanic cones are evidenced by seismic lines (**Modified from Rangel, 2006**).

As well as observed in other regions of Campos and Santos Basin, the Cabo Frio High magmatism was observed from the Late Cretaceous to the Eocene (**Figure 6**). A subdivision specifically proposed for this region is based on seismic, petrographic, chemical, and radiometric data (**Mohriak *et al*., 1990; Mizusaki and Mohriak, 1992**):

I. Sequence I – Composed by the basalts of Cabiúnas Formation (120-130 Ma, Eocretacic). These rocks are correlated to the Camboriú Formation at Santos Basin and Serra Geral Formation at Parana Basin.

II. Sequence II – Composed predominantly of basalts with little representation and Campanian-Turonian age (80 – 90 Ma).

III. Sequence III – Basalts, diabases, and volcanoclastic rocks with ages from Early Paleocene to Eocene (40 – 50 Ma).

Some authors point out that the most significant magmatic event around the Cabo Frio region began in the Albian (**Oreiro and Guerra, 2005**), reached its climax in the Eocene (**Mizusaki and Mohriak, 1992**), and is associated with great uplift of the continental crust, which is correlated to an NW-SE lineament that is extending from the oceanic crust (around the region of Jean Charcot mounts) until the Cabo Frio High (**Zalan and Oliveira, 2005**).

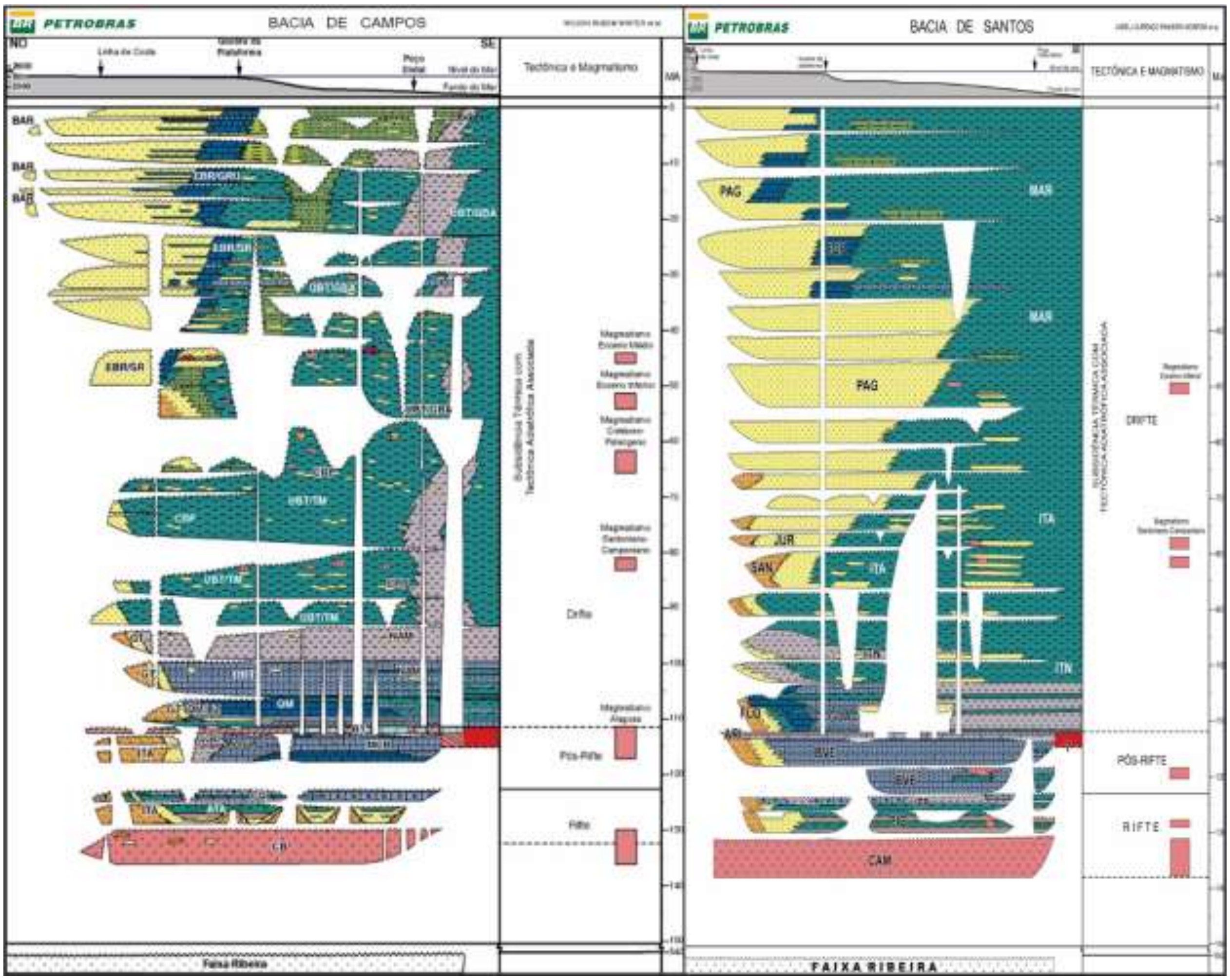

Figure 6. Campos and Santos basins chronostratigraphic chats. Magmatic events are indicated in red rectangles (**Modified from Moreira et al., 2007; Winter et al., 2007**).

Ultimately, the magmatic events in Campos and Santos basins are time-correlated based on the most recent proposals for their chronostratigraphic columns, even though the drift-related, Cretaceous-Paleogene magmatism has been recorded only in Santos (**Figure 7**).

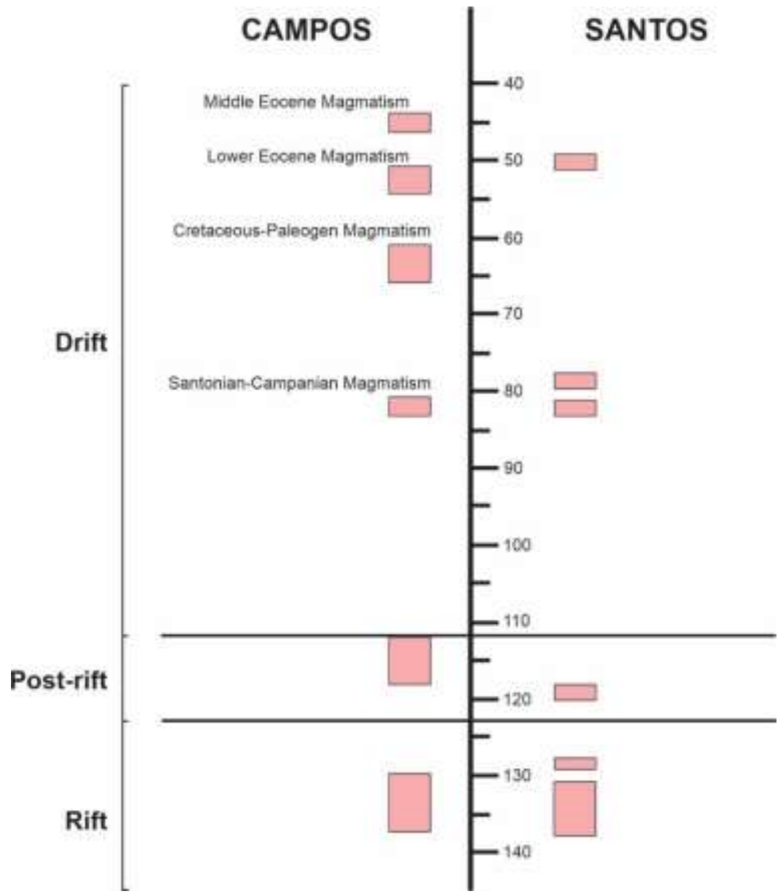

Figure 7. Time correlation of the magmatic processes recorded in Santos and Campos basins (**Modified from Moreira et al., 2007; Winter et al., 2007**).

Alkaline basalt flows and intrusions with 83.2 to 72.4 Ma, as well ash hyaloclastites and bentonites (the so-called 3-Fingers Mark; Marco 3-Dedos), occur mainly in the south area of Campos Basin and represent the drift-related, Santonian-Campanian magmatism (**Mizusaki *et al.*, 1992; Winter *et al.*, 2007**). The 1m-thick, widespread bentonites (Marco 3-Dedos) are taken as altered, volcanic ash deposits interbedded with the marine sediments of the Ubatuba Formation that were originated from a Plinian explosive volcanism (**Caddah *et al.*, 1994; Alves, 2006**). On the other hand, the so-called 3B Mark (Marco 3B) is thought to represent reworked pyroclastic ash that falls from the same emission centers that formed the bentonites. These volcanoclastic sediments mixed with siliciclastic accumulated on the continental shelf where they were further reworked to give rise to Maastrichtian turbidites (**Alves, 2006**).

As referred before, the studied area is located nearby the Cabo Frio Structural High between Santos and Campos basins. Well profiles indicate that the selected magmatic sections are observed in association with shales and marls of the Tamoios Member (Ubatuba Formation) and underlying sandstones of the Carapebus Formation, likely to be linked to the Santonian-Campanian drift magmatism in the Campos Basin. The time-correlated magmatism in the adjoining continental area is recorded in the northern sector of the Serra do Mar Alkaline Province and the Poços de Caldas-Cabo Frio Magmatic Alignment and has been associated with either interaction between lithospheric and asthenospheric Trindade plume-like mantle sources or reactivation of deep-seated lithospheric faults (**Thomaz Filho and Rodrigues, 1999; Thomaz Filho and Misuzaki, 2008; Almeida, 1983; Riccomini *et al*., 2005**).

4.4 Materials and Methods

Materials used in this study consist of well profiles, sidewall and drill cutting samples organized in magmatic sections of three wells. Well profiles were described and samples from post-salt magmatic sections were selected for petrographic and lithogeochemical analysis. When extracted from oil wells, rock samples are exposed to drilling mud which can leave residues that might affect the rock's chemical composition when not removed. Samples were then washed in running water with the assistance of a soft brush for better removal of impurities.

Once dry, drill cutting samples were sieved for loss of fines with two-particle size screens, #48 and #100 respectively. The material retained in the # 100 sieve was stored in 4x4 cm ziplock bags, with the corresponding depth interval for each sample.

The material retained in the # 48 sieve was divided into two rates: magnetic and non-magnetic samples. Both aliquots were grouped by textural type according to color and texture (such as "phaneritic gray" and "aphanitic black") (**Figure 8**). This separation was performed to classify different magmatic lithologies and their estimated depth in the studied sections. Each sample group was stored in a 4x4 cm ziplock bag identified with corresponding code and depth interval.

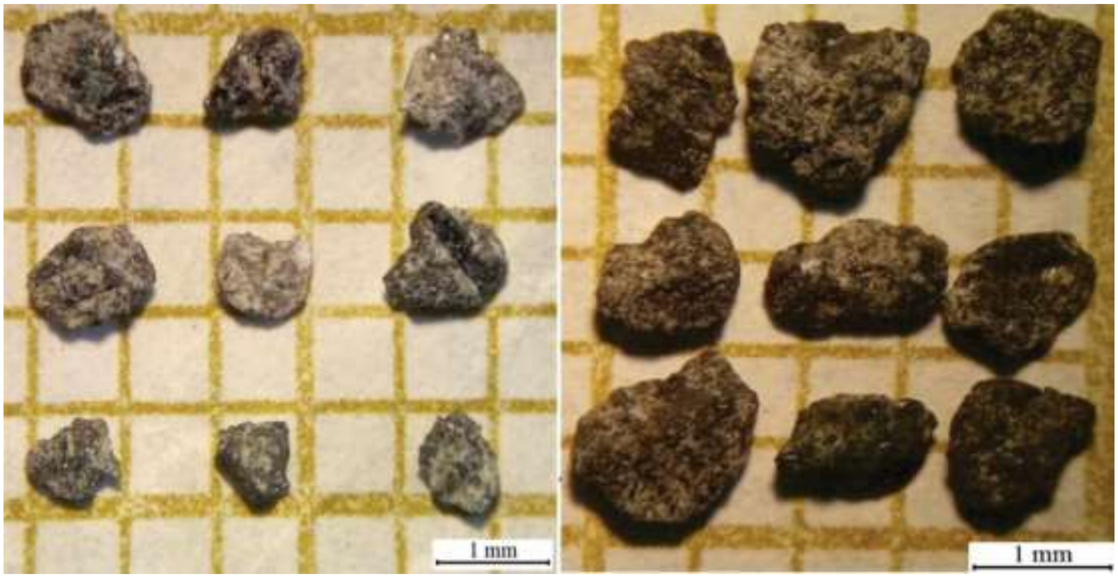

Figure 8. Macroscopic view of drill cutting samples. Separation process evolved the identification of different textural groups divided according to characteristics such as magnetism and color.

Sidewall and selected drill cutting samples were laminated and microscopic descriptions were made using a transmitted-light petrographic microscope Zeiss Axio. Thin section pictures were obtained using a Zeiss Microscope Axio Imager A2 petrographic. These analyses were performed at the Federal Rural University of Rio de Janeiro – Department of Petrology and Geotectonics laboratory.

Lithogeochemical data for fifteen sidewall samples were obtained at the ACTLABS in Canada. Major elements (SiO2, TiO2, Al2O3, Fe2O3t, MnO, MgO, CaO, Na2O, K2O, P2O5) concentrations (in wt.%) were obtained by Inductively Coupled Plasma-Atomic Emission Spectrometry (ICP-AES) whereas selected trace elements (Ba, Rb, Sr, Zr, Y, Nb, Ni, Cr, V, Co, U, Th, Hf, Ta and Pb), including the whole set of rare earth elements (La, Ce, Pr, Nd, Sm, Eu, Gd, Tb, Dy, Ho, Er, Tm, Yb e Lu), were measured (in ppm) by Inductively Coupled Plasma-Mass Spectrometry (ICP-MS). The loss of ignition (LOI) was measured by weight differences between ignited and non-ignited samples. Iron was measured as total iron as ferric iron (Fe2O3t). Analytical precision for major elements measured based on duplicates was between 0.3% and 1.7%, whereas for the selected trace elements was between 0.3% and 2.7% and between 0.5% and 7.9% for the rare earth elements (REE). Analytical accuracy for major elements was calculated based on element concentrations of international standards and was between 0.6% and 6.9%. For trace elements, the accuracy was between 1.0% and 3.39% and between 1.5% and 12.5% for the REE.

4.5 Results

4.5.1 Well data

Schematic sections of wells EG1, EG2 and EG3 are shown in **Figure 9**. Rocks shown in the three sections are stratigraphically above the salt sequence.

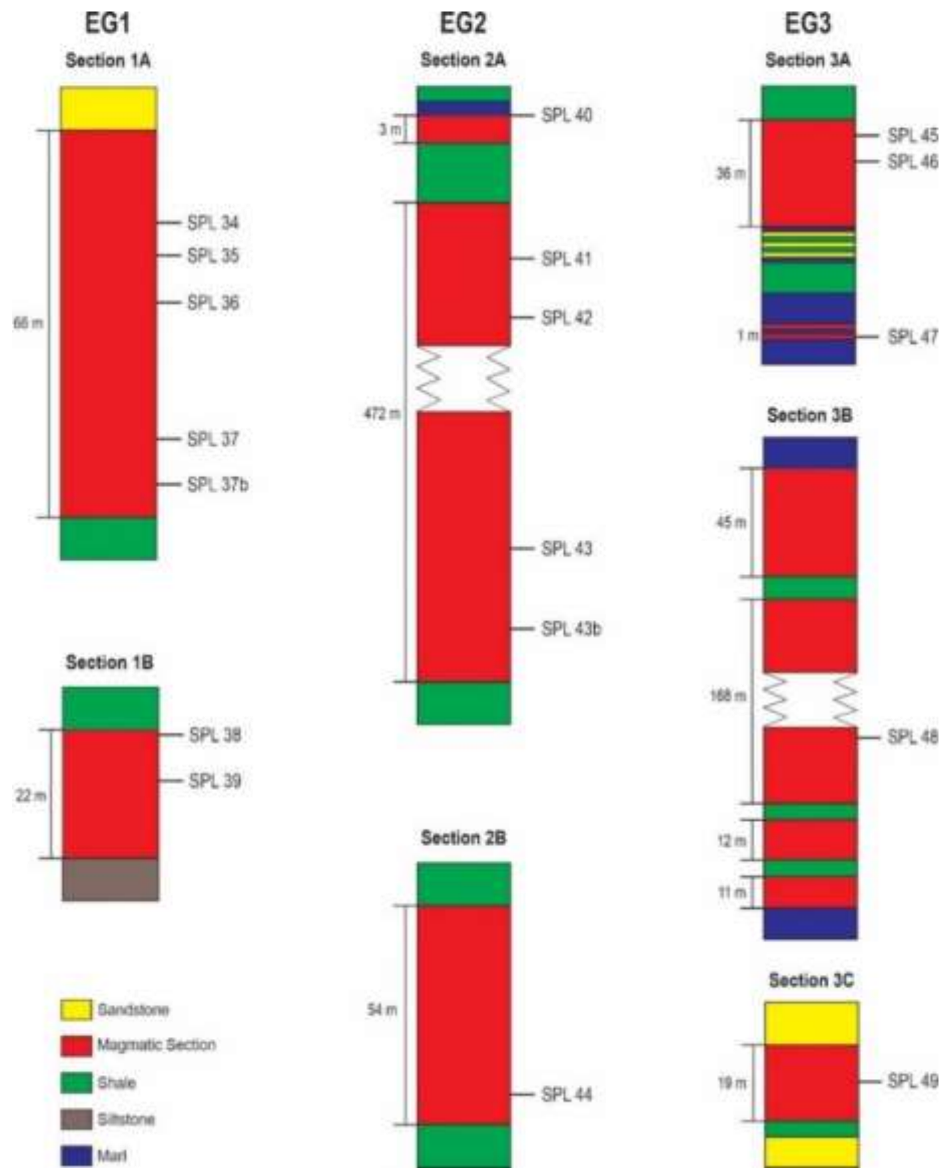

Figure 9. Schematic sections of wells EG1, EG2 and EG3 in northern Santos Basin. Sidewall core samples (SPL) are indicated.

Two magmatic sections were studied in well EG1. Section 1A is a 66 m thick continuous occurrence of dark gray magmatic rocks. These rocks underlie sandstones (Carapebus Formation) and overlie shales (Ubatuba Formation). Section 1B is a 22 m thick continuous occurrence of a diabase associated to shales and marls of the Ubatuba Formation (Tamoios Member). Both sections in well EG2 (2A; 483.5 m thick and 2B; 54 m thick) consist of lapilli tuffs that occur overlain and underlain by shales of the Ubatuba Formation. The well EG3 comprises three magmatic sections, as such: Section 3A comprises 35 m thick and 1 m thick occurrences of magmatic rocks interlayered with shales, sandstones, and marl of the Ubatuba Formation. Section 3B is a 236 m thick occurrence of magmatic rocks interlayered with three thin shale beds. Section 3C is a 19 m thick occurrence of magmatic rocks overlain and underlain by sandstones and shales of the Ubatuba Formation.

4.5.2 Petrography

4.5.2.1 Sidewall and core samples

Well EG1

Pyroclastic lithic ash tuffs with lithoclasts of trachyte (both aphyric and porphytiric) occur in section 1A (**Figure 10A**), as well as olivine-phyric agglutinated scoria (**Figure 10B**), and crystalloclasts of pyroxene and alkali feldspar (**Figure 10C**). The flat shape of vesicles in scoria indicates the presence of spatter cones. The occurrence of trachyte lithoclasts indicates and alkaline basalt-trachyte rock association typical of mildly alkaline series. This magmatic section's intermediate and uppermost rocks are also represented by centimetric bedding that alternates glass-, lithoclast- and carbonate-cemented, and crystalloclast-rich beds. Crystalloclasts are plagioclase, nepheline, biotite and opaque minerals. Clasts of glass are also observed. Some samples may represent mixed volcanoclastic tuffaceous sandstones with little reworking as depicted by the angular shapes of quartz crystalloclasts. As such, deposition was close to the emission center. There are no textures that can be undoubtedly associated with subaqueous volcanism.

Rocks in Section 1B were classified as alkali diabases (**Figure 10D and E**) based on petrographic characteristics. It is difficult to ascertain whether the rocks represent hypabyssal intrusions or flows. However, there are no textures that can be undoubtedly associated with subaqueous volcanism. The top of this magmatic section presents a fine-grained equigranular alkali diabase sample composed of alkali feldspar, clinopyroxene (augite), plagioclase, nepheline (altered to cancrinite), analcime, nosean and devitrified glass (altered to carbonate and chlorite). The partly altered diabase sample is located at the section's intermediate part and is composed of medium-grained plagioclase, alkaline pyroxene and amphibole, biotite, opaque minerals, zircon, apatite, sodalite and devitrified glass (altered to chlorite). Rocks in this section lack textural and structural evidence for pyroclastic processes. The fine- to medium-grained textures might indicate either subvolcanic or volcanic (subaerial), effusive processes.

Well EG2

Five sidewall core samples were used to study the upper, intermediate, and lower parts of section 2A. These rocks present a brecciated texture cemented by carbonate. Lithoclasts are predominantly pyroxene-phyric basalt (**Figure 10F**), basaltic scoria (**Figure 10G**), and fewer felsic, ash tuffs. The brecciated structure could have resulted from either phreatomagmatism associated with monogenetic scoria cones or hydraulic brecciation caused by coeval hydrothermal vents. The primary or secondary origin of the carbonate cement is difficult to discuss based on petrographic features. Nevertheless, the carbonate is itself fragmented, indicating that the brecciation continued after cementation.

Rocks in magmatic section 2B are lithic lapilli tuffs with lithoclasts of basaltic scoria and alkaline basalts. Lithoclasts are mainly altered, amygdaloidal, aphyric basalt with devitrified-brownish-altered glass (**Figure 10H**). Amygdales are irregular in shape and filled with carbonate (**Figure 10I**). Magmatism in section 2B comprises an effusive, subaerial basaltic flow at its lower parts whose volcanic environment is similar to the one observed in section 2A.

Well EG3

Three sidewall core samples, that represent the upper and lower parts of section 3A, are altered agglutinated basaltic scoria (**Figure 10J**) and ash tuffs. Section 3B comprises one lapilli tuff sample (SPL 48) (**Figure 10K**). Fragments includes shards, fiammes, scoria and altered glass. Alteration consists predominantly of chlorite. Compaction is a well-developed structure for very thin deposits (Section 3A) but greater for thicker deposits (Section 3B). Petrographic data obtained for one sidewall core sample (SPL 49) in Section 3C classifies this rock as a welded lapilli tuff with abundant lithoclasts of basaltic scoria (**Figure 10L**). Amygdales are predominantly round to sub round, filled with chlorite and carbonate.

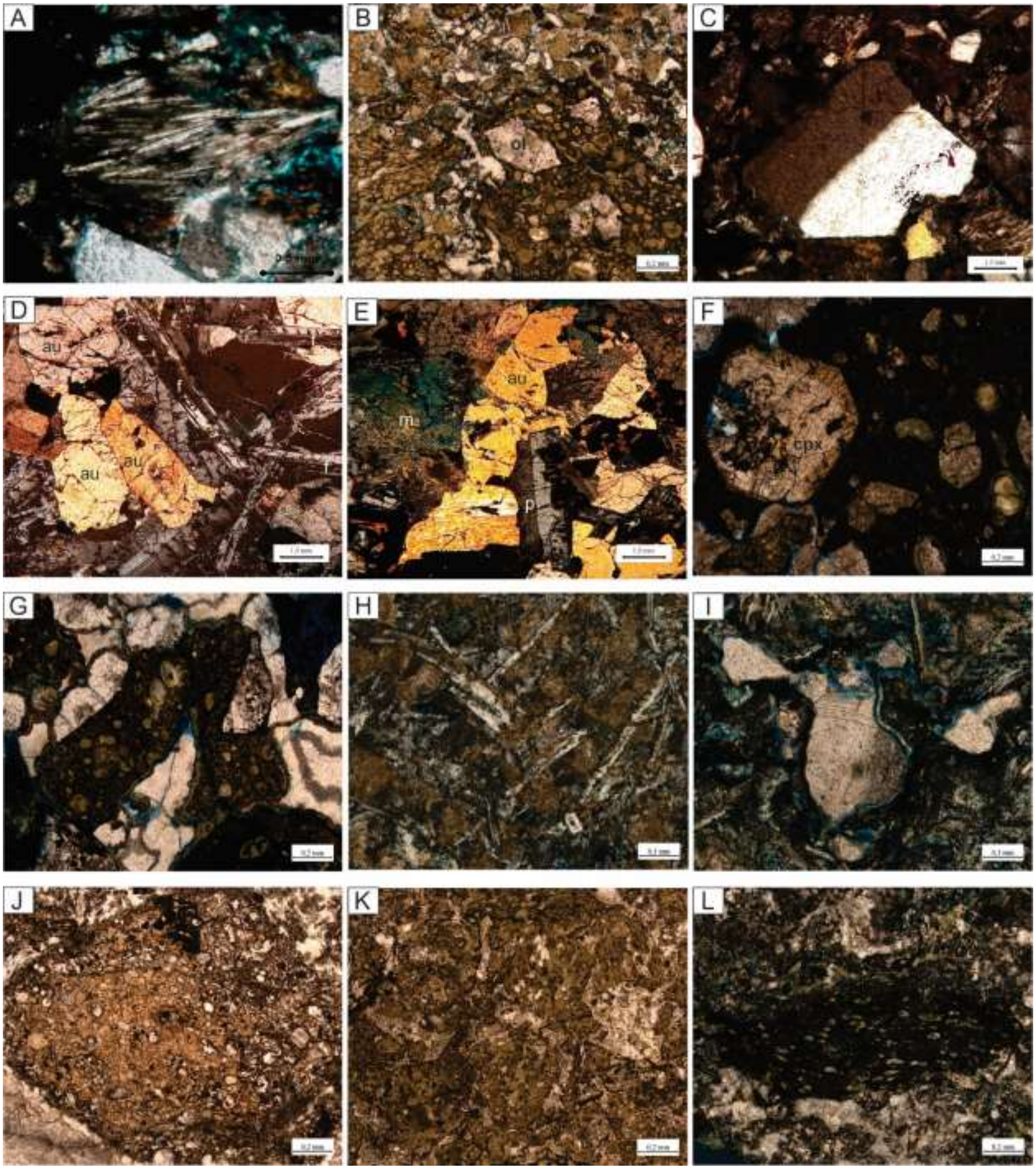

Figure 10. Photomicrographs of sidewall samples from wells EG1, EG2 and EG3. A) lithoclast of trachyte in sample SPL 35 (cross-polarized light); B) lithoclast of scoria with altered olivine (ol) in sample SPL 36 (plane-polarized light); C) alkali feldspar crystalloclast in tuff sample (cross-polarized light); D) equigranular texture in diabase SPL 38 with feldspars (f) and augite (au) (cross-

polarized light); E) alkali diabase sample SPL 39 with devitrified glass altered to a mixture of carbonate and chlorite (m), plagioclase (p) and augite (au) (cross-polarized light); F) pyroxene-phyric basalt lithoclast in SPL 41 (cpx = clinopyroxene) (plane-polarized light); G) basaltic scoria lithoclast in SPL 43 (plane-polarized light); H) Aphyric basalt with altered pyroxene and interstitial glass (brown), and plagioclase laths in sample SPL 44 (cross-polarized light); I) irregular carbonate-infilled amygdales in sample SPL 44 (cross-polarized light); J) basaltic scoria lithoclast in SPL 45 (plane-polarized light); K) welded lapilli tuff SPL 48 (plane-polarized light); L) lithoclast of scoria in lapilli tuff SPL 49 (cross-polarized light).

4.5.2.2 Drill cutting samples

Drill cutting samples represent a 3-meters interval each with 6 meters depth between them. Due to these technical specificities, the spatial positioning of these magmatic rocks is not as exact as sidewall samples are.

Cutting samples macroscopic and microscopic analyses allowed the identification of different lithologies that were occasionally observed in the same sampled intervals. Additionally, it was possible to estimate their stratigraphic positioning in well profiles (**Figure 11**), corroborating and expanding petrographic results obtained with sidewall samples.

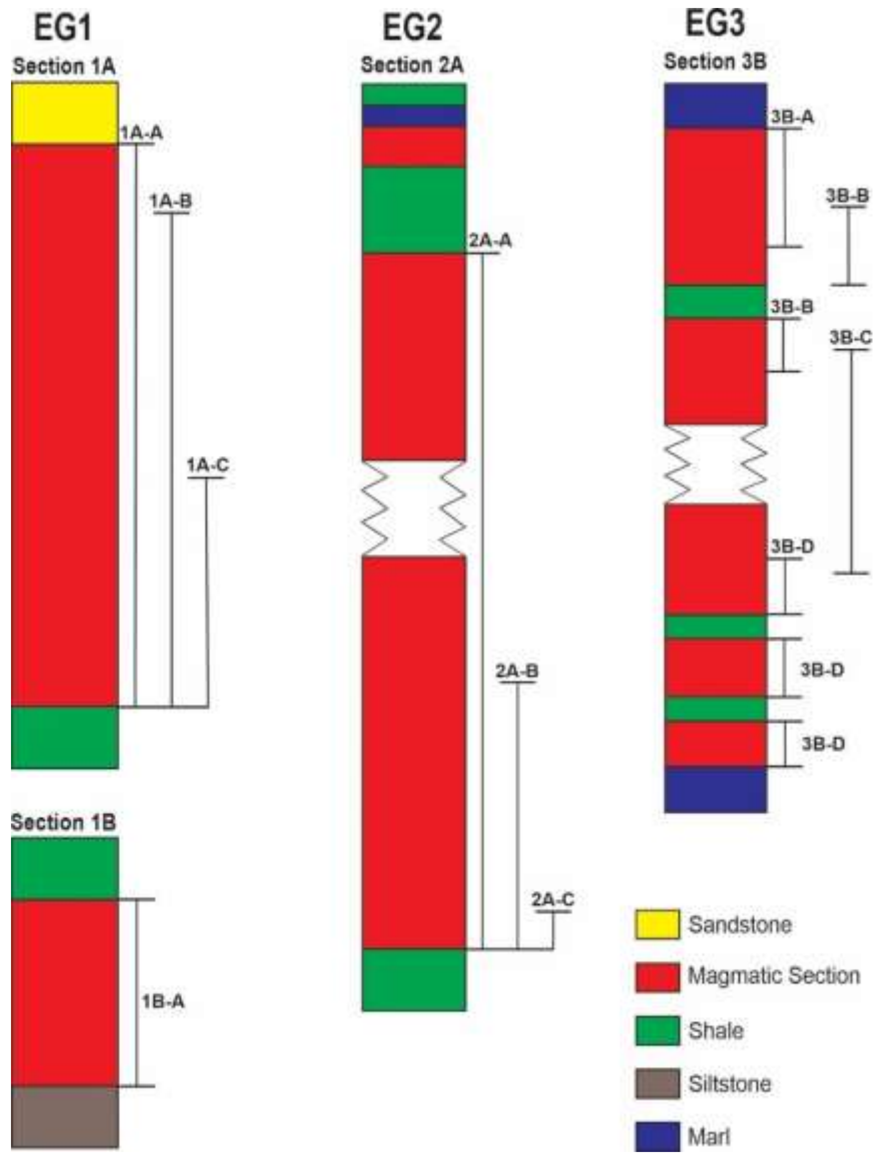

Figure 11. EG1, EG2 and EG3 schematic well profiles, and drill cutting samples magmatic rocks occurrences.

Well EG1

The uppermost and intermediate portions of Section 1A are, as also observed in sidewall samples, mostly tuffaceous sandstones 1A-A samples (**Figure 12A**). These rocks exhibit trachyte lithoclasts, and quartz, biotite, plagioclase and opaque crystalloclasts associated with a micritic matrix. Clasts of altered glass are also present in these samples, as well as rare basalt lithoclasts. Fine-sized lithoclasts and crystalloclasts vary from angular to subangular shape.

Less welded lapilli tuffs (**Figure 12B**) are observed predominantly in the intermediate and lowermost parts of Section 1A. These rocks exhibit the same lithoclasts and crystalloclasts observed in 1A-A. Nevertheless, their igneous components are more abundant than sediments, especially the basalt lithoclasts. Lapilli tuffs rich in basaltic scoria lithoclasts are observed mainly in sections deeper portions. Zeolite and carbonate-filled amygdales are very common and vary from spherical to flat shapes. Olivine fine-grained phenocrysts are replaced by carbonate (**Figure 12C**).

Section 1B consists of a partially altered diabase intrusion. This rock exhibits clinopyroxene phenocrysts and a coarse-to-medium-grained matrix composed of plagioclase, alkali- feldspar, clinopyroxene (augite), analcime, opaque minerals and apatite (**Figure 12D**). Due to size of drill cutting samples, the precise granulometry and intrusive origin of these rocks is difficult to ascertain.

Well EG2

Section 2A is a thick sequence of lapilli tuffs with carbonatic matrix. Lithoclasts consists of porphyritic basaltic scoria (**Figure 12E**) and amygdaloidal basalt (**Figure 12F**). Sample 2A-A basaltic scoria lithoclasts exhibit altered pseudomorphs phenocrysts and, less frequently, more preserved clinopyroxene medium-grained megacrysts. Amygdales are common and predominantly flat, filled with chlorite, carbonate and zeolite. Amygdaloidal basalt lithoclasts exhibits a glassy matrix with very fine-grained pyroxene and carbonate-filled round amygdales.

Pyroxene-phyric basalt 2A-B exhibits an altered matrix with volcanic glass and fine-grained pyroxene, plagioclase and opaque minerals. Pyroxene phenocrysts are mostly altered with very few preserved grains. Amygdales are irregular and filled with carbonate or zeolite (**Figure 12G**). Sample 2A-C consists of scoria lithoclasts observed predominantly on the bottom portion of Section 2A. Amygdales are variable in size but mostly round and filled with carbonate (**Figure 12H**). No mineral was observed among the glassy altered matrix.

Figure 12. Photomicrographs of drill cutting samples from EG1, EG2 and EG3 wells. A) tuffaceous sandstone 1A-A with angular to subangular crystalloclasts (cross-polarized light); B) medium-welded lapilli tuff 1A-B (plane-polarized light); C) pseudomorphs megacrysts in basaltic scoria lithoclast (1A-C). Original mineral was replaced by carbonate (cb) (cross-polarized light); D) altered diabase intrusion in 1B-A sample (cross-polarized light); E) basaltic scoria lithoclasts in 2A-A lapilli tuff (plane-polarized light); F) amygdaloidal basalt lithoclast in 2A-A lapilli tuff (cross-polarized light); G) porphyritic basalt with carbonate-filled amygdales (2A-B) (cross-

polarized light); H) 2A-C scoria sample with carbonate-filled amygdales (plane-polarized light); I) Equigranular basalt 3B-A (cross-polarized light); J) clinopyroxene-phyric basalt in 3B-B sample (cross-polarized light); K) 3B-C sample with partially altered pyroxene phenocryst (plane-polarized light); L) fine-grained matrix in 3B-D sample (plane-polarized light).

Well EG3

Section 3B consists of four volcanic sequences with lapilli tuff, as depicted by the sidewall sample, and basalts, as depicted by drill cutting samples. The top of the section exhibits fine-grained equigranular basalts (**Figure 12I**). These rocks are composed essentially of plagioclase, pyroxene, opaque minerals, apatite and volcanic glass. Few zeolite-filled irregular amygdales are present.

Clinopyroxene-phyric basalt 3B-B (**Figure 12J**) was also observed associated with the first volcanic sequences. They are characterized by coarse-to-medium-grained phenocrysts, and a fine-grained matrix with pyroxene, plagioclase, opaque minerals, apatite and volcanic glass. Alteration is commonly associated with pyroxene grains. Chlorite-filled amygdales are very rare, but always irregular and flat.

Samples 3B-C are recognized as basalts with coarse-grained phenocrysts. Alteration is common in clinopyroxene megacrysts (**Figure 12K**) and in the fine-to-glassy matrix. These rocks occur in the intermediate part of Section 3B.

Another clinopyroxene-phyric basalt occurrence (**Figure 12L**) is described in deeper volcanic sequences of Section 3B. These rocks exhibit a fine-grained matrix composed of clinopyroxene, olivine, plagioclase, opaque minerals and volcanic glass. Alteration is commonly observed associated with glassy portions, pyroxene and olivine grains.

4.5.3 Lithogeochemistry

Studied rocks were geochemically classified based on total alkali *versus* silica (TAS) classification diagram (**Figure 13**). Well EG1 rocks (green color) are classified as trachyte, trachy-andesite, basalt trachy-andesite and basanite-tephrite while EG2 samples (blue color) are classified as basanite-tephrite, basalt and foidite. According to the diagram, well EG3 rocks (red color) are classified as basaltic trachy-andesite, basanite tephrite and basalt.

In Harker diagrams, SiO2, Al2O3, Na2O+K2O, Y, Sm versus MgO (**Figure 14A, B, D, G and H**) and Ti/Y versus Nb/Y (**Figure 15A**) present negative pattern while CaO, Cr, Ni *versus* MgO (**Figure 14C, E and F**) and Nb/Y *versus* Zr/Y (**Figure 15A**) exhibit positive correlation. The square values for the Pearson correlation coefficients (**Schober *et al.,* 2018**) were calculated for both linear $(R2)_L$ and polynomial $(R2)_P$, as well as their respective significance levels (SLL and SLP) for a total of n = 15 samples, with the degree of freedom set as n – 1. Polynomial and linear functions are indicated in diagrams, as well as their respective significance level. As evidenced in both **Figure 14** and **Figure 15**, the absence of compositional hiatus suggests that hybridization or simple assimilation processes did not play a significant role in the evolution of these magmas. The distribution and trends observed in Harker diagrams indicate that possible processes of fractional crystallization or AFC (Assimilation and Fractional Crystallization) might have occurred associated to the studied magmatism. The gaps observed in **Figure 14** are related to reduced sampling. Generally, only in diagrams related to Ni, Y and Sm (**Figure 14C, F, G and H**) it is possible to observe subtly better results in polynomial functions when compared to the linear functions. Nevertheless, it is important to highlight that this situation described above could impact the reliability of interpretation and complex petrogenetic discussions in presented Harker diagrams. **Figure 15A** indicates a negative correlation, suggesting the presence of contamination processes. Nevertheless, the interpretation of this diagram is complicated due to the plot dispersion associated to the low level of significance, probably caused by the problem of sampling hiatus. Conversely, the diagrams presented in **Figure 15B** shows a positive correlation and suggests the absence of contamination processes in the evolution of the studied magmatism.

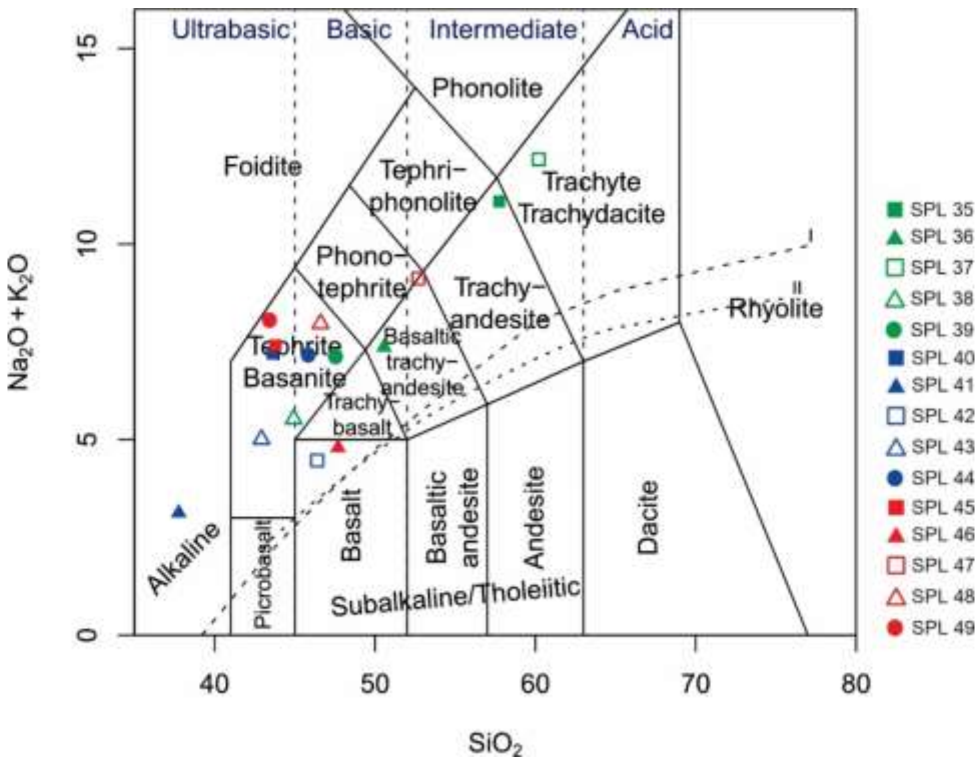

Figure 13. Samples of wells EG1, EG2 and EG3 plotted in the total alkalis versus silica (TAS) classification diagram (**Le Bas et al., 1986**). The subalkaline-alkaline divide curve (dashed line) I is from **Irvine and Baragar (1971)** and II is from **Miyashiro (1978)**. EG1 represented by green symbols, EG2 represented by blue symbols, EG3 represented by red symbols. Values recalculated to 100% on a volatile-free basis.

Taking into consideration the complex geochemistry scenario presented above, it is evident the necessity to elaborate more robust geochemical models. Nevertheless, the generation of new geochemical data, especially isotopic, constitute a step to be carried out in the future.

Petrogenetic discussions and interpretations, mainly involving the behavior of trace elements and rare earths, will be presented separately for each well studied (Wells EG1, EG2 and EG3) below.

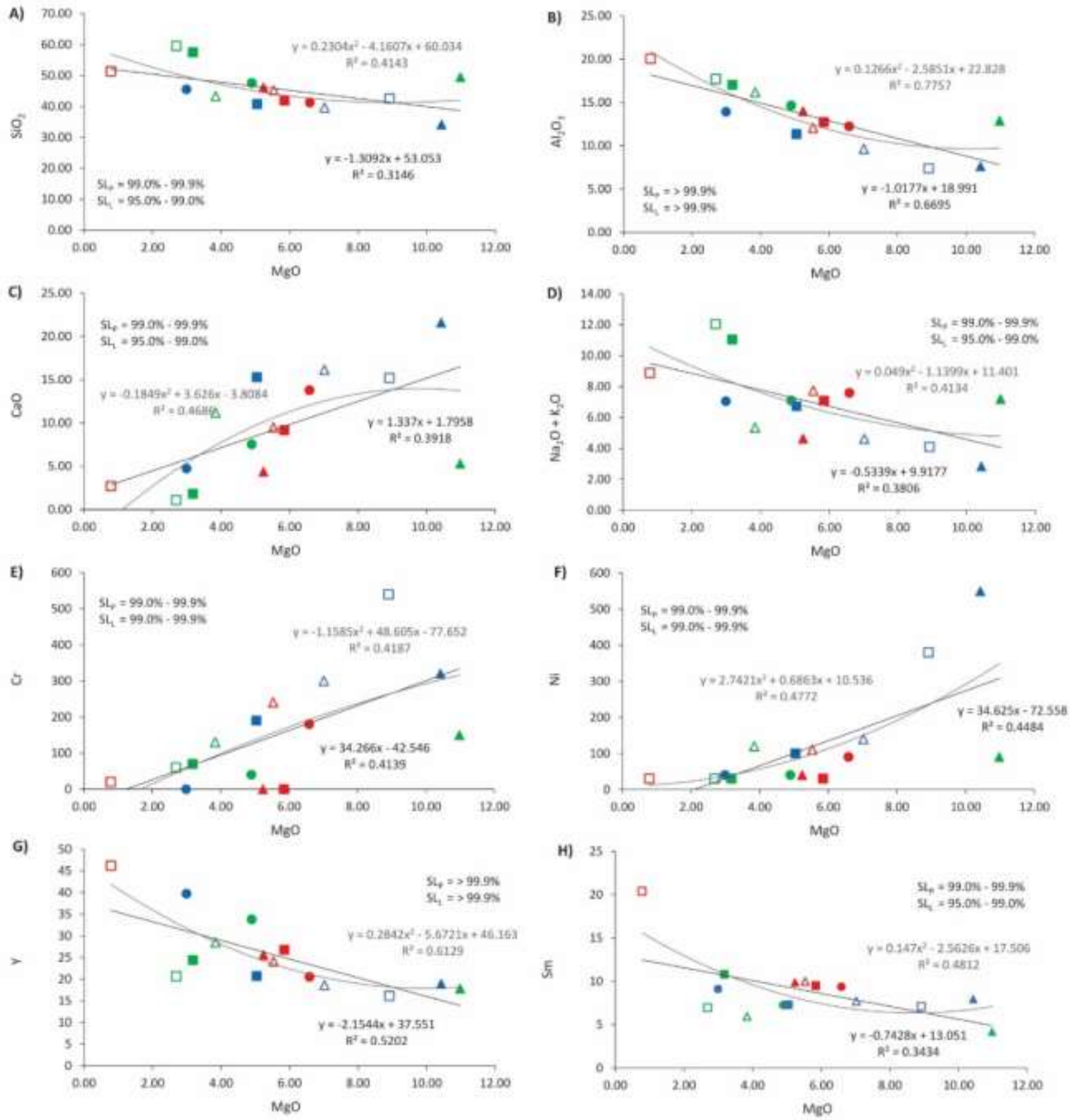

Figure 14. Harker diagrams of major and trace elements for EG1, EG2 and EG3 wells rocks. Samples symbols are same as indicated in figure 11. SLP = polynomial significance level; SLL = linear significance level.

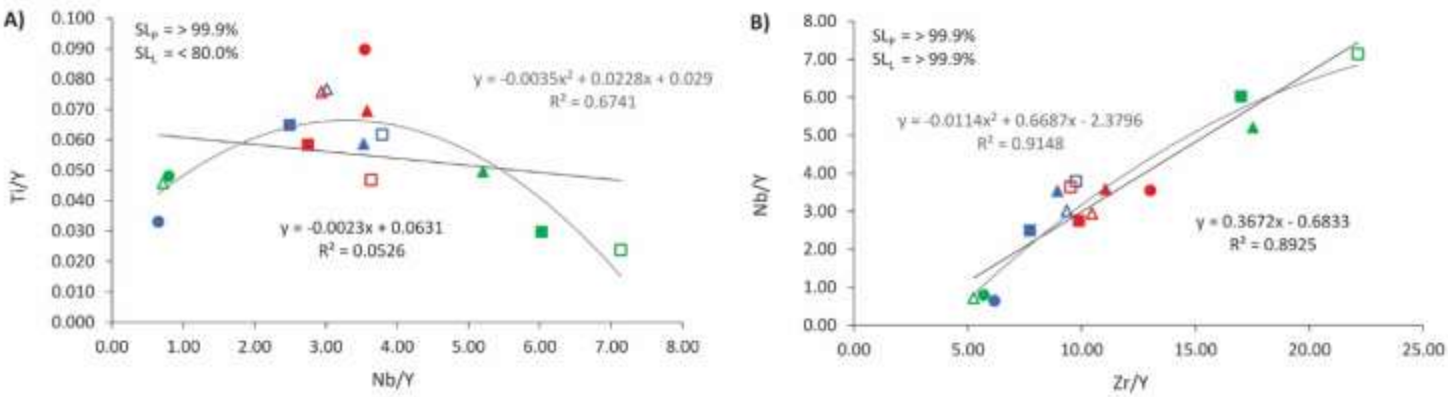

Figure 15. Harker diagrams of Ti/Y x Nb/Y and Nb/Y x Zr/Y for EG1, EG2 and EG3 wells rocks. Samples symbols are same as indicated in figure 11. SLP = polynomial significance level; SLL = linear significance level.

4.5.3.1 Well EG1

Despite some possible mobilization due to alteration, the major and trace element concentrations of the sidewall samples in Well EG1 – Section 1A are likely to represent magmatic compositions. For instance, the lower SiO2 content of sample SPL 36 is largely coherent with its higher contents in MgO and compatible trace elements (Ni, Cr, Sc, Co, and V) and lower contents in incompatible elements (Rb, Sr, Nb, Y, Zr and Hf) when compared with more evolved (silica richer) samples SPL 37 and SPL 35 (**Figure 16**). Samples SPL 35 and SPL 37 with similar SiO_2 contents (respectively, 54.23 and 55.02 wt.%) have also similar concentrations of immobile incompatible trace elements such as Nb (147 ppm), Zr (respectively, 415 ppm and 456 ppm) and Hf (8.6 ppm and 8.5 ppm).

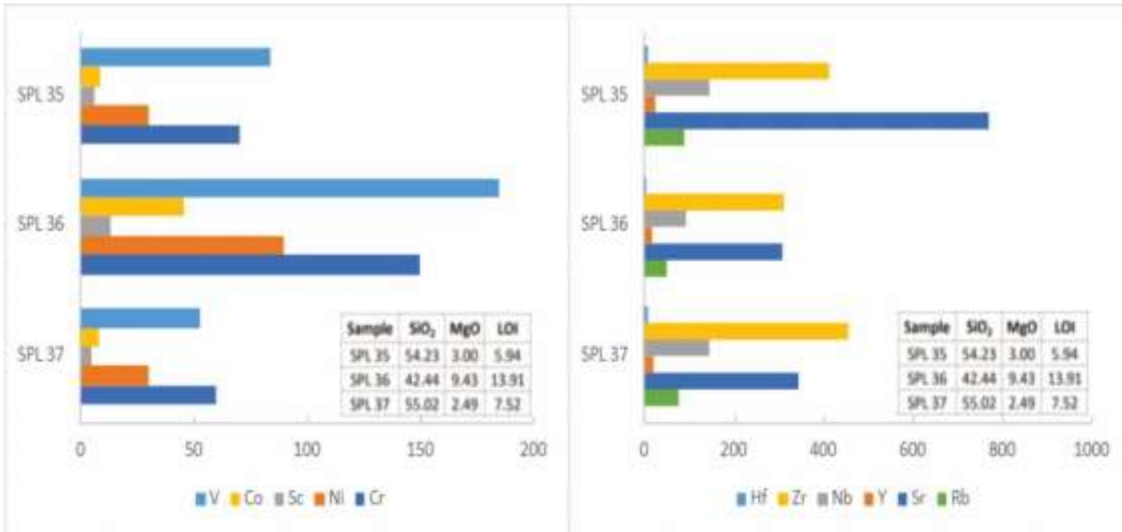

Figure 16. Concentrations (ppm) of selected compatible (Ni, Cr, Sc, Co, V) and incompatible (Hf, Zr, Nb, Y, Sr, Rb) elements of samples SPL 35, SPL 36 and SPL 37 in Well EG1. The SiO2, MgO and LOI contents (in wt.%) of samples are indicated.

In general, the magmatic section 1A represent a sequence of pyroclastic lithic ash tuffs with variable amounts of basalt scoria lithoclasts (more in mid-section; as represented by the least evolved sample SPL 37 and trachyte lithoclasts (towards the top and bottom of section; as represented by samples SPL 35 and SPL 36, respectively).

The pyroclastic tuffs SPL 35 and SPL 37 are intermediate rocks with SiO2 values of 54.23 wt.% and 55.02 wt.%, respectively. Tuff SPL 33 is ultrabasic but the very low values in SiO_2 may also have resulted from some remobilization due to alteration. The tuffs are alkaline (*e.g.* Nb/Y > 0.65; **Pearce and Norry, 1979**) miaskitic (Al/ (Na + K) >1.0, in mol. prop.) rocks and plot as potassic trachyte (SPL 35 and SPL 37) and basaltic trachyandesite (SPL 36) in the total alkalis *versus* silica (TAS) classification diagram (**Figure 13**).

The samples display roughly subparallel patterns in chondrite-normalized multielement diagrams (**Figure 17**). The more evolved samples SPL 35 and SPL 37 are more enriched in trace elements than the least evolved sample SPL 36 as expected if they were to be related by fractional crystallization in subvolcanic magma chambers. Troughs in Sr, P and Ti may be related to fractional crystallization of minor phases, such as apatite and oxides, included in phenocrysts. The existence of carbonate in sample SPL 49 can explain the enriched content of Rb, Sr and K (**Figure 17A, C and E**). Fractional crystallization of amphibole involving the basaltic trachyandesite can explain the concave convex of its REE pattern (**Figure 17B, D and F**). Nevertheless, the cross-cutting patterns of the three tuffs in REE chondrite-normalized diagrams (**Figure 17B and D**) suggest that these rocks possibly have not evolved simply by fractional crystallization (**Brod *et al.*, 2013**) and more complex disequilibrium processes may have occurred in subvolcanic magma chambers (*ie.,* liquid immiscibility).

The patterns of the least evolved tuff (SPL 36) in normalized diagrams (**Figure 17A and B**) are consistent with derivation from fertile, asthenospheric mantle sources based on its $La/Nb_{(N)}$ (< 1, *ie.*, lack of Nb trough) and $La/Yb_{(N)}$ (> 1) ratios. Geochemical modeling was applied to derive possible mantle source compositions of the magmas associated with magmatic section 1A of well EG1. Modeling was done using modal batch melting equations (*e.g.* **Wood and Fraser, 1976**) taking into consideration that alkaline basaltic magmas are derived from low degrees (<11%) of partial melting of lherzolitic mantle sources (*e.g.* **Green, 2015**). Modeling aimed to obtain the $La/Yb_{(N)}$ ratio of the least evolved sample SPL36 in the magmatic section at 10% partial melting of a lherzolitic source with residual Al-rich phase (garnet, spinel, or plagioclase). Results are shown in **Figure 18**.

The $La/Yb_{(N)}$ ratio (~ 12) of typical OIB is just too high to generate the least evolved composition in the magmatic section, considering both the highest and lowest partition coefficients (Kd) values for Yb between garnet and alkaline basaltic magma. One solution for lherzolitic mantle with residual garnet required sources with $La/Yb_{(N)} < 1$ (0.59). However, this solution is unlikely to be applied since such trace element ratio is characteristic of plagioclase-bearing, depleted N-MORB mantle sources. A solution for lherzolitic mantle with residual plagioclase but $La/Yb_{(N)} > 1$ (4.35) is unlikely for similar reason. Possible solutions are either derivation from a more enriched ($La/Yb_{(N)}$ = 4.14) spinel lherzolite residual source or a less enriched ($La/Yb_{(N)}$ = 2.02) garnet lherzolite residual source. The former is consistent with the existence of a strongly attenuated lithosphere at the drifting stage of Campos Basin tectonic evolution.

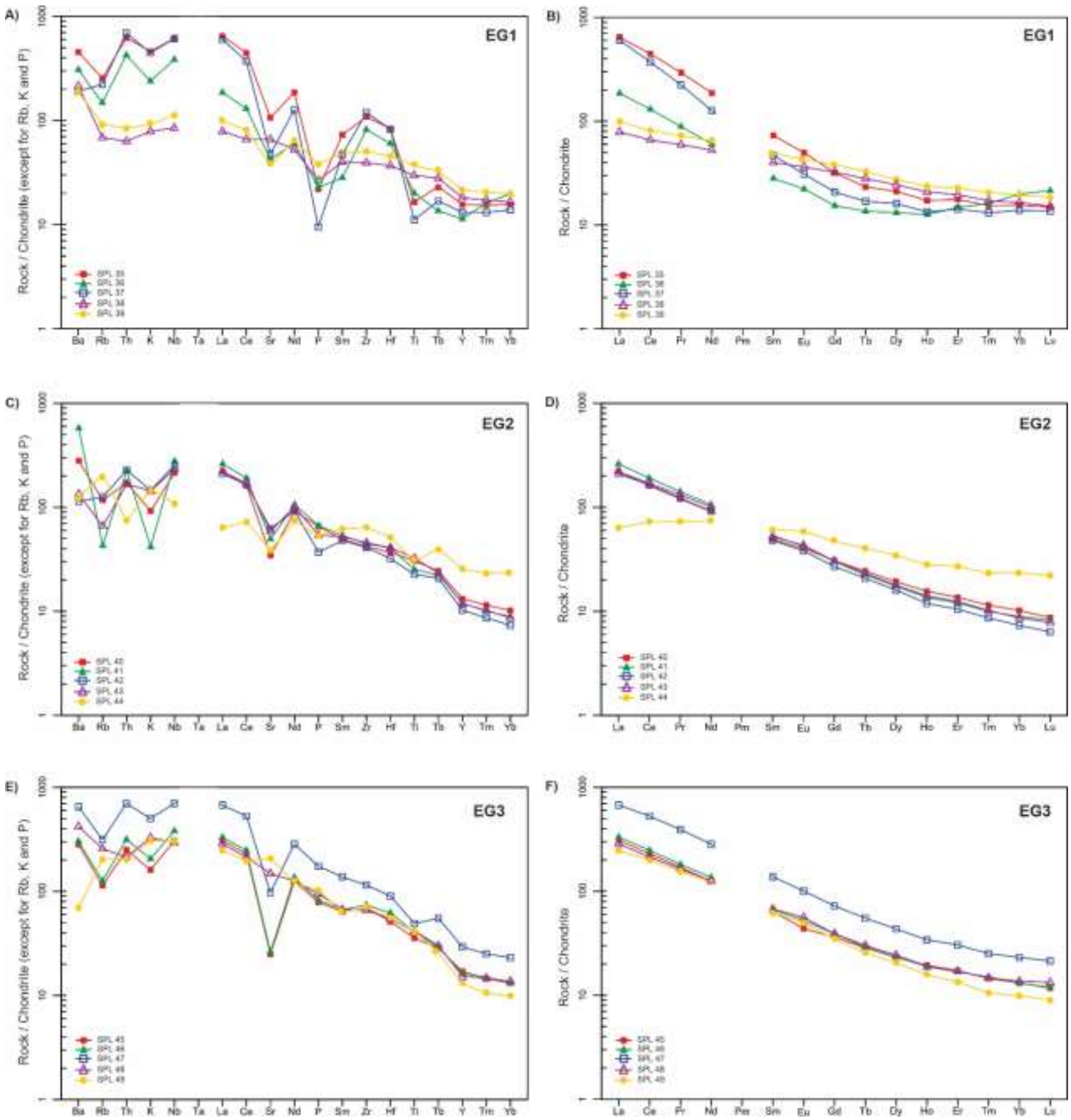

Figure 17. Normalized multielement diagram for samples of magmatic sections of wells EG1 (A), EG2 (C) and EG3 (E). Chondrite normalization factors are from **McDonough and Sun (1995)**. Rb, K and P are from the primitive mantle of Sun (1980); REE chondrite-normalized diagram for samples of magmatic sections of wells EG1 (B), EG2 (D) and EG3 (F). Normalization factors from **McDonough and Sun (1995)**.

In Section 1B, sample SPL 38 is more altered than sample SPL 39 as depicted by their LOI values (15.25 wt.% and 7.57 wt.%, respectively). Both samples are ultrabasic with relatively low

MgO contents (3.29 wt.% and 4.56 wt.%, respectively). They are alkaline (*e.g.* Nb/Y > 0.65; **Pearce and Norry, 1979**) miaskitic (Al/(Na + K) > 1.0, in mol. prop.) rocks and the chemical classification will vary depending on the chosen diagram (**Figure 13 and Figure 19**), possibly because the recalculations required to plot samples in such diagrams are strongly affected by the LOI contents. As such, a classification as alkaline basalts seems appropriate based on immobile trace elements. In general, such classification seems more adequate than the modal classification, implying that samples in section 1B would rather be included in a mildly alkaline magmatic series rather than a strongly undersaturated one.

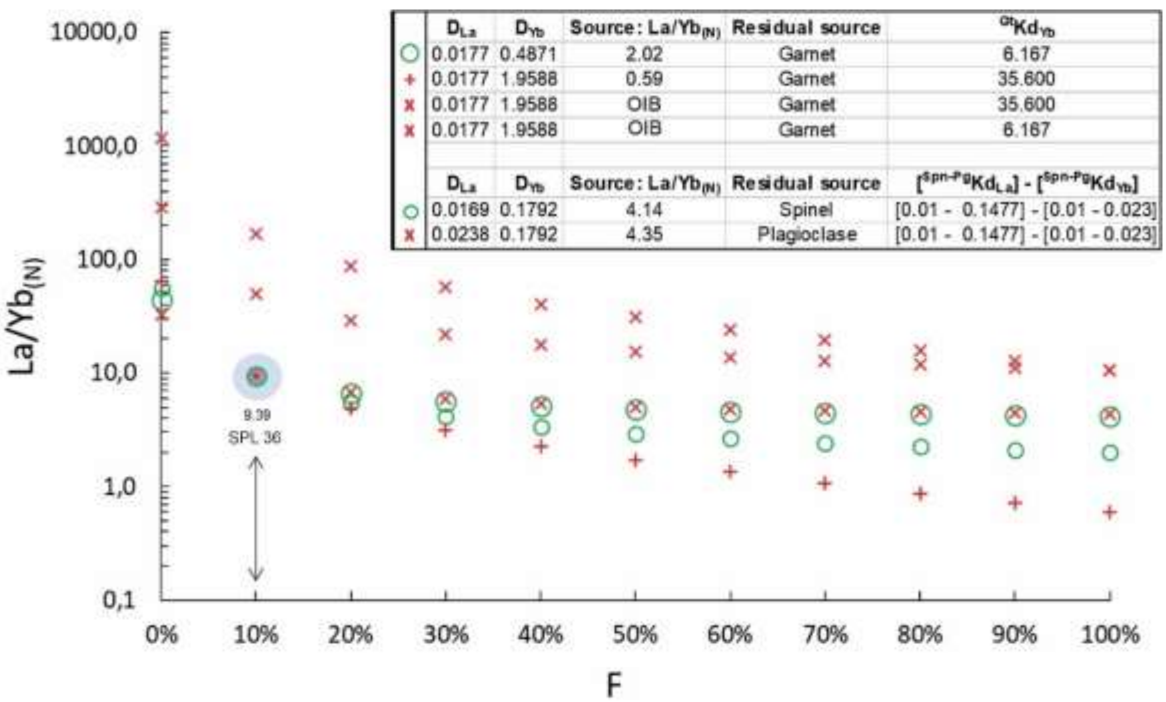

Figure 18. Results of modal batch partial melting modeling for the alkaline magmatism in section 1A of Well EG1. Modal compositions were 60% olivine, 20% orthopyroxene, 15% clinopyroxene and 5% of Al-rich phase (garnet (Gt), spinel (Spn) or plagioclase (Pg)). Partition coefficients (Kd) from table 4.1 in **Rollinson (1993)**. OIB (ocean island basalt; La/Yb(N) ~ 12) composition from **Sun and McDonough (1989)**. Normalization factors from **McDonough and Sun (1995)**. La/Yb(N) of sample SPL 36 / EG1 (9.39, light blue circle) is indicated and can be derived from 10% partial melting. F is the amount of partial melting. La/Yb(N) of required sources are indicated.

Samples display roughly parallel, weakly spiked patterns in chondrite-normalized multi-element diagrams (**Figure 17A**) and REE chondrite-normalized diagrams (**Figure 17B**), being consistent with fractional crystallization. The SiO_2 and MgO values of sample SPL 38 are likely to have been affected by alteration and may not represent magmatic values. The higher contents in immobile incompatible trace elements (*e.g.,* Zr, Hf, Nb, Y, Ti and REE) and lower contents in compatible trace elements (*e.g.,* Ni, Cr and Co) indicate that the mafic rock sample SPL 38 represents the more evolved magma composition. In addition, the similar La/Nb(N), La/Yb(N), $La/Sm_{(N)}$ and $Gd/Lu_{(N)}$ ratios of samples SPL 38 and SPL 39 support a relationship by fractional crystallization.

The patterns of samples SPL 38 and SPL 39 in normalized diagrams (**Figure 17**) are consistent with derivation from fertile, asthenospheric mantle sources based on its $La/Nb_{(N)}$ (<1, *ie.*, lack of Nb trough) and $La/Yb_{(N)}$ (> 1) ratios. The results of the modeling performed for magmatic section 1A can be used to derive possible mantle sources for the magmatic rocks in section 1B. Typical OIB compositions are too enriched in REE (*e.g.,* $La/Yb_{(N)}$ ~ 14) to give rise to least evolved alkaline basalt magmas with $La/Yb_{(N)}$ ~ 5 (**Figure 17B**). The alkaline basalt magmas in section 1B could be related to either a more enriched ($La/Yb_{(N)}$ ~ 2) spinel lherzolite residual source or a less enriched ($La/Yb_{(N)}$ = 1) garnet lherzolite residual source. The former is consistent with the existence of a strongly attenuated lithosphere at the drifting stage of Campos Basin tectonic evolution, similar to the proposed model for section magmatic section 1A.

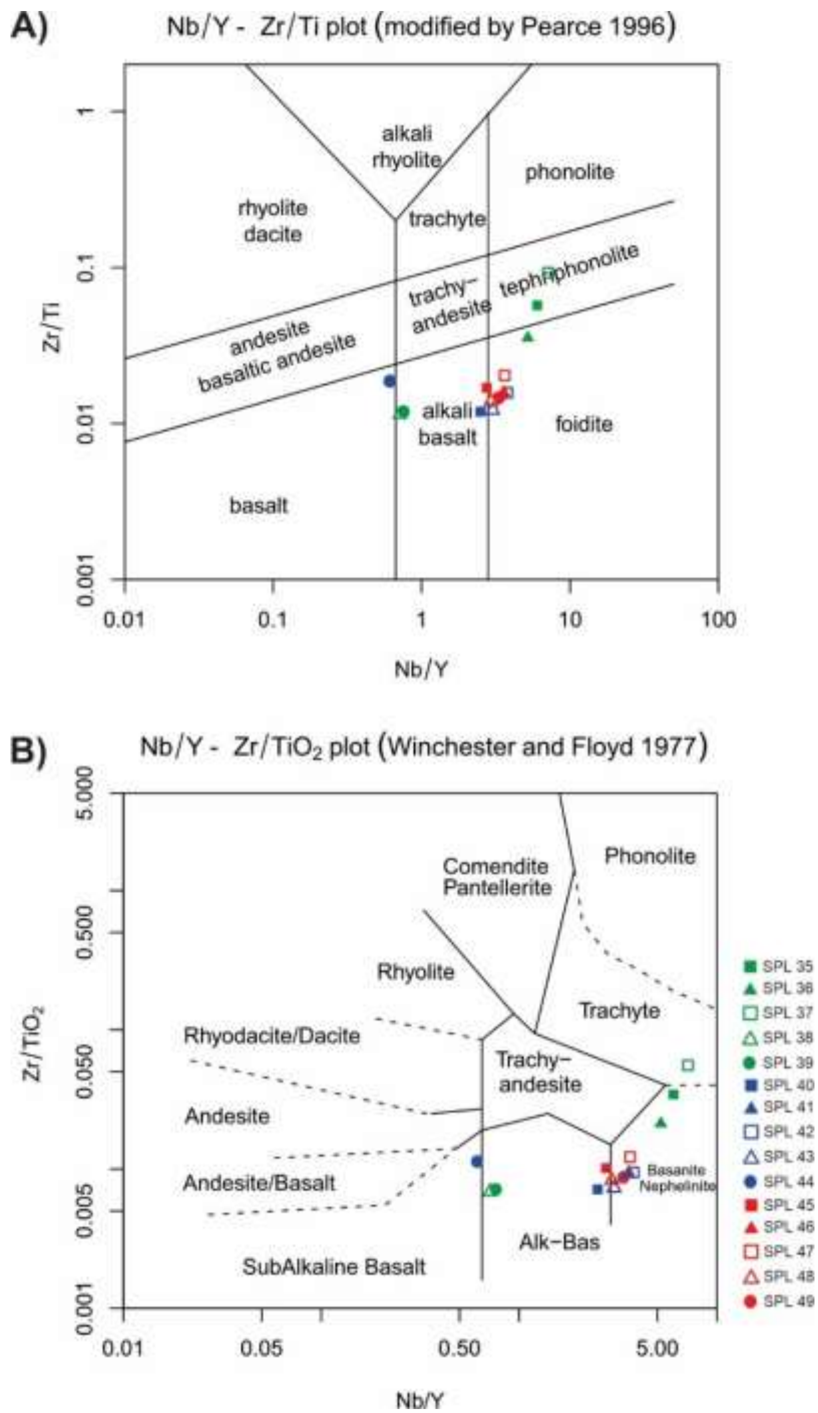

Figure 19. Sidewall core samples of wells EG1, EG2 and EG3 in Campos Basin plotted in classification diagrams based on immobile trace elements. A) Nb/Y versus Zr/Ti diagram (**Pearce and Norry, 1979**); B) Nb/Y versus Zr/TiO_2 diagram (**Winchester and Floyd, 1977**). EG1 represented by green symbols, EG2 represented by blue symbols, EG3 represented by red symbols. Alk-Bas = alkaline basalt.

4.5.3.2 Well EG2

Lithogeochemical data obtained for the five sidewall core samples in magmatic section 2A of Well EG2 indicates that samples are altered as depicted by their high LOI values (> 20 wt.%) and their SiO_2 and MgO contents are unlikely to represent magmatic compositions. Alteration is likely to also have affected the concentrations of mobile trace elements, such as Ba, Sr and Rb. The concentrations of immobile trace elements (Y, Nb, Zr and Hf) are nearly invariable and the concentrations of Ni (100 - 550 ppm) and Cr (190 - 540 ppm) are relatively high and probably reflect the predominantly mafic compositions of the lithic lapilli tuffs in the magmatic section (**Figure 20**). Comparable concentrations of Cr but different concentrations of Ni of samples SPL 41 and SPL 43 could be related to different amounts of clinopyroxene and olivine crystalloclasts in the tuffs, respectively.

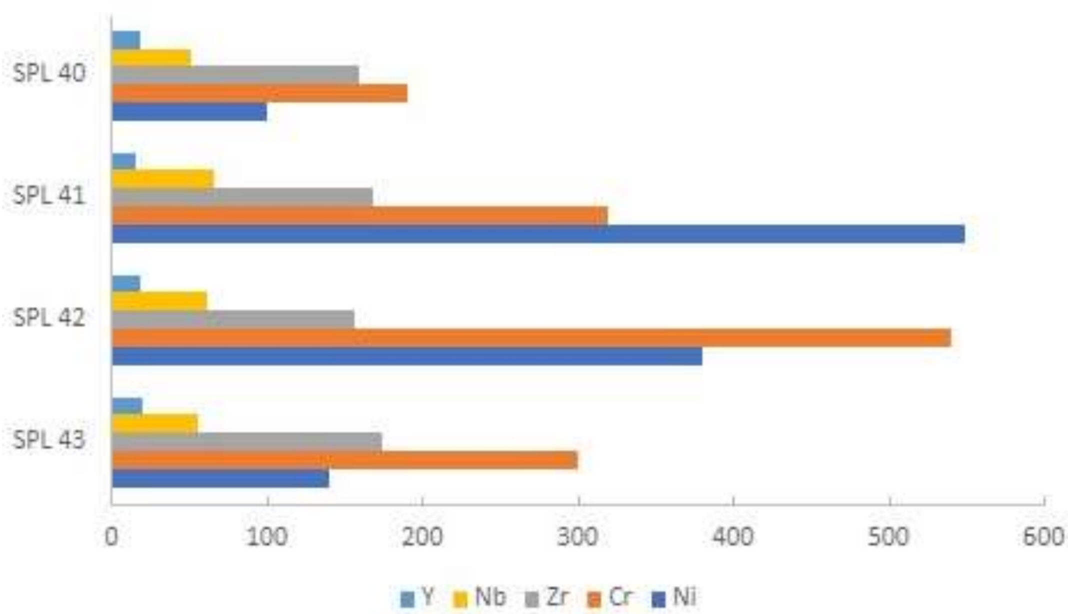

Figure 20. Concentrations (ppm) of selected compatible (Ni and Cr) and incompatible (Y, Nb and Zr) elements of samples SPL 40, SPL 41, SPL 42 and SPL 43 in Well EG2.

Tuffs are mafic, alkaline rocks and plot in the alkaline basalt and foidite fields of the classification diagram based on immobile elements (**Figure 19A**). The similar REE patterns of the four samples are also consistent with a nearly invariable composition of the tuffs (**Figure 17D**).

Selected samples in magmatic section 2A display similar trace element patterns in the normalized multielement diagram (**Figure 17C**). Spiked patterns for mobile trace elements (Ba, Rb, Th, K and Sr) are probably partially related to alteration. Smooth subparallel, almost superimposed patterns for immobile trace elements are consistent with a nearly invariable composition of the tuffs as aforementioned. In general, the immobile trace element compositions of the tuffs attest derivation from the same subvolcanic magma chambers unrelated to prolonged magma differentiation processes.

The $La/Yb_{(N)}$ (>1; **Figure 17D**) and $La/Nb_{(N)}$ (<1; **Figure 17C**) ratios of the tuffs in magmatic section 2A indicate derivation from asthenospheric mantle sources. The $La/Yb_{(N)}$ ratios (~ 22 - 30) of the tuffs cannot be related to derivation from partial melting of typical OIB mantle sources ($La/Yb_{(N)}$ ~ 12) in the garnet stability zone (> 80 km) (**Figure 18**). Derivation from asthenospheric lherzolites in the spinel stability zone (35 - 80 km) requires sources with $La/Yb_{(N)}$ ~ 9. Overall, the results of partial melting modeling indicate that the tuffs in magmatic section 2A of Well EG2 in Campos Basin are related to relatively shallow (35 - 80 km) depths of partial melting of asthenospheric sources.

Partial melting contributions from the enriched subcontinental lithospheric mantle and fertile, either typical OIB or plume-like (*e.g.* Trindade) are unlikely to be related to the studied lithic lapilli tuffs. These results may be related to the existence of a thin lithosphere in Campos Basin at the Santonian-Campanian allowing the uprising asthenosphere to melt at shallow depths. According to the lithogeochemical data obtained for sidewall core SPL 44 (Section 2B), the lithic lapilli tuff is a mafic, alkaline rock and plot in the alkaline basalt field of the classification diagram based on immobile elements (**Figure 19**).

The $La/Nb_{(N)}$ (< 1; **Figure 17C**) and $La/Yb_{(N)}$ (>1; **Figure 17D**) ratios of the tuffs in magmatic section 2B indicate derivation from asthenospheric mantle sources. The $La/Yb_{(N)}$ ratio (2.7) of the tuffs cannot be related to derivation from partial melting of typical OIB mantle sources ($La/Yb_{(N)}$ ~ 12) in the garnet stability zone (> 80 km) (**Figure 18**). Derivation from asthenospheric lherzolites in the spinel stability zone (35 - 80 km) or plagioclase stability zone (< 35 km) require sources with $La/Yb_{(N)}$ ~ 1 - 1.2. Overall, the results of partial melting modeling indicate that the tuffs in magmatic section 2B of Well EG2 in Campos Basin are possibly related to relatively shallow depths of partial melting of asthenospheric sources with the contribution of a more enriched mantle source. Partial melting contributions from the enriched subcontinental lithospheric mantle and fertile, either typical OIB or plume-like (*e.g.*, Trindade) are unlikely to be related to the studied lithic lapilli tuffs. These results may be related to the existence of a thin lithosphere in Campos Basin at the Santonian-Campanian allowing the uprising asthenosphere to melt at shallow depths.

4.5.3.3 Well EG3

Lithogeochemical data obtained for four sidewall core samples in magmatic sections 3A and 3B of Well 3 indicates that the samples are altered as depicted by their high LOI values (11 - 18 wt.%) and are classified mostly as foidites in the classification diagram based on immobile trace elements (**Figure 19A**). Despite their similar classification, ash tuff SPL 47 represents the most evolved composition sampled in the magmatic section (**Figure 21**).

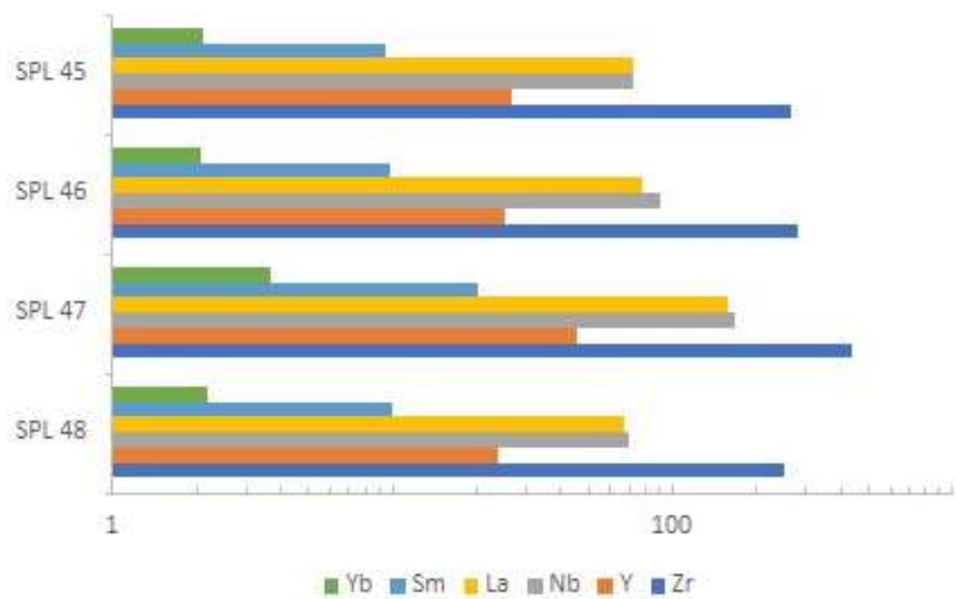

Figure 21. Concentrations (ppm) of selected incompatible, immobile elements of samples SPL 45, SPL 46, SPL 47, and SPL 48 of magmatic section 3A in Well EG3.

The more evolved composition of ash tuff SPL 47 is consistent with its higher values of the REE (**Figure 17F**) and the whole set of trace elements (**Figure 17E**). The little variation in REE ratios indicates that the evolved ash tuff and less evolved basaltic scoria are related by fractional crystallization in subvolcanic magma chambers.

The $La/Yb_{(N)}$ (>1; **Figure 17F**) and $La/Nb_{(N)}$ (≤1; **Figure 17E**) ratios of these samples indicate derivation from asthenospheric mantle sources. The $La/Yb_{(N)}$ ratios (~ 21 - 29) of the samples cannot be related to derivation from partial melting of typical OIB mantle sources (La/Yb(N) ~ 12) in the garnet stability zone (> 80 km) (**Figure 18**). Derivation from asthenospheric lherzolites in the spinel stability zone (35 - 80 km) requires sources with $La/Yb_{(N)}$ ~ 9. Overall, the results of partial melting modeling indicate that the samples in magmatic sections 3A and 3B of Well EG3 in Campos Basin are related to relatively shallow (35 - 80 km) depths of partial melting of asthenospheric sources. Partial melting contributions from the enriched subcontinental lithospheric mantle and fertile, either typical OIB or plumelike (*e.g.*, Trindade) are unlikely to be related to the studied volcanic rocks. These results may be related to the existence of a thin lithosphere in Campos Basin at the Santonian-Campanian allowing the uprising asthenosphere to melt at shallow depths.

Lithogeochemical data obtained for section 3C indicates that sample SPL 49 plots in the foidite field in the classification diagram based on immobile trace elements (**Figure 18A**). The high LOI content of the sample attests to its alteration as also depicted by the petrography.

Sample SPL 49 has $La/Nb_{(N)}$ = 0.8, $La/Yb_{(N)}$ = 25.0, $La/Sm_{(N)}$ = 3.9 and $Gd/Lu_{(N)}$ = 3.9 attesting derivation from asthenospheric mantle sources. Geochemical modeling indicates that partial melting took place in the spinel stability field (35 - 80 km) and involved a source with $La/Yb_{(N)}$ ~ 9.0. This composition is unlikely to be related to contributions from either the subcontinental lithospheric mantle or OIB-like deep mantle components. Overall, the magmatic section 3C of Well EG3 seems related to partial melting of the ascending asthenosphere beneath an attenuated lithosphere in the Santonian-Campanian time. Conclusions related to magmatic section 3C are the same presented previously for magmatic sections 3A and 3B of Well EG3 in Campos Basin.

4.6 Discussion

4.6.1 Well EG1

The following inferences can be made based on the petrographic and lithogeochemical data obtained for Well EG1:

Section 1A is a 66 m thick section formed by lithic ash and lapilli tuffs with variable amounts of basaltic scoria and trachyte lithoclasts. Tuffs are likely to result from bimodal (alkaline basalt-trachyte), mildly alkaline, subaerial explosive volcanism. These pyroclastic rocks represent deposits formed by explosive volcanism from stratovolcanoes in marine environments but high enough to emerge above sea level. Besides that, a little reworking of volcanoclasts took place in a deposition site close to the emission center.

The pyroclastic tuffs are chemically similar to the bentonite thin layers of the 3-Fingers Mark (Marco 3 Dedos) and 3B Mark (Marco 3B). However, section 1A comprises thick (66 m-size) layers of pyroclastic tuff that are neither epiclastic nor related to ash falls. In addition, emission centers seem to be proximal as opposed to those at the continent proposed for the bentonites and ash tuffs elsewhere in Campos.

Explosive eruptions that gave rise to the pyroclastic tuffs in section 1A could have been less energetic (possibly Strombolian or Vulcanian) than the Plinian eruptive styles associated with the bentonites in Campos. Low-magnitude earthquakes and debris flow may be expected to be associated with such explosive eruptions.

Section 1B is a 22 m thick section formed by alkaline diabases that are likely to result from bimodal (alkaline basalt trachyte), mildly alkaline magmatism.

The intrusive or effusive type of magmatism is difficult to ascertain based on well data, petrography and lithogeochemistry.

However, the viscosity of alkaline basaltic lava flows is low enough to allow spreading over relatively large areas from the emission center. Such flows would easily reach the subaqueous depositional environment of the sedimentary rocks of the Campos Group, but no textures indicative of subaqueous volcanism have been observed in the studied samples.

Samples of diabases also display little amounts of glass and are medium-to-coarse-grained, as opposed to glass-rich, very fine-grained textures found in typical basaltic flows. Altogether, the alkaline samples in magmatic section 1B are likely to represent either a chemically differentiated, single or multiple magmatic intrusions. If the magmatic section represents multiple intrusions, the alkaline diabases would be magmas associated with fractional crystallization in shallow, subvolcanic magma chambers.

Partial melting processes in both sections involved asthenospheric mantle sources and took place in depths either related to stable garnet (> 80 km) or stable spinel (35 - 80 km). It is unlikely that the precursor alkaline magmas related to the samples can be associated exclusively with either typical OIB or MORB asthenospheric mantle sources. Derivation from spinel-bearing lherzolitic asthenospheric sources could be related to the existence of an attenuated lithosphere during the drifting stage of Campos Basin.

The following conclusions can be made for the drift-related magmatism recorded in Well EG1 based on the aforementioned interpretations of the petrological data of magmatic sections 1A and 1B:

1. It represents a mildly alkaline, miaskitic series whose either spinel- or garnet-lherzolite mantle sources are less enriched in trace incompatible elements than typical OIB.

2. The pyroclastic tuffs interbedded with the siliciclastic sedimentary rocks of the Campos Group cannot be associated with the typical bentonites and ash falls of the 3-Fingers and 3B-Marks in Campos Basin. They represent the products of subaerial, Strombolian to Vulcanian explosions of high-standing stratovolcanoes that emerged above sea level. The pyroclastics underwent restricted transport from the emission center.

3. The alkaline diabases occur possibly as sills and intrude the shallow marine shales and marls of the Ubatuba Formation. Major temperature increments that might have affected potential petroleum systems due to this intrusion would be relevant for marls and shales at 50 m or less above and below the intrusion.

4.6.2 Well EG2

The following conclusions can be made based on the petrographic and lithogeochemical data obtained for Well EG2:

Both sections 2A (483.5 m thick) and 2B (54 m thick) are lithic lapilli tuffs. These rocks are probably related to low-intensity, subaqueous explosive eruptions (phreatomagmatism) from monogenetic, small scoria cones. Monogenetic, small scoria cones are the most common volcanic edifices associated with basaltic scoria and usually occur in clusters. Brittle structures such as normal and listric faults can be found at the base of scoria cones since they are commonly subjected to subsidence.

Tuffs have nearly invariable trace element compositions predominantly mafic, alkaline rocks. As such, no or limited differentiation process in either deep-seated or subvolcanic magma chambers and pumbling systems is expected and heat conduction to upper levels should be negligible. Hydrothermal processes may have occurred due to interactions of erupted lavas and shallow marine waters.

In both sections, partial melting processes involved asthenospheric mantle sources in the spinel or plagioclase stability zone (< 35 - 80 km) and are unlikely to have involved only the subcontinental lithospheric mantle (SCLM) and either typical OIB or plume-like mantle components.

4.6.3 Well EG3

The following conclusions can be made based on the petrographic and lithogeochemical data obtained for magmatic sections 3A, 3B and 3C of Well EG:

They comprise various occurrences of magmatic rocks interlayered with the sedimentary rocks of the Ubatuba Formation. Magmatic occurrences vary from 1 m to 168 m in thickness.

Basaltic scoria, ash tuff, lapilli tuff and alkaline basalt were sampled along the magmatic sections. They represent extrusive and pyroclastic deposits predominantly less welded and mafic but also more welded, more evolved ash tuffs. These rocks are related to subaerial explosive eruptions from stratovolcanoes that may grow above sea level in marine environments.

Variations in trace element compositions indicate that less and more evolved rocks can be related by fractional crystallization in subvolcanic magma chambers and related pumbling systems. As such, heat conduction to upper levels may be expected. Hydrothermal processes may have been restricted due to the predominantly mafic composition of the lavas.

Partial melting processes involved asthenospheric mantle sources in the spinel or plagioclase stability zone (< 35 - 80 km) and are unlikely to have involved only the subcontinental lithospheric mantle and either typical OIB or plume-like mantle components.

4.7 Conclusion

4.7.1 The drift-related magmatism in Cabo Frio High area

The interpretation of well-log, petrographic and lithogeochemical data obtained for magmatic sections located above the salt sequence in wells EG1, EG2 and EG3 were previously presented in this paper. Even before any geochronological data can be obtained, we can infer that the magmatic rocks are taken as representative of the drift-related, Santonian-Campanian magmatism in Campos Basin (**Winter *et al.*, 2007**). The magmatic sections comprised volcanic rocks, diabases, and phaneritic, massive igneous rocks according to well profiles. Rock classifications were fined based on petrographic descriptions under macro and microscales (**Table 4**).

Table 4. Classification of rocks in magmatic sections studied.

Well	Section	Well profile	Petrography
EG1	1A	Dark grey, massive volcanic rock	Lithic, ash and lapilli tuffs
EG1	1B	Grey diabase	Alkaline diabase
EG2	2A	Volcanic rock.	Lithic lapilli tuffs.
EG2	2B	Grey diabase	Lithic lapilli tuffs
EG3	3A	Volcanic Rock	- Highly vesiculated, less massive basaltic scoria - Less vesiculated, more massive basaltic scoria - Highly vesiculated, less massive basaltic scoria - Welded ash tuff
EG3	3B	Volcanic Rock	- Welded Lapilli tuff - Alkaline Basalt
EG3	3C	Diabase	Welded lapilli tuff

The following conclusions can be made so far about the drift-related magmatism in the study area based on the interpretation of the petrological data:

1. It is mostly explosive and volcanic. The only intrusion (alkaline diabase) was found in magmatic section 1B of well EG1.

2. Volcanic edifices in marine environments are: a) composite stratovolcanoes high enough to stand above sea level giving rise to subaerial explosive and effusive eruptions; b) small, monogenetic scoria cones either parasitic in stratovolcanoes or below sea water. 3. It is alkaline and includes mostly mafic rocks (alkaline basalt, basanite/nephelinite and foidite) with subordinate felsic rocks (tephriphonolite, trachyte) (**Figure 19**).

4. Heat conduction due to magmatic differentiation in subvolcanic magma chambers and related pumbling systems is minimum. Heat due to sill intrusion in EG1 has not been conducted beyond about 50 m away from the contacts.

5. Hydrothermal processes may have been relevant in areas with scoria cones due to interactions with seawater and not because of the composition of the magmas, which are represented by mafic, dry alkaline basalts, basanites and foidites.

A main discussion on the drift-related (or post-breakup) magmatism in sedimentary basins offshore Brazil (Campos included) refers to thermal regimes associated with partial melting processes in the underlain mantle. It is an obvious issue to be addressed since heat is fundamental for hydrocarbon generation in these basins, also affecting the quality of potential reservoirs due to associated hydrothermalism. The usual petrological approach to assess partial melting regimes in the mantle is to use the composition of the least evolved rocks. The trace element ratios and isotope compositions of these rocks are the closest representation of the composition of their mantle sources. Differentiation indexes, such as MgO and SiO_2, can be used to select the least evolved compositions in a set of samples. However, these major elements can change due to alteration, and this seems to be the case for most of the samples in the studied area, whose LOI contents vary from 6 wt.% to 26 wt.%. On the other hand, immobile trace elements such as Zr, Y, Nb and Ti are likely to represent magmatic compositions even in altered samples. These elements are also incompatible during crystal-liquid equilibria processes, such as partial melting, meaning that their concentrations will be the lowest in the least evolved samples. Selected trace elements and LOI concentrations for sidewall core samples in the wells of Campos Basin are listed in **Table 5**.

Table 5. Selected lithogeochemical data of sidewall core samples with different alteration degrees in the studied magmatic sections. LOI in wt.%. Trace elements in ppm. Normalization factors (N) used for trace element ratios are from **McDonough and Sun (1995).**

Wells	Samples	LOI	Ni	Cr	Zr	Y	Nb	Hf	La	Yb	$La/Nb_{(N)}$	$La/Nb_{(N)}$
EG1	SPL 35	5.94	30	70	415	24.4	147	8.6	153	2.5	1.05	41.6
EG3	SPL 47	11.21	30	20	440	46.2	168	9.3	160	3.72	0.96	29.2
EG1	SPL 38	15.25	120	130	150	28.5	20	3.8	18.7	2.66	0.93	4.8
EG2	SPL 41	23.27	550	320	169	18.9	67	4.2	61.8	1.44	0.94	29.2

Sample SPL 35 in well EG1 has the lowest LOI concentration among all sidewall core samples in the studied area. It has high concentrations in Zr, Y, Nb, Hf, La and Yb, and low concentrations in Ni and Cr as would be expected from more evolved magmatic compositions. Sample SPL 47 in well EG3 also has high and low concentrations in incompatible and compatible trace elements, respectively, despite its higher LOI content. On the other hand, sample SPL 38 in well EG1 with high LOI has low and high concentrations in incompatible and compatible trace elements which is consistent with a less evolved magmatic composition. The same applies to sample SPL 41 in well EG2 with much higher LOI contents. Thus, the sample that is more likely to represent trace element ratios compositions of its respective mantle source would be SPL 38, based on its relatively low LOI concentrations, as well as low concentrations in incompatible elements and high concentrations in compatible elements (**Table 5**). This sample was taken from a 22 m thick intrusion of alkaline diabase (**Table 4**) and its composition may have been less affected by the complex differentiation processes that usually take place in subvolcanic magma chambers. On the other hand, sample SPL 41 in well EG2 is a lithic lapilli tuff (**Table 1**) with high LOI contents (**Table 5**) that has been associated with subaqueous explosive volcanism (**Table 5**). However, this sample presents no evidence for changes in REE concentrations due to interactions with seawater such as Ce anomalies, for instance, and its composition may truly reflect those of its respective mantle source. Thus, it is note worthing that the $La/Yb_{(N)}$ ratios of samples SPL 38 and SPL 41 have a 6-fold difference (**Table 5**). Despite differences, the $La/Yb_{(N)}$ and $La/Nb_{(N)}$ ratios of samples SPL 38 and SPL 41, respectively above and below the unity (**Table 5**) cannot be explained by derivation from asthenospheric, shallow, depleted, MORB-like mantle sources ($La/Yb_{(N)} < 1$), but are typical of OIB-like, asthenospheric sources ($La/Yb_{(N)} = 11.6$; $La/Nb_{(N)} = 0.78$, (**McDonough and Sun, 1989**). There is much discussion in the literature about the mantle components involved in OIB-like sources regarding origins in the fertile (incompatible element-rich) deep mantle (such as mantle plumes) or shallow but equally fertile mantle depths. In addition, the involvement of the subcontinental lithospheric mantle source (typically $La/Nb_{(N)} > 1$) would easily produce $La/Nb_{(N)}$ ratios below unit, even considering binary mixing processes with fertile, deep OIB-like mantle components.

The cross-cutting REE patterns of samples SPL 38 and SPL 41 (**Figure 22**) cannot be explained by different amounts of partial melting from the same mantle source. Therefore, either one or both of them do not represent their mantle sources compositions for being changed during differentiation or they are related to derivation from different mantle sources. The latter being true, the higher normalized REE ratios of sample SPL 41 implies partial melting of a more enriched mantle source than the one melted to give rise to sample SPL 38.

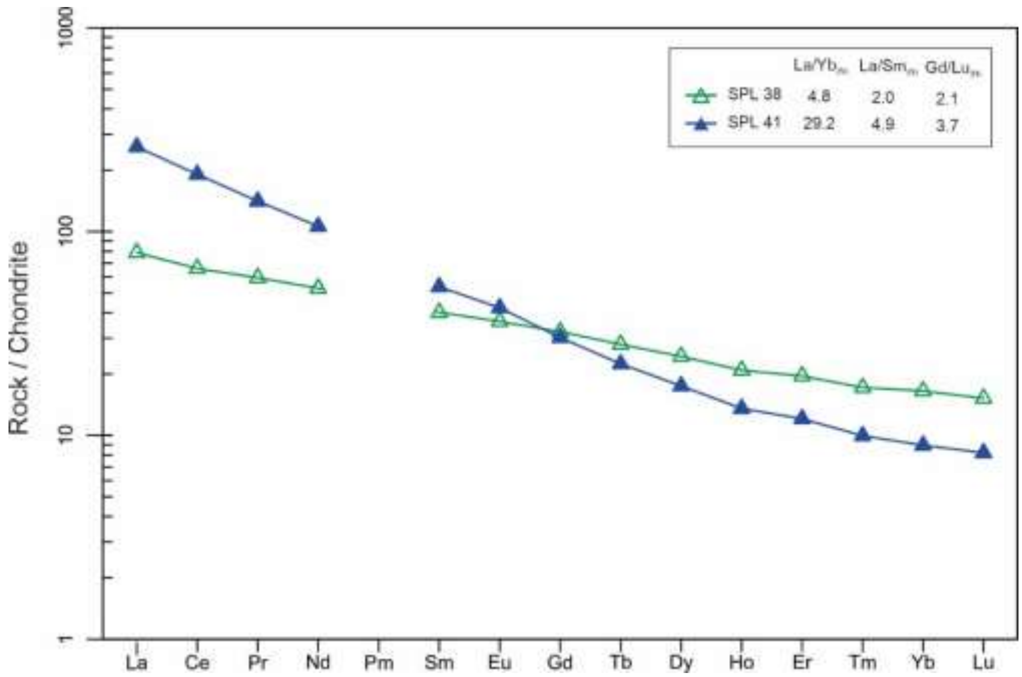

Figure 22. REE chondrite-normalized diagram for samples SPL 38 and SPL 41 in Campos Basin. Normalization factors from **McDonough and Sun (1995)**. Wells and selected trace element ratios are indicated.

Alkaline basalts and basanites primary melts derived from 1 - 11% partial melting of lherzolites according to experimental petrology studies. Lherzolites are peridotites with high amounts of olivine (generally, > 50%), more clinopyroxene than orthopyroxene and about 5-10% of an Al-rich phase that can be plagioclase (< 35 km), spinel (35 - 80 km) or garnet (> 80 km). The low degree of partial melting (< 11%) to generate alkaline basalts implies that it is likely that the Al-rich phase will not melt completely and will remain as a residual phase in the melted lherzolite. In other words, melting is likely to be modal, *ie.* the proportions between phases in the melted lherzolite will be very similar to that in the original lherzolite. In addition, the segregation of melts from the source will not be instantaneous, meaning that partial melting will occur in equilibrium as opposed to fractional.

Modeling of modal batch (equilibrium) melting was elaborated in order to test for possible mantle sources and depths of melting capable of explaining the La/Yb$_{(N)}$ ratios of samples SPL 38 and SPL 41 of wells EG1 and EG2 in Campos Basin and results are shown in **Figure 23**.

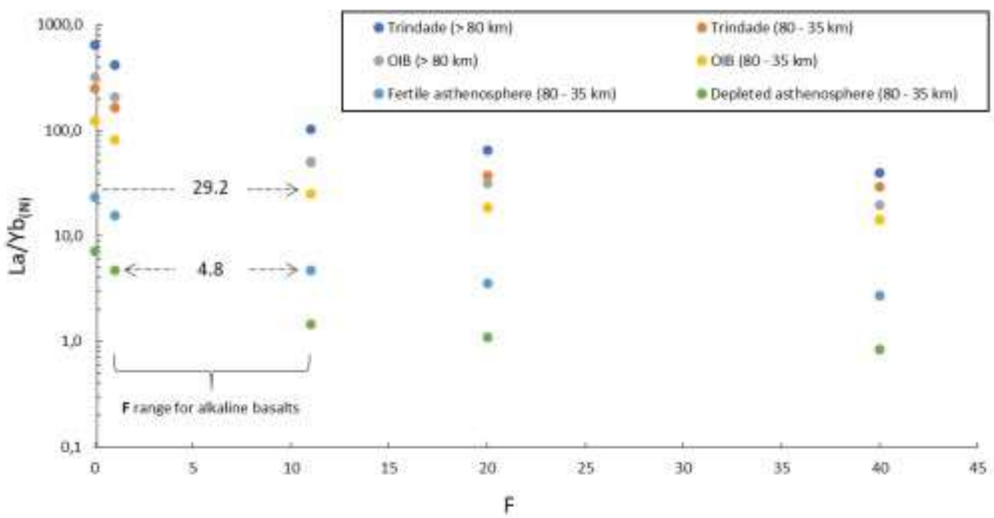

	Depth of melting (km) > 80	Depth of melting (km) 80-35	Depth of melting > 80	Depth of melting 80-35	Depth of melting 80-35	Depth of melting 80-35
	Residual phase Garnet	Residual phase Spinel	Residual phase Garnet	Residual phase Spinel	Residual phase Spinel	Residual phase Spinel
	La/Yb$_{(N)}$ - Trindade 23.5	La/Yb$_{(N)}$ - Trindade 23.5	La/Yb$_{(N)}$ - OIB 11.6	La/Yb$_{(N)}$ - OIB 11.6	La/Yb$_{(N)}$ 2.2	La/Yb$_{(N)}$ 0.7
F (%)	La/Yb$_{(N)}$ - melt	La/Yb$_{(N)}$ - melt	La/Yb$_{(N)}$ - melt	La/Yb$_{(N)}$ - melt	La/Yb$_{(N)}$ - melt	La/Yb$_{(N)}$ - melt
0	644.3	248.3	317.5	122.4	23.4	7.2
1	**418.9**	**164.2**	**206.4**	**80.9**	**15.5**	**4.8**
11	**101.3**	**50.5**	**49.9**	**24.9**	**4.8**	**1.5**
20	64.5	37.7	31.8	18.6	3.6	1.1
40	39.5	29.0	19.5	14.3	2.7	0.8

Figure 23. Results of geochemical modeling of modal batch partial melting process related to the drift magmatism in Campos Basin. See **Wood and Fraser (1976)** and references therein for equations and fundamentals. Trindade data from **Siebel *et al.* (2000)**. OIB data from **McDonough and Sun (1989)**. F is the degree of partial melting (in %). Normalization factors (N) from **McDonough and Sun (1995)**. The La/Yb$_{(N)}$ ratios of samples SPL 38 (4.9) and SPL 41 (29.2) are indicated by dashed arrows.

Results indicate that melting of typical OIB and Trindade plume at depths below 80 km (garnet stability zone) cannot explain neither the low nor the high La/Yb$_{(N)}$ ratios of the sidewall core samples. Melting of OIB-like mantle sources can explain the high La/Yb$_{(N)}$ ratio of sample SPL 41 but much less enriched asthenospheric sources (La/Yb$_{(N)}$ = 2.2) would be required to explain the composition of sample SPL 38. Finally, although a typical, N-MORB mantle source could generate the low La/Yb$_{(N)}$ ratio of sample SPL 38 it can hardly explain the La/Nb$_{(N)}$ ratio (< 1) of the studied samples.

The results of the geochemical modeling and the lithogeochemical data allow inferring that the studied drift magmatism in Campos is related to shallow (35 - 80 km) mantle depths of partial melting. The process seems not to have involved the subcontinental lithospheric mantle, implying the presence of an attenuated lithosphere that allowed the uprising of the underlying asthenosphere. This asthenosphere was neither exclusively depleted (N-MORB type) nor only very enriched (OIB-like of Trindade plume-like). As such, mantle temperatures can be taken as "normal" (~ 1325 - 1430°C; Green, 2015) as opposed to higher temperatures proposed for mantle plume-related magmatism (~ 300°C higher than surrounding mantle; **White and McKenzie, 1989; Campbell, 2007; Spice *et al.*, 2016**).

Once lithogeochemical compositions of the studied samples in wells EG1, EG2 and EG3 cannot be attributed to derivation from partial melting of a single mantle source, mixing processes were then taken into consideration.

Incompatible, immobile trace element ratios of major mantle sources and samples SPL 38, SPL 41 are listed in **Table 6**. References for N-MORB, OIB, Trindade Plume and SCLM are listed. The trace element ratios of samples SPL 38 and SPL 41 were taken as representative of the less and more enriched mantle sources below wells EG1 and EG2, respectively. They have trace element ratios that may reach a 6-fold difference (e.g. La/Yb$_{(N)}$), likely to represent the involvement of compositionally different mantle sources in their petrogenesis (**Figure 24A**).

Table 6. Incompatible, immobile trace element ratios (La/Y and Zr/Nb) of major mantle sources and samples SPL 41 and SPL 38. SCLM1 to SCLM4 are taken as potential representative compositions of the subcontinental lithospheric mantle near studied area.

Reference	Source	La/Y	Zr/Nb
Sun & McDonough, 1989	NMORB	0.1	31.8
Sun & McDonough, 1989	OIB	1.3	5.8
Basanite dyke 10764 (Siebel *et al.*, 2000)	Trindade	2.5	2.3
Lamproite (Rock, 1991)	SCLM1	15.5	8.6
Average lamprophyres SP (Valente, 1997)	SCLM2	2.1	4.3
Average lamprophyres RJ (Valente, 1997)	SCLM3	2.5	1.8

Average lamprophyres Cabo Frio High (Valente, 1997)	SCLM4	4.1	3.4
Composition	**Sample**	**La/Y**	**Zr/Nb**
Less enriched	SPL 38	0.7	7.5
More enriched	SPL 41	3.3	2.5

The analytical mixing model presented below was constrained using the equations presented in **Faure (1994)**. Element ratios of four immobile, incompatible trace elements (La, Y, Zr and Nb) were used in the modelling. The aim of the model is to discriminate two mantle source end members whose mixing can explain the less and more enriched trace element ratios of samples SPL 38 (well EG1) and SPL 41 (well EG2).

Mixing between fertile mantle sources, such as OIB and the Trindade mantle-plume and between them and enriched mantle sources (SCLM1 to SCLM4) are unsuitable to produce mixing curves capable of fitting the compositions of either sample SPL 41 or SPL 38 or even both, as can be depicted by the compositions of these sources in table 3. Particularly, the La/Y ratio (0.7) of the less enriched sample SPL 38 requires the involvement of a depleted mantle source, such as N-MORB, in the mixing process. On the other hand, OIB and Trindade mantle plume compositions are just not enriched enough to produce the enriched trace element ratios of sample SPL 41 when mixed with N-MORB. Therefore, the likely end members in the mixing process would be N-MORB and the SCLM.

The SCLM is probably the most heterogeneous of mantle sources since it is attached to the continental crust throughout geological time. As such, it is difficult to constrain its chemical compositions. However, ultrapotassic-potassic, ultramafic, ultrabasic-basic rocks, such as lamproites and lamprophyres, are probably the best representative of the SCLM compositions, according to many authors (e.g. **Rock, 1991**).

The binary mixing model presented below was done considering 4 possible compositions to represent the SCLM underneath the studied area (**Table 6**). SCLM1 is an average lamproite composition (**Rock, 1991**) whereas the other are average compositions of lamprophyres in São Paulo coastline (SCLM2), Rio de Janeiro coastline (SCLM3) and in Atalaia Peninsula (SCLM4). The Atalaia Peninsula area is taken as the onshore representation of the Cabo Frio Structural High between Campos and Santos basins, close to which studied wells are located offshore. Results of the mixing model are presented in **Figure 24A**.

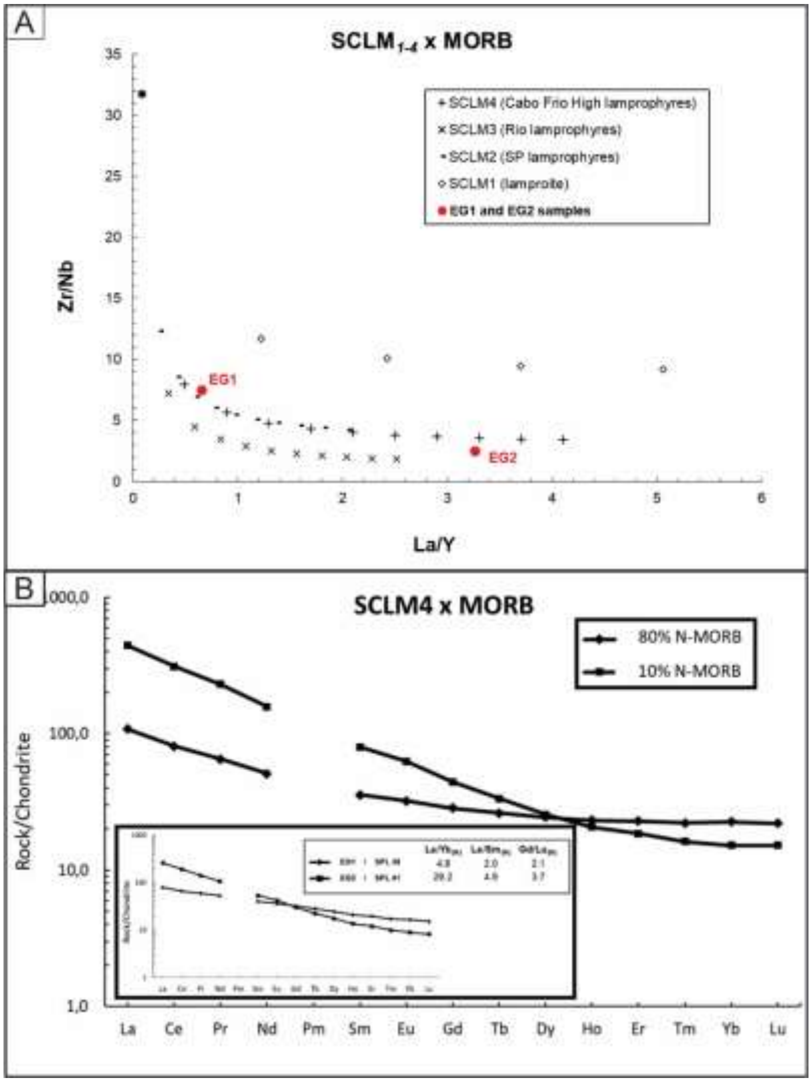

Figure 24. A) results of binary mixing analytical modelling between potential mantle sources. Mixing curves (diamond; cross; dash; x) at 10% intervals between N-MORB and four different subcontinental lithospheric mantle compositions (SCLM1 to SCLM4). Samples SPL 38 (less enriched) and SPL 41 (more enriched) from wells EG2 and EG3, respectively, are also plotted in the diagram. Source and sample compositions are shown in table 3; B) results of binary mixing analytical modelling between N-MORB and SCLM4.

The binary mixing model presented below was done considering 4 possible compositions to represent the SCLM underneath the studied area (**Table 6**). SCLM1 is an average lamproite composition (**Rock, 1991**) whereas the other are average compositions of lamprophyres in São

Paulo coastline (SCLM2), Rio de Janeiro coastline (SCLM3) and in Atalaia Peninsula (SCLM4). The Atalaia Peninsula area is taken as the onshore representation of the Cabo Frio Structural High between Campos and Santos basins, close to which studied wells are located offshore. Results of the mixing model are presented in figure 21A.

The SCLM1 composition is too enriched and unsuitable as an end-member component with mixing processes involving N-MORB. On the other hand, SCLM2 (São Paulo lamprophyres) and SCLM3 (Rio lamprophyres) do not have compositions enriched enough to generate the trace element ratios of SPL 41. The best fitting of a mixing curve was obtained for N-MORB and SCLM4. It is noteworthing that SCLM4 is the average composition of lamprophyres that crop out in the continental area that represents the Cabo Frio Structural High.

The results of the modelling indicate the geodynamic processes that took place in the Cabo Frio High area during the Santonian-Campanian, involved mixing between a depleted, relatively shallow asthenospheric source (N-MORB) and the local subcontinental lithospheric mantle represented by the average composition of the lamprophyres at the Cabo Frio Structural High (SCLM4). Different amounts of mixing are required to explain the less and more enriched compositions of samples SPL 38 and SPL 41, as such: about 87% N-MORB and 13% SCLM4 (sample SPL 38) and about 20% N-MORB and 80% SCLM4 (sample SPL 41).

Another binary mixing model was done to try to reproduce the cross-cutting relationships of chondrite-normalized REE patterns and the $La/Yb_{(N)}$ ratios of samples SPL 41 and SPL 38 and results are shown in figure 21B. Modelling was done using average values of the REE for the same samples used to calculate the SCLM4 composition, i.e. the lamprophyres on the Cabo Frio Structural High in the continental area adjoining Santos Basin). The model reproduced with good approximation the cross-cutting patterns and exactly the same $La/Yb_{(N)}$ ratios of the two samples (**Figure 24B**). The amount of end members in the mixing process is very close to that obtained in the previous modelling (**Figure 24A**) with a predominant and subordinate role for N-MORB in the petrogenesis of the magmatic rocks in wells EG2 and EG1, respectively.

In conclusion, the analytical binary mixing models presented in this section suggest that N-MORB and the subcontinental lithospheric mantle (SCLM) interacted during the geodynamic processes occurring in the Santonian-Campanian within the Cabo Frio High area. However, the potential contribution of other enriched sources can still be considered, and further geochemical and isotopic studies are required to determine the extent of their involvement. The interaction of different sources in the generation of these magmas is supposed to have occurred in a thinned continental lithosphere, allowing the depleted asthenosphere to rise up to the stability zone (35 - 80 km), as supported by **Rigoti (2015)** geophysical-geological modeling for the Santos Basin. Partial melting of the depleted asthenosphere would result from adiabatic decompression, while smaller melt fractions could be generated in the enriched SCLM due to thermal conduction from the convecting asthenosphere below. Melting temperatures in the asthenosphere are believed to be slightly higher than those of the normal mantle (~ 1270 °C), whereas lower temperatures would be required to melt the volatile-rich, enriched SCLM. Partial melting of more enriched and fusible portions or veins within the SCLM could account for the higher proportion of this end member in the mixing models. Ascending melts could accumulate and install plumbing systems within the thin (~ 10-15 km) brittle upper mantle, providing a feeding pathway for the stratovolcanoes above.

4.8 Acknowledgements

We acknowledge the support and funding from Equinor Brazil and the support of ANP (Brazil's National Oil, Natural Gas and Biofuels Agency) through the R&D levy regulation. Master's student Tatiele Marques Jatobá de Barros acknowledges CAPES scholarship, a research funding agency in Brazil.

4.9 Data privacy

The precise location and coordinates of the samples studied in this scientific paper are not given. In addition, the identifier codes of these samples have also been changed. These actions were necessary due to a confidentiality clause in the research project signed between Equinor Brazil and the Federal Rural University of Rio de Janeiro.

4.10 References

ALMEIDA, F. F. M. Relações tectônicas das rochas alcalinas Mesozóicas da região meridional da Plataforma Sul-Americana. **Revista Brasileira de Geociências**, v. 13, n. 3, p. 139-158, Sep. 1983.

ALMEIDA, F. F. M.; CARNEIRO, C. R.; MIZUSAKI, A. M. Correlação do magmatismo das bacias da margem continental Brasileira com a das áreas emersas adjacentes. **Revista Brasileira de Geociências**, v. 26, n. 3, p. 125-138, junho 1996.

ALMEIDA, J.; HEILBRON, M.; GUEDES, E.; NEUBAUER, F.; MANFRED, B.; KLAUSEN, M. B.; VALERIANO, C. M.; BRUNO, H.; GIRO, J. P.; MCMASTER, M.; TETZNER, W. Pre-to-syn-rift tholeiitic magmatism in a transtensive hyperextended continental margin: Onshore and offshore magmatism in the Campos Basin, SE Brazil. **Journal of South American Earth Sciences**, v. 108, n. 103218, June 2021.

ALVES, D. B. Sedimentação vulcanoclástica do Cretáceo Superior da Bacia de Campos, Sudeste do Brasil. **Boletim de Geociências da Petrobras**, v. 14, p. 149-154, maio 2006.

BROD, J. A.; JUNQUEIRA-BROD, T. C.; GASPAR, J. C.; PETRINOVIC, I. A.; VALENTE. S. C.; CORVAL, A. Decoupling of paired elements, crossover REE patterns, and mirrored spider diagrams: Fingerprinting liquid immiscibility in the Tapira alkaline-carbonatite complex, SE Brazil. **Journal of South American Earth Sciences**, v. 41, p. 41-56, Jan 2013

CADDAH, L. F. G.; ALVES, D. B.; HANASHIRO, M.; MIZUSAKI, A. M. P. Caracterização e origem do marco "3-Dedos" (Santoniano) da Bacia de Campos. **Boletim de Geociências da Petrobras**, v. 8, p. 315-334, Abril 1994.

CAMPBELL, I. H. Testing the plume theory. **Chemical Geology**, v. 241, n. 3-4, p. 153-176, July 2007.

CASTRO, R. D.; PICOLINI, J. P., 2014. Principais aspectos da geologia regional da Bacia de Campos. *In*: KOWSMANN, R.O. (Eds.), **Geologia e Geomorfologia.** Rio de Janeiro: Elsevier. Habitats, 2014, p. 1-12.

CHANG, H. K.; ASSINE, M. L.; CORREA, F. S.; TINEN, J. S.; VIDAL, A. C., Koike, L. Sistemas petrolíferos e modelos de acumulação de hidrocarbonetos na Bacia de Santos. **Revista Brasileira de Geociências**, v. 38, p. 29-46, junho 2008.

DANI, A. P. O.; REMUS, M. V. D.; DANI, N.; LIMA, E. F. Magmatismo basáltico do Andar Alagoas (Bacia de Campos). **Geologia USP, Série Científica**, v. 17, p. 269-287, ago. 2017.

DE LUCA, P.; CARBALLO, J.; FILGUEIRAS, A.; PIMENTEL, G.; ESTEBAN, M.; TRITLLA, J.; VILLACORTA, R., 2015. What is the Role of Volcanic Rocks in the Brazilian Pre-salt? *In*: **European Association of Geoscientists and Engineers, 77th EAGE Conference and Exhibition,** 2015, p. 1-5.

FAURE, G. **Principles of isotope geology**. John Wiley & Sons, New York, 1986, p. 590.

FODOR, R. V.; MCKEE, E. H.; ASMUS, H. E. K-Ar Ages and the opening of the South Atlantic Ocean: basaltic rock from the Brazilian margin. **Marine Geology**, v. 54, n. 1-2, p. M1-M8, Dec. 1983.

FODOR, R. V.; VETTER, S. K. Rift-zone magmatism: Petrology of basaltic rocks transitional from CFB to MORB, southeastern Brazil margin. **Contributions to Mineralogy and Petrology**, v. 88, p. 307-321, Dec. 1984.

FRANKE, D. Rifting, lithosphere breakup and volcanism: Comparison of magma-poor and volcanic rifted margins. **Marine and Petroleum Geology**, v. 43, p. 63-87, May 2013.

GREEN, D. H. Experimental petrology of peridotites, including effects of water and carbon on melting in the Earth's upper mantle. **Physics and Chemistry of Minerals**, v. **42**, p. 95-122, Jan. 2015.

GORDON, A. C.; MOHRIAK, W. U.; SANTON, N.; SANTOS A. C. Magmatic cycles in Santos Basin (S.E. Brazil): Tectonic control in the temporal-spatial distribution and geophysical signature. **Journal of South American Earth Sciences**, v. 121, n. 104111, Jan. 2023.

HEILBRON, M.; MOHRIAK, W. U.; VALERIANO, C. M.; MILANI, E. J.; Almeida, J., Tupinambá, M. From collision to extension: the roots of the southeastern continental margin of Brazil. *In*: Mohriak, W.; TANKARD, U. (Ed.), **Atlantic Rifts and Continental Margins American Geophysical Union**, Geophysical Monograph Series, 2000, v. 115, p. 1-32.

IRVINE, T. N.; BARAGAR, W. R. A. A guide to the chemical classification of the common volcanic rocks. **Canadian Journal of Earth Sciences**, v. 8, p. 523–548, May 1971.

LE BAS, M. J.; LE MAITRE, R. W.; STRECKEISEN, A.; ZANETTIN, B. A chemical classification of volcanic rocks based on the Total Alkali-Silica Diagram. **Journal of Petrology**, v. 27, n. 3, p. 745-750, June 1986.

LOBO, J. T. **Petrogênese de rochas basálticas do Eocretáceo das Bacias de Campos e Pelotas e implicações na geodinâmica de rifteamento do Gondwana Ocidental**. Tese de Doutorado, FGEL-UERJ, p. 250. 2007.

MACEDO, J. M. Evolução tectônica da Bacia de Santos e áreas continentais adjacentes. **Boletim de Geociências da Petrobrás**, v. 3, p. 159-173, 1989.

MCDONOUGH, W. F.; SUN, S. The composition of the Earth. **Chemical Geology**, v. 120, p. 223-253, March 1995.

MIYASHIRO, A. Nature of alkalic volcanic rock series. **Contributions to Mineralogy and Petrology**, v. 66, n. 1, p. 91-104, March 1978.

MIZUSAKI, A. M. P.; PETRINI, R.; BELLIENI, G.; COMIN-CHIARAMONTI, P.; DIAS, J., DE MIN, A.; PICIRILLO, E. M. Basalt magmatism along the passive continental margin of SE Brazil (Campos basin). **Contributions to Mineralogy and Petrology**, v. 111, p. 143-160, June 1992.

MIZUSAKI, A. M. P.; MOHRIAK, W. U. Sequências vulcanosedimentares na região da plataforma continental de Cabo Frio, RJ. *In*: **Resumos Expandidos, 37, Congresso Brasileiro de Geologia,** São Paulo, SP, v. 2, p. 468-469, 1992.

MOHRIAK, W. U.; DE BARROS, A. Z. N. Novas evidências de tectonismo cenozóico na região Sudeste do Brasil: O Graben de Barra de São João, na plataforma de Cabo Frio, RJ. **Revista Brasileira de Geociências**, v. 20, n. 1–4, p. 187-196, dez. 1990.

MOHRIAK, W. U.; MACEDO, J. M.; CASTELANI, R. T.; RANGEL, H. D.; BARROS, A. Z. N.; LATGÉ, M. A. L.; RICCI, J. A.; MIZUSAKI, A. M. P.; SZATMARI, P.; DEMERCIAN, L. S.; RIZZO, J. G.; AYRES, J. R. Salt Tectonics and Structural Styles in the Deep – Water Province of the Cabo Frio Region, Rio de Janeiro, Brazil. *In*: JACKSON D.G., ROBERTS, D.G., SNELSON S. (Eds.), **Salt Tectonics: A Global Perspective**. AAPG Memoir, 1995, v. 65, p. 273-304.

MOHRIAK, W. U. Bacias Sedimentares da Margem Continental Brasileira. *In*: C. S. L. A. BIZZI, R. M. VIDOTTI; J. H. GONÇALVES (Eds.), **Geologia, Tectônica e Recursos Minerais do Brasil**, 2003. Brasília, DF, Brasil, CPRM, v. 1, p. 87-165.

MOHRIAK, W. U.; GORDON, A.; MELLO, M. R. Origin and Petroleum System of the Cabo Frio High Between Santos and Campos Basins: Reviewed Integration of Structural and Paleogeographic Reconstruction with the Oil and Gas Systems. *In*: MELLO, M. R.; YILMAZ, P. O.; KATZ, B. J. (Eds), **The Supergiant Lower Cretaceous Pre-Salt Petroleum Systems of the Santos Basin, Brazil: AAPG Memoir 124**. AAPG Special Volumes, 2021. p. 273-324.

MOREIRA, J. L. P.; ESTEVES, C. A.; RODRIGUES, J. J. G.; VASCONCELOS, C. S. Magmatismo, sedimentação e estratigrafia da porção norte da Bacia de Santos. **Boletim de Geociências da Petrobrás**, v. 14, n. 1, p. 161-170, 2006.

MOREIRA, J. L. P.; MADEIRA, C.V.; GIL, J. A.; MACHADO, M. A. P. Bacia de Santos. **Boletim de Geociências da Petrobras**, v. 15, n. 2, p. 531-549, nov. 2007.

OREIRO, S. G.; GUERRA, M. C. M. Expressão sísmica de eventos magmáticos e não-magmáticos na Bacia de Santos. **Anais do 11 Simpósio de Vulcanismo e Ambientes Associados**, Cabo Frio, p. 195-200, 2005.

OREIRO, S. G. Magmatismo e sedimentação em uma área na Plataforma Continental de Cabo Frio, Rio de Janeiro, Brasil, no intervalo Cretáceo Superior–Terciário. **Boletim de Geociências da Petrobras**, v. 14, p. 95-112, maio 2006.

OREIRO, S. G.; CUPERTINO, J. A.; SZATMARI, P.; THOMAZ FILHO, A. Influence of pre-salt alignments in post-Aptian magmatism in the Cabo Frio High and its surroundings, Santos and Campos basins, SE Brazil: An example of non-plume-related magmatism. **Journal of South American Earth Sciences**, v. 25, p. 116-131, Feb. 2008.

PEARCE, J. A.; NORRY, M. J. Petrogenetic implications of Ti, Zr, Y and Nb variations in intrusive rocks. **Contributions to Mineralogy and Petrology**, v. 69, p. 33-47, May 1979.

PEARCE, J. A. A user's guide to basalt discrimination diagrams. *In*: D. A. WYMAN (Ed.), Trace element geochemistry of volcanic rocks: applications for massive sulphide exploration. ***Geological Association of Canada***, 1996. v. 12, p. 79-113.

PEDRO, A. J. **Utilização da sismoestratigrafia no estudo da atuação do alto de Cabo Frio sobre a sedimentação na porção sul da Bacia de Campos**. Dissertação de mestrado, Lagemar, UFF, Niterói, RJ, Brasil, p. 97. 2005.

RANCAN, C. C.; OLIVEIRA, L. C.; DE CARMO, I. O.; MARINS, G. M.; PESSOA, V. C. O.; DE ANDRADE, H.; PENATTI, A. P. R.; BORGES, T. A.; DA SILVA, R. C. B.; CARLOTTO, M. A.; BASSETTO, M.; ZANATTA, A. S. Rochas ígneas do Bloco de Libra, Bacia de Santos. **Anais do 49° Congresso Brasileiro de Geologia***,* 2012.

RANGEL, H. D. Manifestações magmáticas na parte sul da Bacia de Campos (Área de Cabo Frio) e na Bacia de Jequitinhonha. **Boletim de Geociências da Petrobras**, v. 14, n. 1, p. 155-160, maio 2006.

RICCOMINI, C.; FERNANDEZ, V. V.; GOMES, C. Tectonic controls of the Mesozoic and Cenozoic alkaline magmatism in central-southern Brazilian Platform. *In*: COMIN-CHIARAMONTI, P., GOMES, P. B. (Eds.), **Mesozoic to Cenozoic alkaline magmatism in the Brazilian Platform**, 2005. EDUSP-FAPESP, p. 31-56.

RIGOTI, C. A. **Evolução tectônica da Bacia de Santos com ênfase na geometria crustal: Interpretação integrada de dados de sísmica de reflexão e refração, gravimetria e magnetometria**. Dissertação de mestrado, FGEL-UERJ, Rio de Janeiro, RJ, Brasil, p. 134. 2015.

ROCK, N. M. S. **Lamprophyres**. Glasgow: Blackie and Son Ltd, 1991, p. 285.

ROLLINSON, H. R. **Using geochemical data: evaluation, presentation, interpretation**. Routledge, New York, USA, 1993, p. 384.

SCHMITT, R. S.; TROUW, R. A. J.; VAN SCHMUS, W. R.; PIMENTEL, M. M. Late amalgamation in the central part of West Gondwana: new geochronological data and the characterization of a Cambrian orogeny in the Ribeira Belt (SE Brazil). **Precambrian Research**, v. 133, p. 29-61, Aug. 2004.

SCHMITT, R. S.; VAN SCHMUS, W. R.; TROUW, R. A. J.; PASSCHIER, C. W. Cambrian orogeny in the Ribeira Belt (SE Brazil) and correlations within West Gondwana: Ties that bind underwater. **Geological Society, Special Publications**, v. 294, p. 279-296, 2008.

SCHOBER, P.; BOER, C.; SCHWARTE L. A. Correlation Coefficients: Appropriate Use and Interpretation. **Anesth Analg**., v. 126, n. 5, p. 1763-1768, 2018.

SIEBEL, W.; BECCHIO, R.; VOLKER, F.; HANSEN, M. A. F.; VIRAMONTE, J.; TRUMBULL, R. B.; HAASE, G.; ZIMMER, M. Trindade and Martín Vaz Islands, South Atlantic: isotopic (Sr, Nd, Pb) and trace element constraints on plume related magmatism. **Journal of South American Earth Sciences**, v. **13**, n. 1-2, p. 79-103, May 2000.

SPICE, H. E.; FITTON, J. G.; KIRSTEIN, L. A. Temperature fluctuation of the Iceland mantle plume through time. **Geochemistry, Geophysics, Geosystems**, v. **17**, n, 2, p. 243-254, Jan. 2016.

SUN, S. S. Lead isotopic study of young volcanic rocks from mid-ocean ridges, ocean islands and island arcs. **Philosophical Transactions of The Royal Society. Series A, Mathematical, Physical and Engineering Sciences**, v. 297, p. 409-445, July 1980.

SUN, S. S.; MCDONOUGH, W. F. Chemical and isotopic systematics of oceanic basalts; implications for mantle composition and processes. *In*: SAUNDERS, A. D.; NORRY, M. J. (Eds.), **Magmatism in the ocean basins**. London: Geological Society of London, 1989, v. 42, p. 313-345.

THOMAZ-FILHO, A.; RODRIGUES A. L. O alinhamento de rochas alcalinas Poços de Caldas-Cabo Frio (RJ) e sua Continuidade na Cadeia Vitória-Trindade. **Revista Brasileira de Geociências**, v. 29, n. 2, p. 189-194, junho 1999.

THOMAZ-FILHO, A.; CESERO, P.; MIZUSAKI, A. M.; LEÃO, J. G. Hot spot volcanic tracks and their implications for South American plate motion, Campos basin (Rio de Janeiro state), Brazil. **Journal of South American Earth Sciences**, v. 18, p. 383-389, 2006.

THOMAZ-FILHO, A.; MIZUSAKI, A. M. P.; ANTONIOLI, L. Magmatismo nas bacias sedimentares brasileiras e sua influência na geologia do petróleo. **Revista Brasileira de Geociências**, v. 38, n. 2, p. 128-13, junho 2008.

THOMPSON, R. N.; GIBSON, S. A.; MITCHELL, J. G.; DICKIN, A. P.; LEONARDOS, O. H.; BROD, J. A.; GREENWOOD, J. C. Migrating Cretaceous – Eocene Magmatism in the Serra do Mar Alkaline provinces, SE Brazil: melts from the deflected Trindade Mantle Plume? **Journal of Petrology**, v. **39**, n. 8, p. 493-526, Aug. 1998.

TUPINAMBÁ, M.; HEILBRON, M.; DUARTE, B. P.; NOGUEIRA, J. R.; VALLADARES, C.; ALMEIDA, J.; EIRADO SILVA, L. G.; MEDEIROS, S. R.; ALMEIDA, C. G.; MIRANDA, A.; RAGATKY, C. D.; MENDES, J., LUDKA, I. Geologia da Faixa Ribeira Setentrional: Estado da arte e conexões com a Faixa Araçuaí. **Genomos**, v. 15, n. 1, p. 67-79, fev. 2007.

VALENTE, S. C. **Geochemical and isotopic constraints on the petrogenesis of the Cretaceous dykes of Rio de Janeiro, Brazil**. Belfast, PhD. Thesis, The Queen's University of Belfast, p. 366. 1997.

WHITE, R.; MCKENZIE, D. Magmatism at rift zones: the generation of volcanic continental margins and flood basalts. ***Journal of Geophysical Research: Solid Earth*****,** v. 94, n. B6, p. 7685-7729, June 1989.

WINCHESTER, J. A.; FLOYD, P. A. Geochemical discrimination of different magma series and their differentiation products using immobile elements. **Chemical Geology,** v. 20, p. 325-343, 1997.

WINTER, R. W.; JAHNERT, R. J.; FRANÇA, A. B. Bacia de Campos. **Boletim de Geociências da Petrobras**, v. 15, n. 2, p. 511-529, nov. 2007.

WOOD, B., J., FRASER, D. C. ***Elementary thermodynamics for geologists***. Oxford University Press, Oxford, England, 1976. p. 303.

ZALAN, P. V.; OLIVEIRA, J. A. B. Origem e Evolução Estrutural dos Riftes cenozóicos do Sudeste do Brasil. **Boletim de Geociências da Petrobras**, v. 13, n. 2, p. 269–300, nov. 2005.

5 ARTIGO CIENTÍFICO 2: Petrogenesis of the drift magmatism in the Cabo Frio High, Campos Basin, Brazil: evidence from Sr-Nd-Pb-Hf isotopes

5.1 Abstract

Situated between the Campos and Santos basins, the Cabo Frio High emerges as a focal point of heightened magmatic activity during the Santonian-Campanian and Eocene following the breakup of these basins. The geodynamic framework associated with these events took place during the passive margin stage of these basins, wherein magmatic occurrences could potentially be attributed to the reactivation of significant geological structures or thermal enhancement facilitated by proximal hotspots, notably the Trindade Martin Vaz Plume, within a context of lithospheric thinning. (*i.e.*, Trindade Martin Vaz Plume). This investigation unveils novel Sr-Nd-Pb-Hf isotope data derived from alkaline magmatic rocks extracted from three boreholes strategically positioned within the Cabo Frio High area. The evolutionary trajectory of these rocks reflects intricate processes of assimilation and fractional crystallization. Results of analysis and binary mixing modeling point out to an involvement of both depleted (characterized by Depleted Mantle (DM)/Midi-Ocean Ridge Basalt (MORB) or HIMU compositions) and enriched sources (manifesting as the Enriched Mantle I (EMI) and the Enriched Mantle II (EMII)) in the genesis of these magmas. Moreover, the discerned incorporation of a fertile Ocean Island Basalt (OIB-like) reservoir hints at a plausible association with the Trindade Martin Vaz Plume, amplifying the complexity of the magmatic genesis within the studied region.

5.2 Introduction

During the Late Cretaceous and Paleogene, southeastern Brazil experienced a significant surge in magmatic activity, particularly notable within the Campos and Santos basins. This period saw the emergence of post-breakup magmatism, characterized by both extrusive and intrusive phenomena, predominantly exhibiting alkaline compositions. Coinciding temporally and spatially with other noteworthy magmatic events, these occurrences are observable in the onshore Poços de Caldas-Cabo Frio Alignment and the offshore Vitória-Trindade Chain (*e.g.* **Chang *et al.*, 1992; Thomaz Filho and Rodrigues, 1999; Alves, 2006; Bongiolo *et al.*, 2015**).

Studies on magmatic rocks in the Cabo Frio High area have predominantly relied on geophysical data, either independently or in tandem with petrological and lithogeochemical analyses, to characterize these events (*e. g.* **Oreiro *et al.*, 2003; Moreira *et al.*, 2006; Stanton and Schmitt, 2015; Gordon *et al*., 2023a)**. Despite the considerable attention devoted to this subject, there remains a notable dearth of lithogeochemical and geochronological data pertaining to post-breakup magmatism in this region. The understanding of mantle sources and associated evolutionary processes remains incomplete, with the precise contribution of geodynamic elements to magma generation yet to be fully elucidated.

This study endeavors to address these knowledge gaps by presenting novel isotopic data derived from volcanic and volcaniclastic rocks associated with the drift phase in the Cabo Frio High area, situated within the Campos Basin along Brazil's southeastern margin (**Figure 25**). Through the analysis of samples obtained from three wellbores, our primary objective is to shed light on the potential evolutionary processes and mantle sources contributing to the genesis of these magmatic formations. Central to our investigation is the exploration of the geodynamic context surrounding these magmatic episodes, aiming to ascertain whether a mantle plume, such as the Trindade plume, played a role in magma formation, in conjunction with tectonic reactivation and uplift processes.

Magmatic events play a crucial role in sedimentary basins and petroliferous systems, profoundly shaping their geological and thermal trajectories. The thermal effects stemming from magmatic intrusions and extrusions permeate the surrounding lithosphere, inducing a notable increase in temperature. This thermal energy imparts a transformative impact on organic matter, dictating its maturation processes and consequently influencing the genesis, migration, and entrapment of hydrocarbons. Structural perturbations induced by magmatic intrusions further augment this intricate geological narrative, precipitating deformations characterized by faulting, fracturing, and uplifting. These structural alterations serve as architects of hydrocarbon reservoirs, sculpting intricate traps and seals pivotal for the containment and preservation of petroleum deposits. By studying the interactions between magmatic phenomena and sedimentary contexts, it is possible to unlock invaluable insights into the genesis and distribution of hydrocarbon resources. Such insights hold particular significance in regions like the Brazilian southeastern margin, where the convergence of magmatic and sedimentary processes underscores the intricate dynamics shaping the hydrocarbon systems landscape (**Thomaz Filho *et al.*, 2008**).

By strategically integrating isotopic data with geological context and tectonic processes, our study seeks to unravel the complex dynamics underlying the magmatic evolution of the Cabo Frio High region. In doing so, we aim to provide valuable insights into the subsurface processes of the Earth within this captivating geological setting.

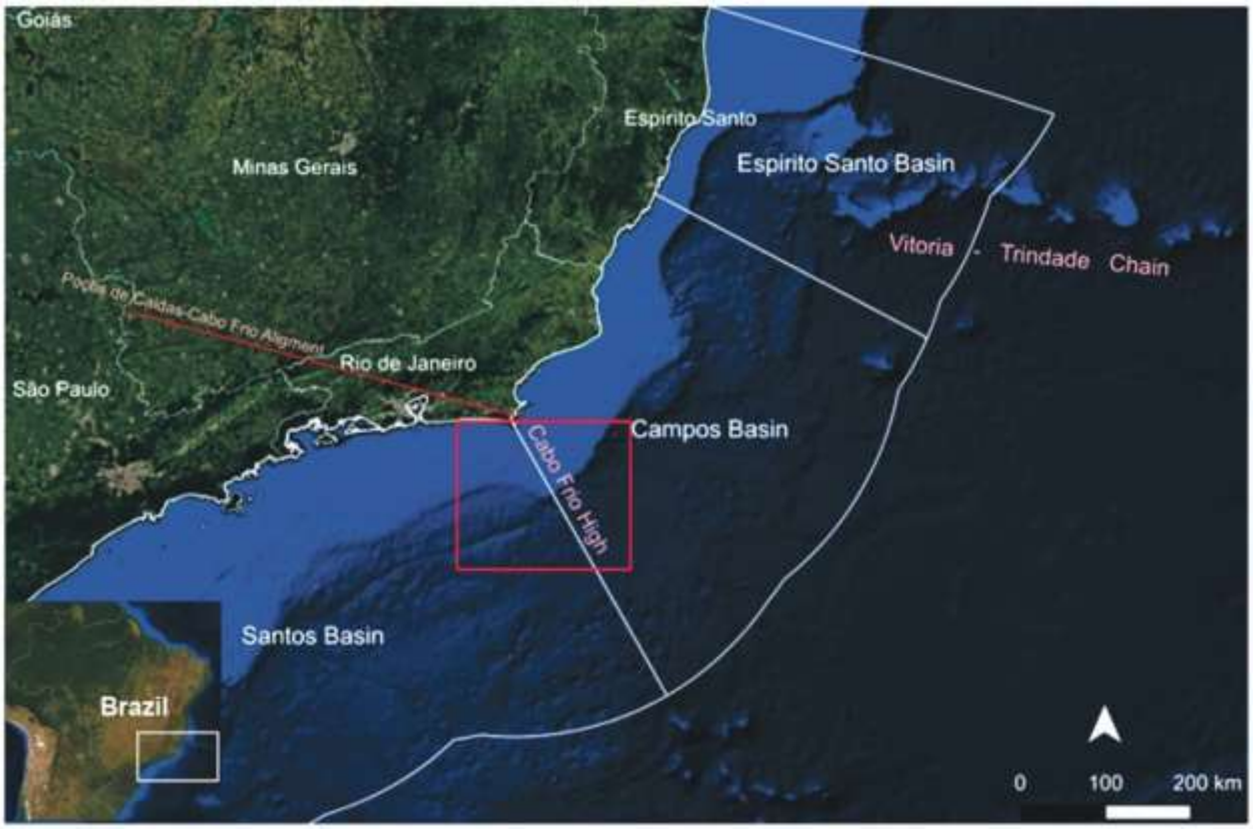

Figure 25. The delineated study area is demarcated within the red square. The figure also encompasses adjacent geological features, including sedimentary basins, the Cabo Frio High, the Poços de Caldas – Cabo Frio Alignment, and the Vitória – Trindade Chain.

5.3 Geological Setting

5.3.1 Drift Magmatism in the Cabo Frio High Area, Campos Basin

The sedimentary basins along the Brazilian southeastern margin, specifically Campos and Santos, were originated as rift systems resulting from the breakup between South America and Africa during the Upper Jurassic/Lower Cretaceous. Crustal extension movements subsequently led to the development of the present passive margin basins (**Chang *et al*., 1992, Cainelli and Mohriak, 1999; Mohriak, 2003**).

The Cabo Frio High is situated between Campos and Santos basins, prominent oil provinces in the southeastern margin of Brazil (**Mohriak *et al.*, 2005; Moreira *et al.*, 2007; Winter *et al.*, 2007**). This region exhibits intense intrusive and extrusive magmatic events that date from the Santonian to the Eocene and that contributed to the geophysical and tectonostratigraphic characteristics of these basins (**Mohriak *et al.*, 2005; Oreiro, 2006**). Geophysical investigations reveal the presence of various magmatic features, including dikes, sills, floods, volcanic cones and thick volcaniclastic sequences associated with distinct episodes (**Figure 26**) (*e. g.* **Moreira *et al.*, 2006; Oreiro, 2006; Oreiro *et al.*, 2008; Gordon *et al*., 2023a**). These rocks compositions consist predominantly of tuffs, hyaloclastites, breccias and basalts, with an overall alkaline character (*e. g.* **Moreira *et al.*, 2006; Oreiro, 2006; Rangel, 2006; Frank and Valente, 2023**). Possible fertile deep mantle sources are identified as potential elements in the origin of Santos Basin drift magmas, with a minor contribution of EMI and EMII mantle components (**Gordon *et al*., 2023b**).

Tectonic implications of the magmatism observed in studied area are strongly related to the extension movements during the South Atlantic Ocean opening and posterior tectonic, upwelling and thermal events that took place in the region (**Gibson et al., 1997; Thomaz Filho *et al.*, 2000; Thomaz Filho *et al.*, 2008; Almeida *et al.*, 2021**). Further elaboration of these aspects and hypotheses will be provided in subsequent discussions.

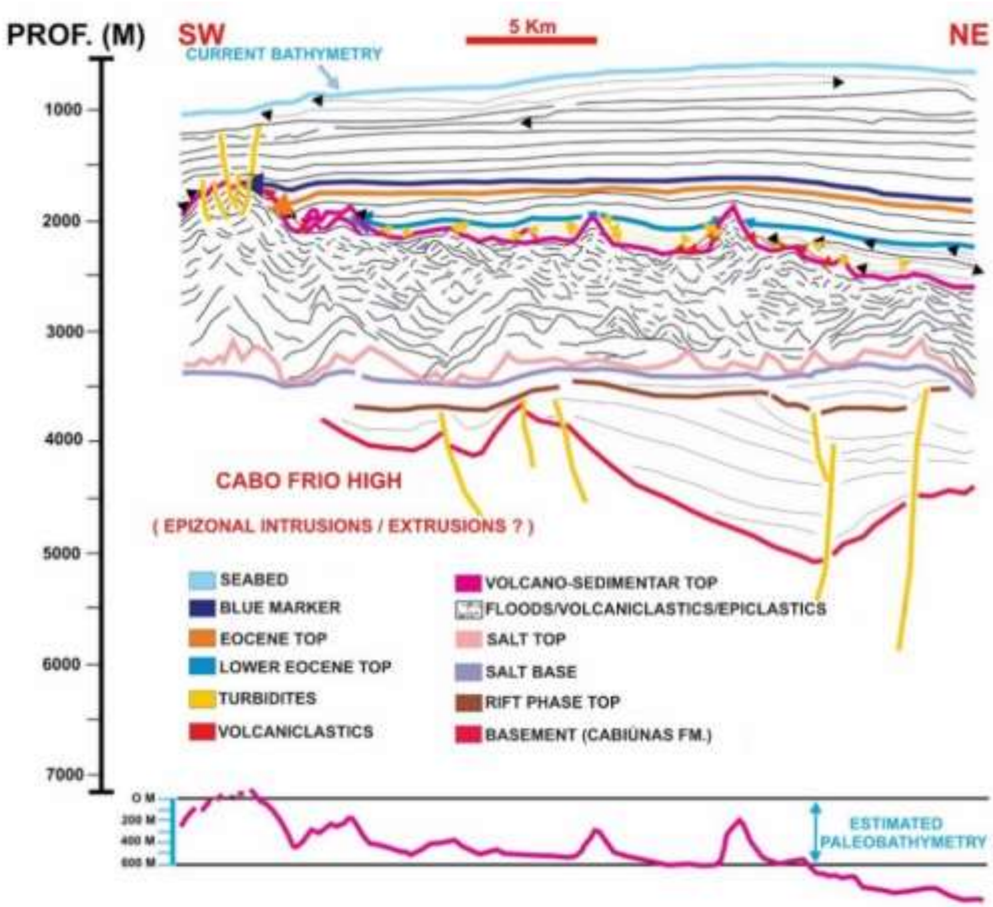

Figure 26. Volcano-sedimentary model proposed for the Cabo Frio High Area. Modified from **Oreiro (2006)**.

Detailed petrographic and lithogeochemical data from the rocks studied in this paper are available in **De Barros *et al.* (2023)**. The classification of these magmatic rocks is summarized in **Table 4**. Analysis of major and trace elements suggests that the origin of these magmas can be traced back to shallow mantle depths ranging from 35 to 80 km. They are associated with mixing processes involving a depleted source (N-MORB-like) and the local subcontinental lithospheric mantle (Cabo Frio High area lamprophyres) (**De Barros *et al.*, 2023**). However, the present study addresses and deliberates on the potential contribution of other enriched sources as the origin of these rocks. Moreover, additional constraints are imposed on possible evolutive processes that may have influenced the development of these magmas.

Table 4. Petrographic and lithogeochemical classification of studied rocks. Modified from **De Barros *et al.*, 2023**. Lithogeochemical classification based on Nb/Y versus Zr/Ti diagram (**Pearce and Norry, 1979**).

Well	Sample	Petrography	Lithogeochemistry
EG1	SPL 37	Ash tuff	Tephriphonolite
EG1	SPL 39	Alkaline diabase	Alkali basalt
EG2	SPL 40	Lapilli tuff	Alkali basalt
EG2	SPL 44	Basalt	Basalt
EG3	SPL 45	Lapilli tuff	Alkali basalt
EG3	SPL 47	Lapilli tuff	Foidite
EG3	SPL 48	Lapilli tuff	Foidite

5.3.2 Cretaceous Alkaline Magmatism in Brazilian Southeastern

The alkaline magmatism in the Cabo Frio High area contemporaneously coincides with numerous magmatic events observed in the southeastern region of Brazilian. Manifestations of the Trindade Martin Vaz plume are evident in alkaline provinces throughout southeastern Brazil, spanning the Upper Cretaceous to Paleogene, including areas such as Poroxeu, Alto do Paranaíba, Itaporá and Serra do Mar (**Gibson *et al.*, 1995; Gibson *et al.*, 1997; Thompson *et al.*, 1998; Thomaz Filho and Rodrigues, 1999; Siebel *et al.*, 2000**).

The Vitória-Trindade Chain comprises a group of seamounts oriented in an E-W, extending from the Brazilian margin to the Trindade and Martín Vaz islands. In sequence from west to west, these seamounts are Vitória, Montague, Jaseur, Davis, Dogaressa, Columbia, Trindade and Martín Vaz. Ranging in age from 40 Ma to the present, these seamounts predominantly consist of subaerial volcanoes composed of highly alkaline silica unsaturated rocks (**Fodor and Hanan, 2000; Siebel *et al.*, 2000; Pires *et al.*, 2016**). Contributions of HIMU, EMI, and N-type MORB mantle sources are suggested to have participated in the origin of these magmas (**Siebel *et al.*, 2000; Quaresma *et al.*, 2023**).

The Abrolhos Archipelago, dated between 40 to 60 Ma, is situated northward of the Vitória-Trindade Chain, and constitutes an igneous province of mildly alkaline basalts genetically linked to the Trindade hotspot (**Marques *et al.*, 1999; Siebel *et al.*, 2000; Geraldes *et al.*, 2013**).

The Poços de Caldas-Cabo Frio Alkaline Alignment represents a prominent magmatic lineament stretching approximately 1,150 km in length and 60 km in width, extending Poços de Caldas to Cabo Frio (**Almeida, 1991**). This geological province, developed in extensive shear zones exhibiting a WNW-ESE trend as depicted in **Figure 27**. The alignment is associated with a complex geological history involving at least two distinct magmatic and reactivation episodes during the Upper Cretaceous-Paleocene and Eocene (**Riccomini *et al.*, 2004**). Manifestations of both extrusive (floods and pyroclastic flows) and intrusive (dikes, stocks, and plugs) magmatic activity are observed along the entire alignment (**Thomaz Filho and Rodrigues, 1999**).

The principal complexes aligned along the Poços de Caldas-Cabo Frio Alignment, arranged from west to east, encompass Poços de Caldas, Passa Quatro, Itatiaia, Morro Redondo, Serra dos Tomazes, Tinguá, Marapicu-Gericinó-Mendanha, Tanguá, Soarinho, Rio Bonito, Morro de São João, and Cabo Frio (**Riccomini *et al.,* 2005**).

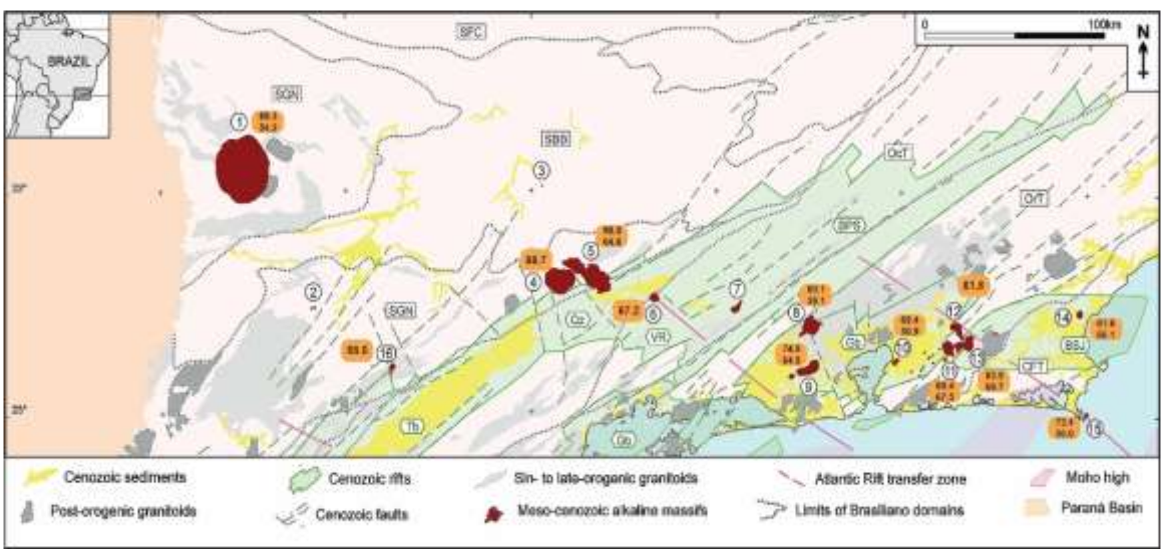

Figure 27. Distribution of the Meso-Cenozoic Poços de Caldas-Cabo Frio magmatic occurrences: Poços de Caldas (1), Bom Repouso (2), Caxambú (3), Passa Quatro (4), Itatiaia (5), Morro Redondo (6), Serra dos Tomazes (7), Tinguá (8), Mendanha-Mapicuru (9), Itaúna (10), Tanguá (11), Soarinho (12), Rio Bonito (13), Morro de São João (14), Cabo Frio (15) Modified from **Rosa and Ruberti (2018)**. K-Ar ages from **Sonoki and Garda (1998)**.

These complexes are predominantly felsic, characterized by a limited occurrence of mafic expressions such as dikes, sills, and lavas. The prevailing lithologies consist of nepheline syenite, often associated with trachyte, phonolite, and breccia (*e.g*. **Brotzu *et al.*, 1992; Brotzu *et al.*, 2007; Motoki *et al.*, 2010; Rosa and Ruberti, 2018**). Additionally, ankaramitic lavas have been identified in the Itaboraí and Volta Redonda basins (**Thompson *et al.*, 1998**).

The origin and potential continuity of the Poços de Caldas-Cabo Frio Alignment and offshore alkaline magmatism with the Vitória-Trindade Chain have been predominantly explored through plume-related hypotheses. **Thompson *et al.* (1998)** propose a connection between the Poços de Caldas alkaline magmatism and the Trindade mantle plume, suggesting that between 80 to 55 Ma, the plume's upwelling was deflected by the thick São Francisco craton lithosphere. This deflection could have induced decompression melting processes along the craton's southern margin, giving rise to the alkaline complexes observed in the Poços de Caldas-Cabo Frio Alignment.

Alternatively, a theory posits the displacement of the South American plate over a hot spot, with manifestations of this structure observed from Poços de Caldas to Cabo Frio alkaline magmatism. During the Eocene, as implicated in this model, a clockwise plate rotation would have led to intense magmatism and tectonic manifestations in the surrounding areas, such as the Cabo Frio Platform and the Abrolhos Archipelago, ultimately contributing to the formation of the Vitória-Trindade Chain formation (**Thomaz Filho and Rodrigues, 1999; Thomaz Filho and Misuzaki, 2008**).

In contrast, a non-plume-related hypothesis attributes the magmatic episodes to the reactivation of major Proterozoic crustal discontinuities during the extensional processes that affected the South American Platform. **Almeida (1983)** and **Riccomini *et al.* (2005)** propose that, through these reactivated structural weaknesses and potential mantle upwelling, the alkaline magmatism was generated and emplaced. This intense tectonic control is then suggested to be connected to the alkaline drift magmatism observed in offshore Santos Basin (**Gordon *et al.*, 2023b**) and onshore portions of both the Campos and Santos basins (**Oliveira *et al.*, 2023**).

5.4 Materials and Methods

The present study utilized seven sidewall core samples (SPL 37, SPL 39, SPL 40, SPL 44, SPL 45, SPL 47, and SPL 48) comprising volcanic and volcaniclastics rocks obtained from three wells drilled in the Cabo Frio High area, situated between the Campos and Santos basins. Well profiles were employed to characterize and estimate the emplacement time of these magmas and the associated stratigraphic formations. Both the samples and well profiles were acquired through the Brazilian National Agency for Petroleum, Natural Gas and Biofuels (ANP).

The selection of sidewall core samples was based on criteria such as minor Loss on Ignition (LOI), petrographic and lithogeochemical data, and spatial distribution. Subsequently, the samples underwent a thorough washing process using running water and a soft brush to enhance the removal of impurities. Post-cleaning, the samples were dried, crushed, and powdered, preparing them for subsequent isotopic analysis.

Sr-Nd-Pb-Hf isotopic data were acquired at the New Mexico State University Johnson Mass Spectrometer Laboratory in the United States. The analyses were conducted using the Thermo Scientific Neptune Plus Multicollector-Inductively Coupled Plasma Mass Spectrometer (MC – ICPMS). Standard reference material, NBS 987, yielded the following results: $^{87}Sr/^{86}Sr = 0.710284 \pm 0.000011$; $^{143}Nd/^{144}Nd = 0.512099 \pm 0.000008$; $^{206}Pb/^{204}Pb = 18.898 \pm 0.001$; $^{207}Pb/^{204}Pb = 15.485 \pm 0.001$; $^{208}Pb/^{204}Pb = 38.678 \pm 0.002$; $^{176}Hf/^{177}Hf = 0.282161 \pm 0.000007$.

A compilation effort was undertaken to gather isotopic data and endmembers pertaining to the following mantle reservoirs: DM/MORB, HIMU, EMI, and EMII, and data for Poços de Caldas-Cabo Frio and Vitória-Trindade magmas. This data was employed in the formulation of petrological models, contributing to the advancement of geodynamic discussions regarding the Santonian-Campanian magmatism in the studied area. The compiled information was sourced from the GEOROC (https://georoc.eu/georoc/new-start.asp) and EarthRef (https://earthref.org/) databases. The compiled spreadsheets containing this information can be accessed in the Complimentary Material associated with this study.

5.5 Results

Volcanic and volcaniclastic rocks analyzed in this study were collected in three wells, namely EG1, EG2 and EG3, located within the Cabo Frio High area situated between the Campos and Santos basins. These rocks occur interbedded to Cretaceous sedimentary deposits, which encompass sandstones, shales, siltstones, and marls (**Figure 28**), associated with the drift phase.

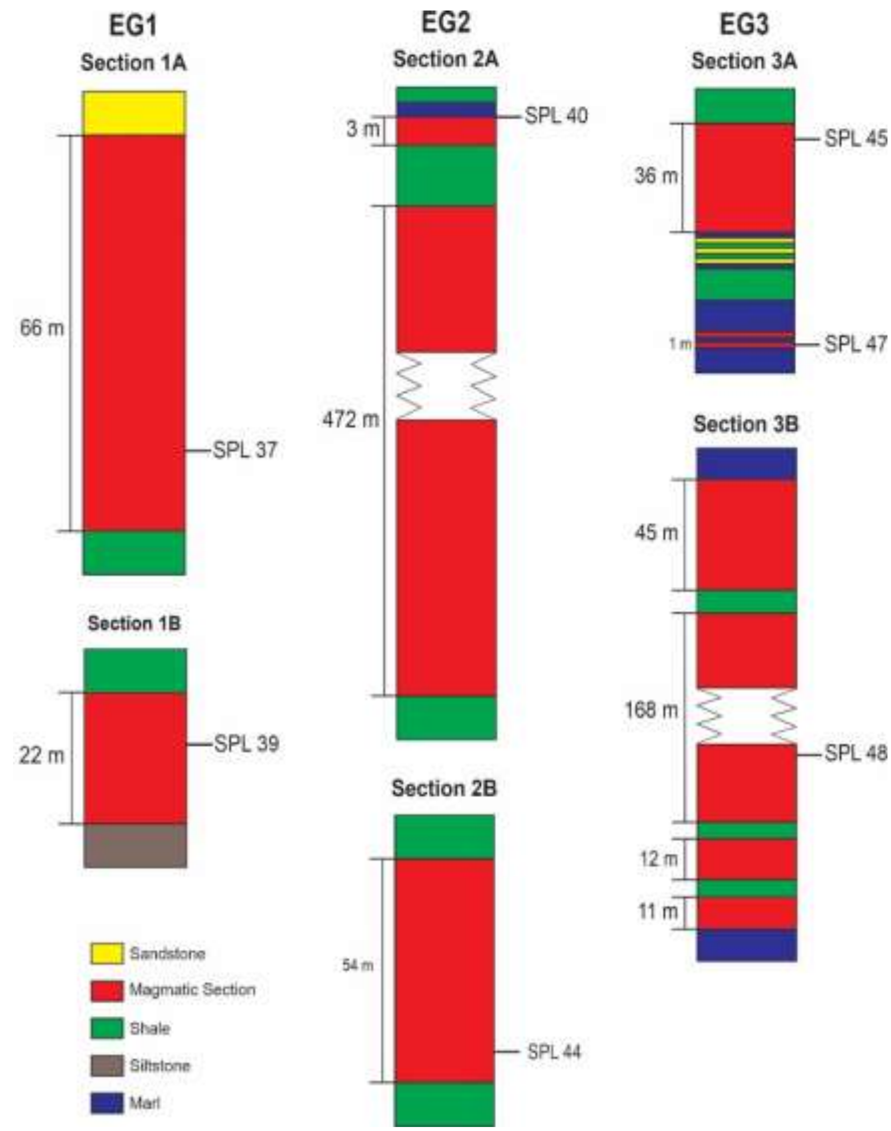

Figure 28. Schematic sections of EG1, EG2 and EG3 wells. Studied sidewall core samples are indicated. Modified from **De Barros *et al.*, 2023.**

5.5.1. Magma Evolution Processes

As depicted by **De Barros *et al.* (2023)**; lithogeochemical data from alkaline volcanic and volcaniclastic rocks in the Cabo Frio High area have their evolution associated with fractional crystallization processes. According to the authors, more complex disequilibrium processes, such as liquid immiscibility, are also possibly to be associated with these magmas and can be observed in the crossover pattern of EG1, EG2, and EG3 most and less evolved samples.

Despite that, simple fractional crystallization processes may not be sufficient to explain certain concentrations observed in trace and REE elements in studied magmas. Peaks observed in Ba, Rb, Sr, Th, and K are thought to be associated with alteration processes, very commonly observed in these rocks as depicted by their loss on ignition (LOI) and petrographic data (**De Barros *et al.*, 2023**). Nevertheless, crystallization processes and associated assimilation of different magmas can be explained by the high concentrations observed in such mobile trace elements. Notorious variations in Sr and Nd isotopic ratios (**Table 5**) are also strong evidence that these magmas went through assimilation-fractional crystallization processes.

In magmas derived from a common source, discernible distinctions in the fourth decimal place for $^{87}Sr/^{86}Sr$ and the fifth decimal place for $^{143}Nd/^{144}Nd$ ratios serve as robust indicators, suggesting that the exclusive influence of crystallization processes is insufficient to account for such dissimilarity. Notably, samples SPL 37 and SPL 39 from well EG1 representing the least and most evolved states, exhibit significant fluctuations in both $^{87}Sr/^{86}Sr$ (0.705180 – 0. 704578) and $^{143}Nd/^{144}Nd$ (0. 512294 – 0. 512726) ratios, commencing at the third decimal place. This data implies that crystallization processes may have been intricately associated with assimilation processes (assimilation and fractional crystallization – AFC) in the genesis of the studied rocks. A similar pattern can be observed in EG2 and EG3 samples. Nonetheless, the observed isotopic variation cannot be explained solely by single crystallization processes.

It is crucial to consider that these samples show significant alteration and high LOI contents (**De Barros *et al.*, 2023)**, potentially affecting Nd and mainly in Sr isotopic ratios. Furthermore, is worth noting that the number of samples studied, and the amount of isotopic data is quite limited. A more robust discussion in a petrological scenario involving more complex evolutionary processes requires more evidence.

Table 5. Isotopic ratios from studied samples and their respective wells. MgO (wt.%), LOI (wt.%), La (ppm), Yb (ppm) and Nb (ppm) content from **De Barros *et al.*, 2023**. Initial (i) content refers to measured data (m) recalculated to 82 Ma (based on **Moreira *et al.* (2006)** and geological setting bibliographic research). Normalization factors (N) are from **McDonough and Sun (1995)**.

Well	**EG1**	**EG1**	**EG2**	**EG2**	**EG3**	**EG3**	**EG3**
Sample	**SPL 37**	**SPL 39**	**SPL 40**	**SPL 44**	**SPL 45**	**SPL 47**	**SPL 48**
SiO2	55.02	44.31	32.41	39.12	33.83	45.88	38.71
MgO	2.49	4.56	4.01	2.57	4.73	0.7	4.74
LOI	7.52	7.57	19.95	14.02	17.52	11.21	14.68
$La/Yb_{(N)}$	43.562	5.036	21.663	2.714	23.567	29.218	20.905
$La/Nb_{(N)}$	0.9851	0.8814	1.0264	0.5927	1.0058	0.9644	0.9669
$^{87}Sr/^{86}Sr_{(m)}$	0.705942	0.704979	0.716609	0.708871	0.705719	0.704951	0.705604
$^{87}Sr/^{86}Sr_{(i)}$	0.705180	0.704578	0.716055	0.708016	0.704970	0.704426	0.705323
$^{143}Nd/^{144}Nd_{(m)}$	0.512333	0.512806	0.512396	0.512893	0.512605	0.512584	0.512647
$^{143}Nd/^{144}Nd_{(i)}$	0.512294	0.512726	0.512339	0.512805	0.512551	0.512533	0.512591
$^{176}Hf/^{177}Hf_{(m)}$	0.282576	0.283074	0.282856	0.283136	0.282843	0.282811	0.282860
$^{176}Hf/^{177}Hf_{(i)}$	0.282575	0.283072	0.282855	0.283134	0.2828418	0.282810	0.282859
$^{206}Pb/^{204}Pb$	17.929	18.804	18.581	19.058	18.704	19.166	18.973
$^{207}Pb/^{204}Pb$	15.529	15.574	15.553	15.589	15.521	15.569	15.536
$^{208}Pb/^{204}Pb$	39.437	38.984	38.767	39.124	38.861	39.590	39.011

In EG3, two samples, SPL 45 (MgO = 4.73) and SPL 48 (MgO = 4.74) despite sharing a similar level of evolution, display unexpected differences in $^{87}Sr/^{86}Sr$ and $^{143}Nd/^{144}Nd$ rations. Unlike expectations for cogenetic magmas, the Sr isotopic ratio is higher for the less evolved sample, diverging from the trend observed in EG2 samples. However, the. Nd isotopic ratio, aligns with ordinary assimilation processes, with the more evolved sample showing a lower content of $^{143}Nd/^{144}Nd$. This supports the notion that alteration processes may have influenced these samples, particularly in Sr isotopic data mobility.

In a broader context, assimilation and fractional crystallization emerges as the predominant process shaping the origin of these magmas, given the notable variation in $^{87}Sr/^{86}Sr$ and $^{143}Nd/^{144}Nd$ content that cannot be exclusively attributed to fractional crystallization. It is essential to note challenges such high LOI values, especially in EG2 and EG3 samples, and their petrographic characterization as highly altered rocks, susceptible to Sr remobilization. The limited sample number constrains a more in-depth discussion regarding the evolution of these magmas. The existence of magmas with the same MgO composition but remarkably different Sr and Nd composition are strong indicators that different sources are related to the origin of these rocks, as depicted by **De Barros *et al.* (2023**) and the subsequent results regarding possible mantle sources involved in studied magmatic events.

5.5.2. Mantle Sources

Both N-MORB and fertile asthenospheric mantle sources (SCLM in onshore Cabo Frio) are suggested to be the origin of magmas from EG1, EG2 and EG3 (**De Barros *et al.,* 2023**). $La/Yb_{(N)}$ (> 1) and $La/Nb_{(N)}$ (<1) ratios from SPL 37, SPL 47 and SPL 48 (**Table 2**) are very likely to represent enriched mantle source. Despite that, values that close to unit might also account for more enriched or fertile mantle sources. $La/Nb_{(N)}$ (>1) ratios in studied rocks SPL 40 and SPL 45 indicates they are supposed to have the contribution of a more fertile mantle source, such as a OIB plume-like, during their formation.

Based on lithogeochemical data results from **De Barros *et al.* (2023**) and on the major geodynamic context in which Cabo Frio High post-breakup magmas were emplaced, it is possible to ascertain that mantle sources involved to give origin to these magmas are not completely clear. Among a diverse possibility of mantle sources, discrimination diagrams using $^{87}Sr/^{86}Sr$, $^{143}Nd/^{144}Nd$, $^{176}Hf/^{177}Hf$, $^{206}Pb/^{204}Pb$ (**Figures 29 and 30**) were then used to help elucidate such contributions. Data from coeval and adjoining alkaline magmatism from the Poços de Caldas-Cabo Frio alignment and Vitória-Trindade Chain were also compared to studied samples.

In general, diagrams in **Figures 29 and 30** supports the hypothesis of an enriched mantle source along with N-MORB (here represented by depleted mantle + mantle sources) to have given origin to the magmatism in the offshore Cabo Frio High area during the Santonian-Campanian.

EG1 samples, SPL 37 and SPL 39, isotopic data suggest these rocks originated from an enriched mantle source, either EMI-type (**Figure 29A, B, C, D, and E**, and **Figure 30C**) or EMII-type (**Figure 29A, B, C, D, and E**). Possible contribution of a depleted source (such as MORB) is evidenced by **Figure 29C and E**, and **Figure 30C**. As for EG2 samples, SPL 40 and SPL 44), they exhibit similar pattern, being associated to EMII mantle sources (**Figure 29A, B, C, D and E, and Figure 30B**). Contribution of DM/MORB sources are indicated by **Figure 29C and E**, and **Figure**

30, as well as possible involvement of HIMU (**Figure 29A, D and E**). It is important to emphasize that particularly high $^{87}Sr/^{86}Sr$ isotopic ratios in EG2 samples are possible to be associated with Sr remobilization, given the stage of alteration these rocks exhibit.

Samples SPL 45, SPL 47 and SPL 48 from EG3 possess similar isotopic ratios. They can be associated with EMI enriched mantle source (**Figure 29A, B and D, and Figure 30A and B**). Some diagrams also suggest the contribution of EMII (**Figure 29B, C and D, and Figure 30C**). Data from the subcontinental lithospheric mantle (SCLM) is supposed to be similar to the ones found in EMI.

The genetic association of the Cabo Frio High alkaline post-breakup magmatism with either Vitória-Trindade Chain or the Poços de Caldas-Cabo Frio Alignment is still in discussion and the thermal or geochemical contribution of these features is not a consensus among studies in the area (*e. g.* **Almeida, 1991; Almeida, 1993; Thompson *et al.*, 1998; Thomaz Filho and Rodrigues, 1999; Gordon *et al.*, 2023a; Gordon *et al.*, 2023b**). Some samples from studied wells exhibits isotopic signatures similar to the ones observed in both adjacent magmatic provinces (**Figure 29**) and are correspondent with enriched and fertile $La/Yb_{(N)}$ and $La/Nb_{(N)}$ indicators (**Table 5**). Despite that, considering the predominancy of results and the discrimination diagrams, these association can only be suggested, not determined. Further studies involving petrogenesis, geophysics and geodynamic data are needed to clarify such association.

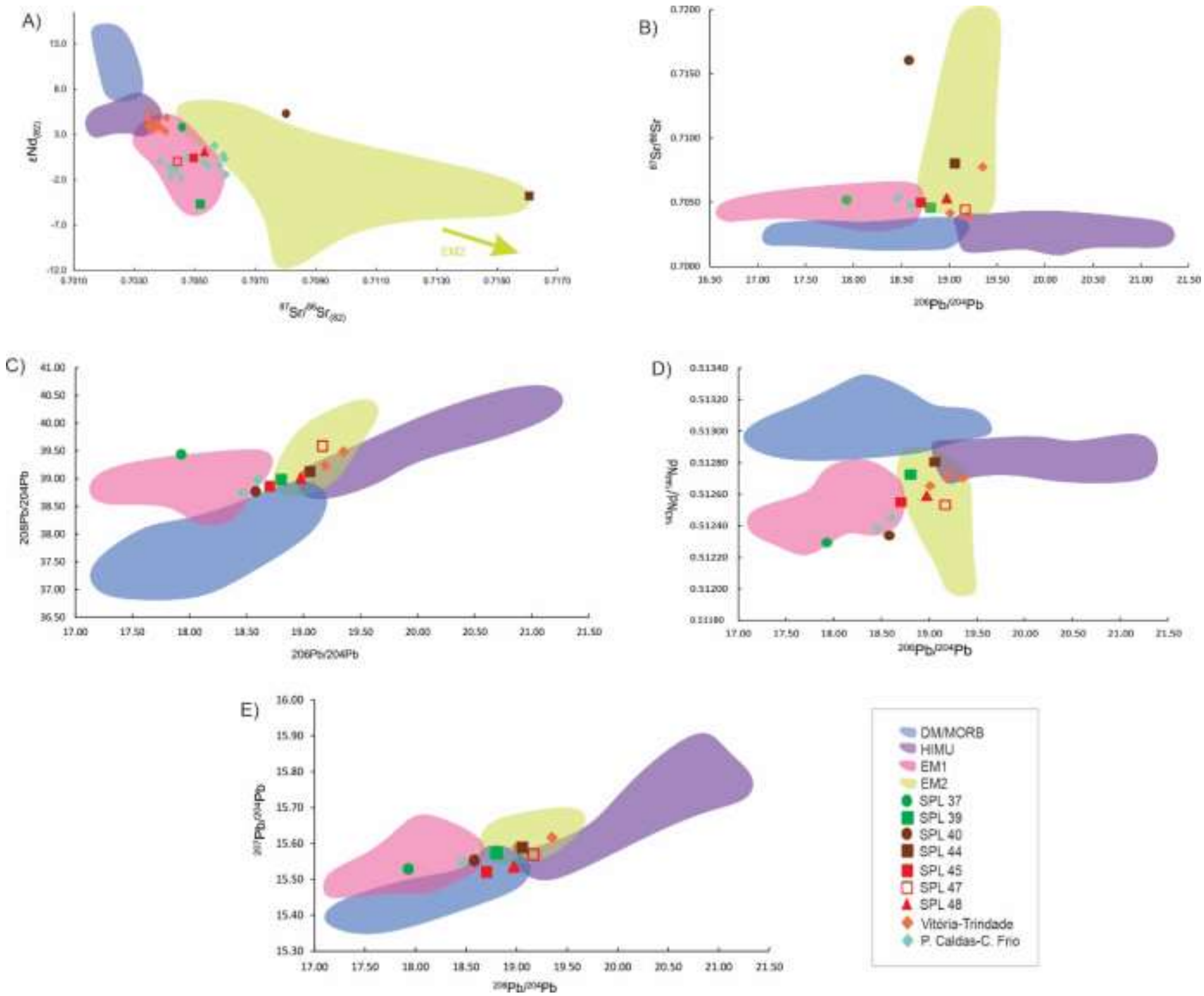

Figure 29. Mantle source discrimination diagrams for studied samples. EG1 (SPL 47 and SPL 39), EG2 (SPL 40 and SPL 44) and EG3 (SPL 45, SPL 47 and SPL 48) rocks $^{87}Sr/^{86}Sr$, $^{143}Nd/^{144}Nd$ and $^{176}Hf/^{177}Hf$ ratios were recalculated to estimated initial age 82 Ma (based on **Moreira *et al.* (2006)** and geological setting bibliographic research). Data from Vitória-Trindade Chain are from **Siebel *et al.*, 2000; Marques *et al.*, 1999; Peyve and Skolotnev, 2014; Bongiolo *et al.*, 2015; Quaresma *et al.*, 2023; and Fodor and Hanan, (2000)**. Data from Poços de Caldas-Cabo Frio Alkaline Alignment are from **Guarino *et al.*, 2021; Thompson *et al.*, 1998; Valente, 1997; and Rosa, 2017**. DM/MORB stands for general depleted mantle sources. DM/MORB, HIMU, EMI and EMII data can be found in complimentary material and were obtained in GEOROC (https://georoc.eu/georoc/new-start.asp) and EarthRef (https://earthref.org/) databases.

Precise mantle sources remain unclear even considering discrimination diagrams. Despite that, it is possible to ascertain the contribution of both enriched and depleted mantle sources.

Additionally, a fertile OIB-like source is to be considered given discrimination diagrams and La/Yb$_{(N)}$ and La/Nb$_{(N)}$ ratios. Binary mixing models were then elaborated to help determine EMI, EMII, DM/MORB, HIMU and OIB-like mantle sources possible input to the formation of studied magmas and their rate of contribution.

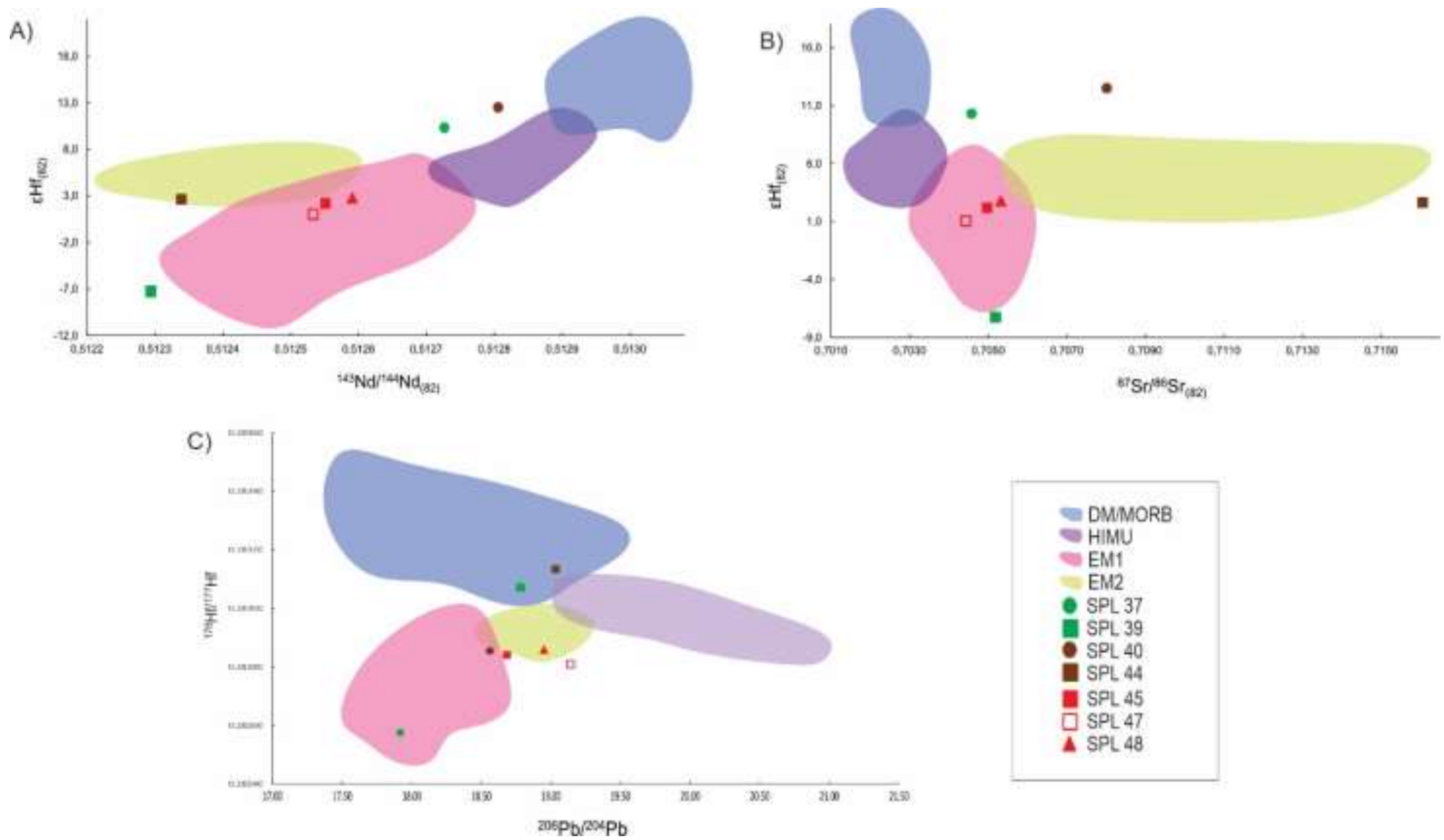

Figure 30. Mantle source discrimination diagrams for studied samples. EG1 (SPL 47 and SPL 39), EG2 (SPL 40 and SPL 44) and EG3 (SPL 45, SPL 47 and SPL 48) rocks $^{87}Sr/^{86}Sr$, $^{143}Nd/^{144}Nd$ and $^{176}Hf/^{177}Hf$ ratios were recalculated to estimated initial age 82 Ma (based on **Moreira *et al.* (2006)** and geological setting bibliographic research). stands for general depleted mantle sources. DM/MORB, HIMU, EMI and EMII data can be found in complimentary material and were obtained in GEOROC (https://georoc.eu/georoc/new-start.asp) and EarthRef (https://earthref.org/) databases.

5.6 Discussions

The indication that more than one mantle source originated the studied magmatism made it necessary to elaborate binary mixing modeling to determine which sources are involved in this mixture and their specific percentage of contribution. Previous studies indicate the contribution of EMI and EMII and mainly fertile mantle sources for drift magmatism in Campos and Santos basins (**Gordon *et al.*, 2023b**), as well as the SCLM and N-MORB (**De Barros *et al.* 2023**).

In general, binary mixing modeling results suggest the involvement of a depleted and an enriched mantle source for studied samples. EG1 sample SPL 37 exhibits a high contribution of DM (99.7% - 95%) in a possible mixing with EMI and EMII (**Figure 31A and B**). In the case of mixing between EMI and HIMU, the enriched mantle source exhibits higher values (approximately 85%), as observed in sample SPL 39 (about 95% contribution from EMI) (**Figure 31C**).

Samples from EG2 exhibit a discrepant pattern in mixing using $^{87}Sr/^{86}Sr$ and $^{143}Nd/^{144}Nd$ ratios (**Figure 31A, D and E**). Such values may reflect an increment of radiogenic strontium by alteration and contamination with seawater (**Hofmann and White, 1981**). This alteration is also observed in LOI values and petrographic descriptions of these samples (**De Barros *et. al.*, 2023**). As for diagrams using radiogenic Pb data, results were very precise and indicate the contribution of about 99% of DM for SPL 44 and 99.7% for SPL 40 in the case of a mixing with EMII (**Figure 31B**), and 10% of EMI for sample SPL 40 and 19% for sample SPL 44 when mixed with HIMU (**Figure 31C**). Another possible mixing between HIMU and EMI could have generated SPL 45 and SPL 47, with a considerable contribution of EMI (**Figure 31D**). Lastly, OIB sources from the Trindade plume were modeled with EMI and SPL 47 could represent about 10% of OIB in this mixture (**Figure 31E**).

All three EG3 samples can be associated with an equalized mixing between EM and EMI (**Figure 31A**). When observed in a mixing EMI and HIMU, they plot slightly out of the curve, but still following the same trend, indicating possible contribution of these mantle sources, accounting for 10% to 20% of HIMU for SPL 45, SPL 47 and SPL 48 respectively (**Figure 31C**).

The numerous possible mantle sources and combinations can be associated with the heterogeneity and enrichment of the SCLM underneath the Campos and Santos basins during the Neoproterozoic events that originated the Ribeira Orogen (*e. g.* **Valeriano et al., 2004; Heilbron et al., 2008; Schmitt et al., 2008**). Contributions of EMI and EMII end members are commonly observed in literature, mainly regarding the drift magmatism in the studied area (**Louback *et al.*, 2021; Gordon *et al*., 2023b).** A HIMU component could be associated to metasomatic processes in the subcontinental lithospheric mantle (**Stracke and Hofmann, 2005**). This mantle source is also observed as end member of the Vitória-Trindade magmatism (*e. g.* **Marques *et al.*, 1999; Santos et al., 2019**; **Maia *et al.*, 2022; Quaresma *et al.*, 2023**).

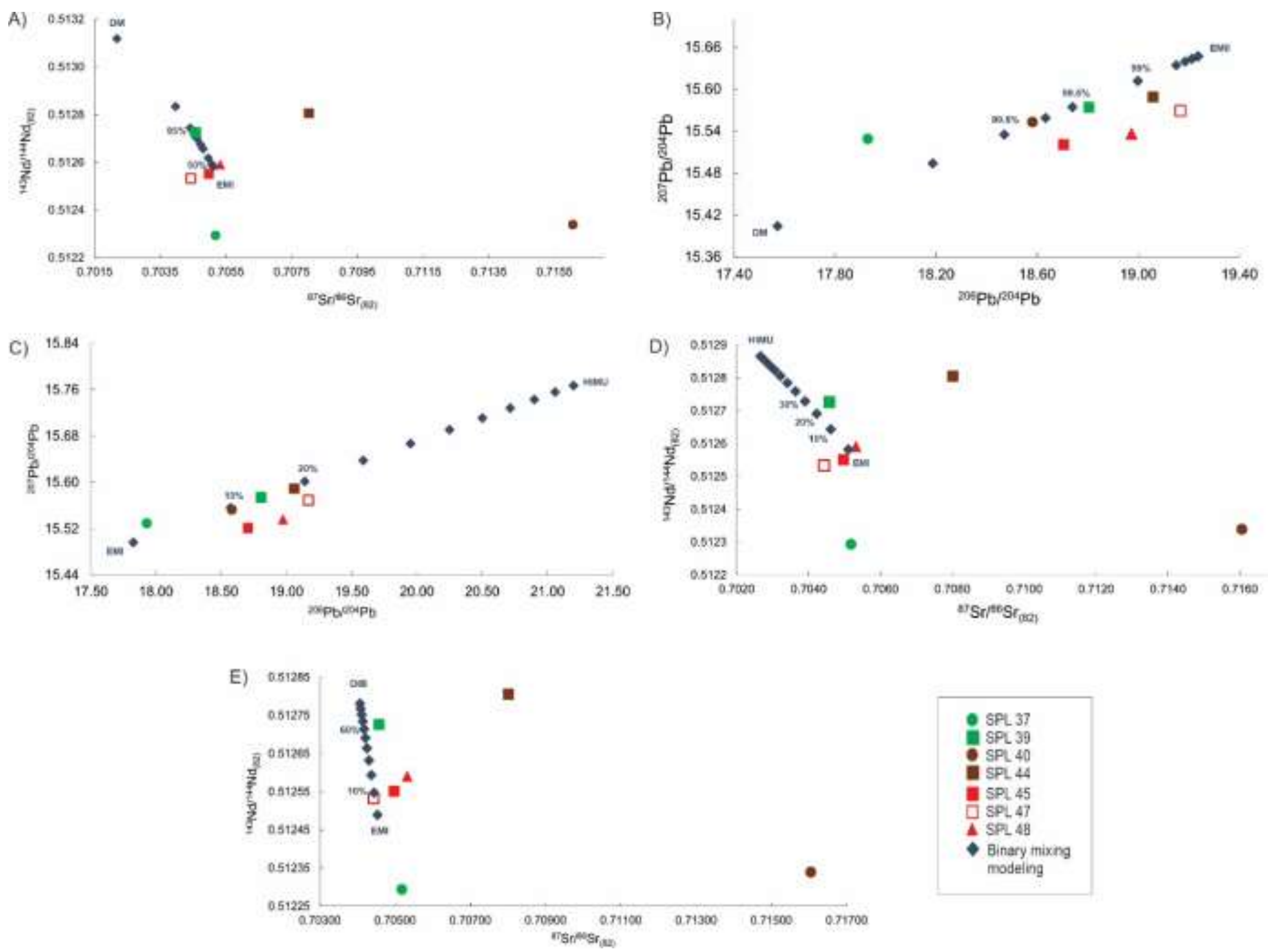

Figure 31. Binary mixing models involving mantle sources EMI, EMII, HIMU, DM/MORB and OIB-like (Trindade Martin Vaz Plume). Studied wells and respective samples are: EG1 (SPL 47 and SPL 39), EG2 (SPL 40 and SPL 44) and EG3 (SPL 45, SPL 47 and SPL 48). $^{87}Sr/^{86}Sr$ and $^{143}Nd/^{144}Nd$ ratios were recalculated to estimated initial age 82 Ma (based on **Moreira *et al.* (2006)** and geological setting bibliographic research). End-members: DM ($^{87}Sr/^{86}Sr$ = 0.701978; $^{143}Nd/^{144}Nd$ = 0.513266; $^{206}Pb/^{204}Pb$ = 18.275; $^{207}Pb/^{204}Pb$ = 15.486; $^{208}Pb/^{204}Pb$ = 37,920 / **Salters and Stracke (2004); Workman and Hart (2005)**); EMI ($^{87}Sr/^{86}Sr$ = 0.705108; $^{143}Nd/^{144}Nd$; = 0.512582; $^{206}Pb/^{204}Pb$ = 17.826; $^{207}Pb/^{204}Pb$ = 15.496; $^{208}Pb/^{204}Pb$ = 38.887 / **Jackson and Dagsputa (2008); Eisele *et al.* (2002)**); EMII ($^{87}Sr/^{86}Sr$ = 0.708478; $^{143}Nd/^{144}Nd$ = 0.512453; $^{206}Pb/^{204}Pb$ = 19.237; $^{207}Pb/^{204}Pb$ = 15.647; $^{208}Pb/^{204}Pb$ = 39.862 / **Workman *et al.* (2004)**); HIMU ($^{87}Sr/^{86}Sr$ = 0.702663; $^{143}Nd/^{144}Nd$ = 0.512865; $^{206}Pb/^{204}Pb$ = 21.199; $^{207}Pb/^{204}Pb$ = 15.767; $^{208}Pb/^{204}Pb$ = 40.382 / **Jackson and Dagsputa (2008)**); OIB ($^{87}Sr/^{86}Sr$ = 0.704065; $^{143}Nd/^{144}Nd$ = 0.512781 / **Bongiolo et al. (2015)**).

The contribution of the Trindade Martin Vaz plume for the offshore magmatism in studied area, observed specifically in the SPL 47, is still debated in literature (**Thompson et al., 1998; Thomaz Filho and Rodrigues, 1999**). Despite that, is important to consider that the plume head positioning in 85 Ma was near the Alto Paranaiba province (**Gibson *et al.*, 1997**), considerably far from the studied area. Its geochemical contribution for the magmatic events in the Cabo Frio High area could then represent an indirect effect and possibly a reflect of the main events in the onshore Brazil alkaline events.

5.7 Conclusions

The following conclusions can be made based on previously presented data and discussions.

1. The studied drift related magmatism in the Cabo Frio High area is characterized by alkaline rocks that evolved by assimilation and fractional crystallization processes as depicted by $^{87}Sr/^{86}Sr$ and $^{143}Nd/^{144}Nd$ range of variation. Despite that, further studies are needed to determine such contribution. The fact is that the amount of isotopic data available is still insufficient for more refined petrological modeling of the magmatic differentiation processes involved in the genesis of these rocks.
2. Cogeneticity of EG1, EG2 and EG3 is still unclear, but discrepancy in $^{87}Sr/^{86}Sr$ and $^{143}Nd/^{144}Nd$ ratios in samples with same level of evolution (SPL 45 and SPL 48) indicates that different mantle sources were involved in the formation of studied rocks.
3. Binary mixing models suggest the contribution of EMI, EMII, DM/MORB and HIMU as origin for the Cabo Frio High area drift magmatism. Such mixing can reflect the SCLM characteristics and its origins that should be related to the previous mantle complex subduction events underneath studied area (**Valente *et al.*, 2007)**. Possible contribution of OIB (plume-like) mantle sources can still be taken into consideration, and in this case, the more probably is associated with the Trindade Martin Vaz plume.
4. Studied magmatism is possibly associated with the partial melt of asthenospheric mantle sources in shallow depths, corresponding to a relatively thinned lithosphere (**Figure 32**). Contribution of SCLM to generate these magmas would be reflected in EMI end members, observed in binary mixing models for all studied samples. HIMU components may indicate the involvement of metasomatic processes in the mantle that gave origin to these magmas, while

EMII could reflect the complex and enriched mantle affected by crustal contamination during preterits subduction processes. OIB like, represented by the Trindade Martin Vaz plume should be taken into consideration, but given the restrict results (a positive association with only one of the studied samples) and the plume head positioning during the formation of these magmas, more studies should be taken to determine the contribution of this source. Nevertheless, trace and isotopic data indicates a strong fertile component in these magmas' origin.

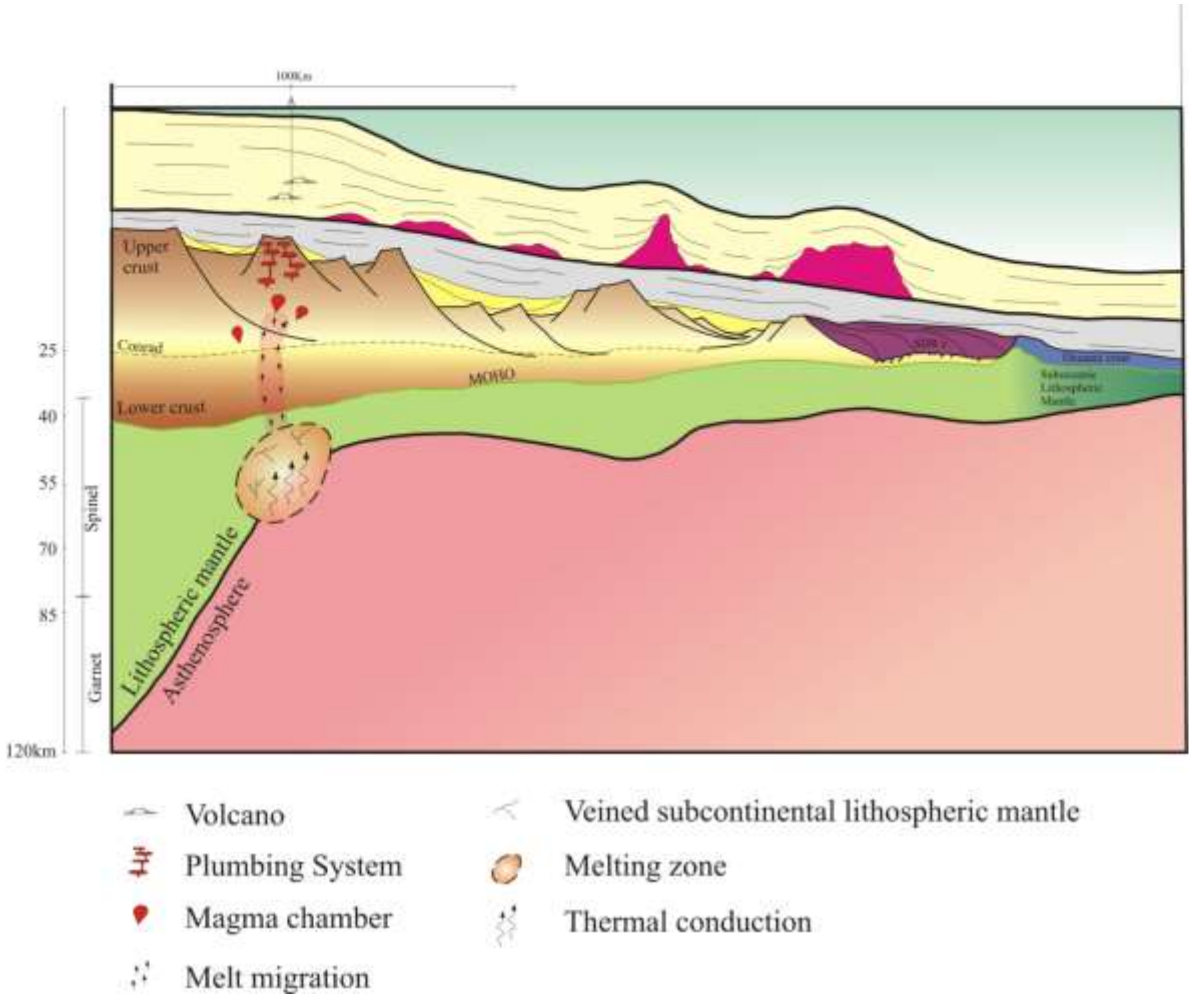

Figure 32. Conceptual geodynamic model for the origin of magmatism in the Alto de Cabo Frio region during the Santonian-Campanian.

The diversity of potential mantle sources contributing to the formation of the magmas under study indicates the heterogeneous nature of the mantle and the geodynamic setting in which they are emplaced. The origins of these magmatic events within the Campos and Santos passive margin basins during the Santonian-Campanian period remain uncertain, as do the principal geotectonic processes responsible for significant thermal input or the reactivation of deep structures necessary for generating such magmatism.

Given the relevance of the Campos and Santos basins for the hydrocarbon industry and for the understanding of Brazilian geological evolution, further studies are necessary to clarify the geodynamic context associated to the drift magmatism, its effects in tectono-sedimentary evolution of this regions and the reflects caused in the adjacent petroliferous systems.

5.8 Acknowledgements

We acknowledge the support and funding from Equinor Brazil and the support of ANP (Brazil's National Oil, Natural Gas and Biofuels Agency) through the R&D levy regulation. Master's student Tatiele Marques Jatobá de Barros acknowledges CAPES scholarship, a research funding agency in Brazil.

5.9 Data Privacy

The precise location and coordinates of the wells and samples studied in this scientific paper are not given. In addition, the identifier codes of these samples have also been changed. These actions were necessary due to a confidentiality clause in the research project signed between Equinor Brazil and the Federal Rural University of Rio de Janeiro.

5.10 Complimentary Material

Compiled data of the Poços de Caldas-Cabo Frio Alignment, Vitória-Trindade Chain, and mantle reservoirs (DM/MORB, HIMU, EMI and EMII).

5.11 References

ALMEIDA, F. F. M. Relações tectônicas das rochas alcalinas Mesozóicas da região meridional da Plataforma Sul-Americana. **Revista Brasileira de Geociências**, v. 13, n. 3, p. 139-158, Sep. 1983.

ALMEIDA, F. F. M. O alinhamento magmático de Cabo Frio. In: **Atas do 2 Simpósio de Geologia do Sudeste**, p. 423-423, 1991.

ALMEIDA, J.; HEILBRON, M.; GUEDES, E.; NEUBAUER, F.; MANFRED, B.; KLAUSEN, M. B.; VALERIANO, C. M.; BRUNO, H.; GIRO, J. P.; MCMASTER, M.; TETZNER, W. Pre-to-syn-rift tholeiitic magmatism in a transtensive hyperextended continental margin: Onshore and offshore magmatism in the Campos Basin, SE Brazil. **Journal of South American Earth Sciences**, v. 108, n. 103218, June 2021.

ALVES, D. B. Sedimentação vulcanoclástica do Cretáceo superior da Bacia de Campos, sudeste do Brasil. **Boletim de Geociências da Petrobrás**, v. 14, n. 1, p. 149-152, 2006.

BONGIOLO, E. M.; PIRES, G. L. C.; GERALDES, M. C.; SANTOS, A. C.; NEUMANN, R. Geochemical modeling and Nd–Sr data links nephelinite–phonolite successions and xenoliths of Trindade Island (South Atlantic Ocean, Brazil). **Journal of Volcanology and Geothermal Research**, v. 306, p. 58-73, 2015.

BROTZU, P.; BARBIERI, M.; BECCALUVA, L.; GARBARINO, C.; GOMES, C. B.; MACCIOTTA, G.; MELLUSO, L.; MORBIDELLI, L.; RUBERTI, E., SIGOLO, J. B.; TRAVERSA, G. Petrology and geochemistry of the Passa Quatro alkaline complex, southeastern Brazil. **South American Earth Sciences**, v. 6, n. 4, p. 237-352, 1992.

BROTZU, P.; MELLUSO, L.; BENNIO, L.; GOMES, C. B.; LUSTRINO, M.; MORBIDELLI, L.; MORRA, V.; RUBERTI, E.; TASSINARI, C.; ANTONIO, M. D., 2007. Petrogenesis of the Early Cenozoic potassic alkaline complex of Morro de São João, southeastern Brazil. **South American Earth Sciences**, v. 24, p. 93-115, 2007.

CAINELLI, C., MOHRIAK, W. U. Some remarks on the evolution of sedimentary basins along the eastern Brazilian continental margin. **Episodes**, v. 22, n. 3, p. 206-216, 1999.

CHANG, H. K.; KOWSMANN, R. O.; FIGUEIREDO, A. M. F.; BENDER, A. A. Tectonics and stratigraphy of the East Brazil Rift system: an overview. In: ZIEGLER, P. A. (Ed), **Geodynamics of Rifting, Volume II. Case History Studies on Rifts: North and South America and Africa**. Tectonophysics, p. 97-138, 1992.

CHANG, H. K.; ASSINE, M. L.; CORREA, F. S.; TINEN, J. S.; VIDAL, A. C., Koike, L. Sistemas petrolíferos e modelos de acumulação de hidrocarbonetos na Bacia de Santos. **Revista Brasileira de Geociências**, v. 38, p. 29-46, junho 2008.

DE BARROS, T. M. J.; BRITO, P. C.; CORVAL, A.; VALENTE, S. C.; MIRANDA, A. W. A. The post-breakup magmatism in Cabo Frio High, Campos Basin, Brazil: implications to a thinned lithosphere contribution in magma formation. **Comunicações Geológicas**, v. 110, n. 1, p. 39-60, Nov. 2023.

EISELE, J.; SHARMA, M.; GALER, S. J. G.; BLICHERT-TOFT, J.; DEVEY, C. W.; HOFMANN, A. W. The role of sediment recycling in EM-1 inferred from Os, Pb, Hf, Nd, Sr isotope and trace element systematics of the Pitcairn hotspot. **Earth and Planetary Science Letters**, v. 196, p. 197-212, 2002.

FODOR, R, V.; HANAN, B. B. Geochemical evidence for the Trindade hotspot trace: Columbia seamount ankaramite. **Lithos,** v. 51, p. 293-304, 2000.

FRANK, Y. V. M.; VALENTE, S. C. Volcaniclastic rocks and reconstruction of a volcanosedimentary paleoenvironment in Campos Basin, SE Brazil. **Brazilian Journal of Geology**, v. 53, n. 2, 2023.

GERALDES, M. C.; MOTOKI, A.; COSTA, A.; MOTA, C. E.; MOHRIAK, W. U. Geochronology (Ar/Ar and K-Ar) of the South Atlantic post-break-up magmatism. *In*: MOHRIAK, W. U.; DANFORTH, A.; POST, P. J.; BROWN, D. E.; TARI, G. C.; NEMOOK, M.; SINHA, S. T. (Eds). **Conjugate Different Margins**. Geological Society, Special Publications, p. 41-74, 2013

GIBSON, S. A.; THOMPSON, R. N.; LEONARDOS, O. H.; DICKIN, A. P.; MITCHELL, J. G. The Late Cretaceous Impact of the Trindade Mantle Plume: Evidence from Large-volume, Mafic, Potassic Magmatism in SE Brazil. **Journal of Petrology**, v. 36, n. 1, p. 189-229, 1995.

GIBSON, S. A.; THOMPSON, R. N.; WESKA, R. K.; DICKIN, A. P.; LEONARDOS, O. H. Late Cretaceous rift-related upwelling and melting of the Trindade starting mantle plume head beneath western Brazil. **Contrib. Mineral Petrol.** v. 126, p. 303-314, 1997.

GORDON, A. C.; SANTOS, A. C.; CAITANO, G. R.; STANTON, N.; MOHRIAK, W. U. Magmatic cycles in Santos Basin (S.E. Brazil): Geochemical characterization and magmatic sources. **Journal of South American Earth Sciences**, v. 126, n. 104323, April 2023.

GORDON, A. C.; MOHRIAK, W. U.; STANTON, N.; SANTOS, A. C. Magmatic cycles in Santos Basin (S.E. Brazil): Tectonic control in the temporal-spatial distribution and geophysical signature. **Journal of South American Earth Sciences**, v. 121, n. 104111, Jan. 2023.

GUARINO, V.; LUSTRINO, M.; ZANETTI, A.; TASINARI, C. C. G.; RUBERTI, E.; GENNARO, R.; MELLUSO, L. Mineralogy and geochemistrry of a giant agpaitic magma reservoir. The Late Cretaceous Poços de Caldas potassic alkaline complex (SE Brazil). **Lithos**, n. 106330, June, 2021.

HEILBRON, M. et al. Correlation of Neoproterozoic terranes between the Ribeira Belt, SE Brazil and its African counterpart: comparative tectonic evolution and open questions. **Geological Society, Special Publications**, London, v. 294, p. 211-237, 2008.

HOFMANN, A. W.; WHITE, W. M. Mantle plumes from ancient oceanic crust. **Earth and Planetary Science Letters**, v. 57, p. 421-436, 1982.

JACKSON, M. G.; DAGSPUTA, R. Compositions of HIMU, EM1, and EM2 from global trends between radiogenic isotopes and major elements in ocean island basalts. **Earth and Planetary Science Letters**, v. 276, p. 175-186, 2008.

LOUBAK, V. S.; VALENTE, S. C.; ALMEIDA, C. N.; ROSS, J.; BORGHI, L. Petrogenesis and geodynamics of Eocene alkaline intrusions in the pre-salt sedimentary sequence of Santos Basin, Brazil. **Lithos**, v. 106400, July 2021.

MARQUES, L. S.; ULBRICH, M. N. C.; RUBERTI, E.; TASSINARI, C. G. Petrology, geochemistry and Sr-Nd isotopes of the Trindade and Martin Vaz volcanic rocks (Southern Atlantic Ocean). **Journal of Volcanology and Geothermal Research**, v. 93, p. 191-216, 1999.

MOHRIAK, W. U.; MACEDO, J. M.; CASTELANI, R. T.; RANGEL, H. D.; BARROS, A. Z. N.; LATGÉ, M. A. L.; RICCI, J. A.; MIZUSAKI, A. M. P.; SZATMARI, P.; DEMERCIAN, L. S.; RIZZO, J. G.; AYRES, J. R. Salt Tectonics and Structural Styles in the Deep – Water Province of the Cabo Frio Region, Rio de Janeiro, Brazil. *In*: JACKSON D.G., ROBERTS, D.G., SNELSON S. (Eds.), **Salt Tectonics: A Global Perspective**. AAPG Memoir, 1995, v. 65, p. 273-304.

MAIA, T. M.; SANTOS, A. C.; VALENTE, S. C.; ROCHA-JÚNIOR, E. R. V.; BARROS, G. P. W.; HEILBRON, M.; VALERIANO, C. M.; ARENA, M. Abrolhos Magmatic Province petrogenesis and its link with the Vitória-Trindade Ridge, Southeast Brazilian Margin, South Atlantic Ocean. **Journal of South American Earth Sciences**, v. 120, n. 104075, Oct. 2022.

MARQUES, L. S.; ULBRICH, M. N. C.; RUBERTI, E.; TASSINARI, C. G. Petrology, geochemistry and Sr-Nd isotopes of the Trindade and Martin Vaz volcanic rocks (Southern Atlantic Ocean). **Journal of Volcanology and Geothermal Research**, v. 93, p. 191-216, 1999.

MCDONOUGH, W. F.; SUN, S. The composition of the Earth. **Chemical Geology**, v. 120, p. 223-253, March 1995.

MOHRIAK, W. U. Bacias Sedimentares da Margem Continental Brasileira. *In*: C. S. L. A. BIZZI, R. M. VIDOTTI; J. H. GONÇALVES (Eds.), **Geologia, Tectônica e Recursos Minerais do Brasil**, 2003. Brasília, DF, Brasil, CPRM, v. 1, p. 87-165.

MOREIRA, J. L. P.; ESTEVES, C. A.; RODRIGUES, J. J. G.; VASCONCELOS, C. S. Magmatismo, sedimentação e estratigrafia da porção norte da Bacia de Santos. **Boletim de Geociências da Petrobrás**, v. 14, n. 1, p. 161-170, maio, 2006.

MOREIRA, J. L. P.; MADEIRA, C.V.; GIL, J. A.; MACHADO, M. A. P. Bacia de Santos. **Boletim de Geociências da Petrobras**, v. 15, n. 2, p. 531-549, nov. 2007.

MOTOKI, A.; SICHEL, S. E.; VARGAS, T.; AIRES, J. R.; IWANUCH, W.; MELLO, S. L. M.; MOTOKI, K. F.; SILVA, S.; BALMANT, A.; GONÇALVES, J. Geochemical evolution of the felsic alkaline rocks of Tanguá and Rio Bonito intrusive bodies, state of Rio de Janeiro, Brazil. **Geociências**, v. 29, n. 3, p. 291-310, 2010.

PEYVE, A. A.; SKOLOTNEV, S. G. Systematic variations in the composition of volcanic rocks in tectono-magmatic seamount chaines in the Brazil Basin. **Geochemistry International**, v. 52, p. 111-130, 2014.

QUARESMA, G. O. A.; SANTOS, A. C.; ROCHA-JÚNIOR, E. R. V.; BONIFÁCIO, J. REGO, C. A. Q.; MATA, J.; VALERIANO, C. M.; JOURDAN, F.; MATTIELLI, N.; GERALDES, M. C. Isotopic constraints on Davis bank, Vitória-Trindade Ridge: A Revised Petrogenetic Model. **Journal of South American Earth Sciences**, v. 122, n. 104099, 2023.

RANGEL, H. D. Manifestações magmáticas na parte sul da Bacia de Campos (Área de Cabo Frio) e na Bacia de Jequitinhonha. **Boletim de Geociências da Petrobrás**, v. 14, n. 1, p. 155-160, maio 2006.

RICOMMINI, C.; SANT'ANNA, L. G.; FERRARI, A. L. Evolução geológica do rift continental do Sudeste do Brasil. *In*: MANTESSO-NET, V.; BARTORELLI, A.; CARNEIRO, C. D. R.; BRITO-NEVES, B. B. (Eds**). Geologia do Continente Sul-Americano: Evolução da obra de Fernando Flávio Marques de Almeida**. Editora Beca, p. 385-405, 2004.

RICCOMINI, C.; FERNANDEZ, V. V.; GOMES, C. Tectonic controls of the Mesozoic and Cenozoic alkaline magmatism in central-southern Brazilian Platform. *In*: COMIN-CHIARAMONTI, P., GOMES, P. B. (Eds.), **Mesozoic to Cenozoic alkaline magmatism in the Brazilian Platform**, EDUSP-FAPESP, p. 31-56, 2005.

OLIVEIRA, M. J. R.; SCHIMITT, R. S.; ARAÚJO, M. N. C.; VALENTE, S. C.; SAVASTANO, V. L. M.; INOCÊNCIO, L. C.; CARMO, I. O. Tectonic influence of Cenozoic post-rift alkaline magmatic intrusions on the onshore basement of the Campos and Santos basins, SE Brazil. **Journal of South American Earth Sciences**, v. 132, n. 104638, Oct. 2023.

OREIRO, Sérgio Goulart; CUPERTINO, José Antônio; THOMAZ FILHO, Antônio. Diagnostic features of volcanic and volcaniclastic rocks in seismic sections on the Continental Shelf of Cabo Frio Area, SE Brazil. In: **8th International Congress of the Brazilian Geophysical Society**. European Association of Geoscientists & Engineers, p. cp-168-00039, 2003.

OREIRO, S. G. Magmatismo e sedimentação em uma área na Plataforma Continental de Cabo Frio, Rio de Janeiro, Brasil, no intervalo Cretáceo Superior–Terciário. **Boletim de Geociências da Petrobras**, v. 14, p. 95-112, maio 2006.

OREIRO, S. G.; CUPERTINO, J. A.; SZATMARI, P.; THOMAZ FILHO, A. Influence of pre-salt alignments in post-Aptian magmatism in the Cabo Frio High and its surroundings, Santos and Campos basins, SE Brazil: An example of non-plume-related magmatism. **Journal of South American Earth Sciences**, v. 25, p. 116-131, Feb. 2008.

PEARCE, J. A.; NORRY, M. J. Petrogenetic implications of Ti, Zr, Y and Nb variations in intrusive rocks. **Contributions to Mineralogy and Petrology**, v. 69, p. 33-47, May 1979.

ROSA, P. A. S. **Geologia e Evolução Petrogenética do Maciço Alcalino de Itatiaia, MG-RJ**. Tese de Doutorado, Instituto de Geociências, Universidade de São Paulo, São Paulo, SP, Brasil, p. 137. 2017.

ROSA, P. A. S.; RUBERTI, E. Nepheline syenites to syenites and granitic rocks of the Itatiaia Alkaline Massif, Southeastern Brazil: new geological insights into a migratory ring Complex. **Brazilian Journal of Geology**, v. 48, n. 2, p. 347-372, June 2018.

SALTERS, V. J. M.; STRACKE, A. Composition of the depleted mantle. **Geochemistry, Geophysics, Geosystems**, v. 5, n. 5, May 2004.

SANTOS, A. C.; GERALDES, M. C; SIEBEL, W.; MENDES, J.; BONGIOLO, E.; SANTOS, W. H.; GARRIDO, T. C. V.; RODRIGUES, S. W. O. Pleistocene allkaline rocks of Martin Vaz volcano, South Atlantic low-degree partial melts of a CO2 metasomatized mantle plume. **International Geology Revie**w, v. 61, n. 3, p. 296-313, 2019.

SCHMITT, R. S. et al. Cambrian orogeny in the Ribeira Belt (SE Brazil) and correlations within West Gondwana: ties that bind underwater. **Geological Society, Special Publications,** London, v. 294, p. 279-296, 2008.

SIEBEL, W.; BECCHIO, R.; VOLKER, F.; HANSEN, M. A. F.; VIRAMONTE, J.; TRUMBULL, R. B.; HAASE, G.; ZIMMER, M. Trindade and Martín Vaz Islands, South Atlantic: Isotopic (Sr, Nd, Pb) and trace element constraints on plume related magmatism. **Journal of South American Earth Sciences,** v. 13, p. 79-103, 2000.

SONOKI, I. K.; GARDA, G. M. Idades K-Ar de rochas alcalinas do Brasil Meridional e Paraguai Oriental: compilação e adaptação às novas constantes de decaimento. Bol. IG-USP, **Sér. Cient**., v. 19, p. 63-85, 1988.

STANTON, Natasha; SCHMITT, Renata. Onshore-offshore prolongation of structures between Campos and Santos Basins from aeromagnetic datanshore-offshore prolongation of structures between Campos and Santos Basins from aeromagnetic data. In: **14th International Congress of the Brazilian Geophysical Society & EXPOGEF, Rio de Janeiro, Brazil, 3-6 August 2015**. Brazilian Geophysical Society, p. 445-448, 2015.

STRACKE, A.; HOFMANN, A. W. FOZO, HIMU, and the rest of the mantle zoo. **Geochemistry, Geophysics, Geosystems**, v. 6, n. 5, May 2005.

THOMAZ-FILHO, A.; RODRIGUES A. L. O alinhamento de rochas alcalinas Poços de Caldas-Cabo Frio (RJ) e sua Continuidade na Cadeia Vitória-Trindade. **Revista Brasileira de Geociências**, v. 29, n. 2, p. 189-194, junho 1999.

THOMAZ FILHO, A.; MIZUSAKI, A. M. P.; MILANI, E. J.; CESERO, P. Rifting and magmatism associated with the South America and Africa break up. **Revista Brasileira de Geociências**, v. 30, n. 1, p. 17-19, March 2000.

THOMAZ-FILHO, A.; MIZUSAKI, A. M. P.; ANTONIOLI, L. Magmatismo nas bacias sedimentares brasileiras e sua influência na geologia do petróleo. **Revista Brasileira de Geociências**, v. 38, n. 2, p. 128-13, junho 2008.

THOMPSON, R. N.; GIBSON, S. A.; MITCHELL, J. G.; DICKIN, A. P.; LEONARDOS, O. H.; BROD, J. A.; GREENWOOD, J. C. Migrating Cretaceous – Eocene Magmatism in the Serra do Mar Alkaline provinces, SE Brazil: melts from the deflected Trindade Mantle Plume? **Journal of Petrology**, v. **39**, n. 8, p. 493-526, Aug. 1998.

VALENTE, S. C. **Geochemical and isotopic constraints on the petrogenesis of the Cretaceous dykes of Rio de Janeiro, Brazil**. Belfast, PhD. Thesis, The Queen's University of Belfast, p. 366. 1997.

VALERIANO, C. M. U-Pb geochronology of the southern Brasília belt (SE-Brazil):
Sedimentary provenance, Neoproterozoic orogeny and assembly of West Gondwana. **Precambrian Research**, v. 130, n. 4, p. 27–55, 2004.

WINTER, R. W.; JAHNERT, R. J.; FRANÇA, A. B. Bacia de Campos. **Boletim de Geociências da Petrobras**, v. 15, n. 2, p. 511-529, nov. 2007.
WORKMAN, R. K.; HART, S. R.; JACKSON, M.; REGELOUS, M.; FARLEY, K. A.; BLUSZTAJN, J.; KURZ, M.; STAUDIGEL, H. Recycled metasomatized lithosphere as the origin of the Enriched Mantle II (EM2) end-member: Evidence from the Samoan Volcanic Chain. **Geochemistry, Geophysics, Geosystems**, v. 5, n. 4, April 2004.
WORKMAN, R. K.; HART, S. R. Major and trace element composition of the depleted MORB mantle (DMM). **Earth and Planetary Science Letters**, v. 231, p. 52-72, Jan. 2005.

6 CONCLUSÕES

Os poços estudados, EG1, EG2 e EG3, apresentam seções magmáticas compostas por rochas vulcânicas e vulcaniclásticas associadas aos eventos do Santoniano-Campaniano que afetaram a região do Alto de Cabo Frio, localizado entre as bacias de Campos e Santos.

Por meio de análises petrográficas de amostras da calha e laterais, foi possível identificar as seguintes litologias nos poços: tufos piroclásticos, lapilli tufos, diabásio, escórias altamente vesiculadas, cinzas e basaltos. Tais rochas estão associadas a um vulcanismo subaéreo explosivo, no qual estratovulcões teriam gerado os depósitos vulcânicos e mistos observados nas amostras.

Dados litogeoquímicos indicam que essas rochas são alcalinas, predominantemente foiditos, basaltos alcalinos e, subordinadamente, tefrifonolitos. O grau de alteração e a grande presença de vesículas e amígdalas afetaram principamente a composição geoquímica destas amostras, especialmente os elementos maiores e elementos traços móveis, como Ba, Rb, Th, K e Sr. Apesar disso, foi possível identificar que tais rochas estão associadas a processos de cristalização fracionada. Posteriores estudos com base em dados isotópicos de Sr e Nd revelaram que processos de assimilação também afetaram estes magmas durante sua formação, sendo AFC (assimilação e cristalização fracionada) o principal representante dos processos evolutivos associados às rochas estudadas.

Com base nas razões $La/Yb_{(N)}$ e $La/Nb_{(N)}$ foi possível identificar fontes férteis e enriquecidas como sendo componentes mantélicos associados à formação do magmatismo do Alto de Cabo Frio. Posteriores modelagens com base em elementos traço e dados isotópicos revelaram o envolvimento de fontes depletadas do tipo N-MORB e enriquecidas do tipo EMI (incluindo o

Manto Litosférico Subcontinental, MLSC) e EMII. Subordinadamente, os resultados de mistura binária também implicam na possível participação de fontes do tipo OIB e HIMU.

O contexto tectônico no qual estes eventos magmáticos estão inseridos podem ser associados a uma litosfera pouco espessa, que possibilitaria a ascensão astenosférica e geração de magmas por descompressão adiabática entre 35 – 80 km de profundidade (zona de estabilidade do espinélio). A presença de uma astenosfera levaria a um incremento de temperatura suficiente para que poucas frações de fusão parcial fossem geradas no manto MLSC enriquecido.

A associação dos eventos magmáticos com eventos adjacentes como o Alinhamento Magmático Poços de Caldas-Cabo Frio e a Cadeia de Vitória Trindade ainda permanece incerta, bem como a presença de tal atividade termal durante o estágio de formação das bacias estudadas. Dados isotópicos apontam para uma possível contribuição da pluma de Trindade na geração destes magmas. Entretanto, trabalhos mais aprofundados e com maior quantitativo de amostras são necessários para realizar tais determinações e esclarecer mais profundamente o cenário geodinâmico ao qual o magmatismo estudado está inserido.

7 REFERÊNCIAS BIBLIOGRÁFICAS

ALVES, Daisy Barbosa. Sedimentação vulcanoclástica do Cretáceo superior da Bacia de Campos, sudeste do Brasil. **Boletim de Geociências da Petrobrás**, v.14, n.1, p.149-152, 2005.

CADDAH, L. F. G. et al. Caracterização e origem do Marco" 3-Dedos" (Santoniano) da Bacia de Campos. **Boletim de Geociências da Petrobrás**, v.8, n.2, p.315-334, 1994.

CASTRO, R. D.; PICOLINI, J. P., 2014. Principais aspectos da geologia regional da Bacia de Campos. *In*: KOWSMANN, R.O. (Eds.), **Geologia e Geomorfologia.** Rio de Janeiro: Elsevier. Habitats, 2014, p. 1-12.

CHANG, H.K.; KOWSMANN, R.O.; FIGUEIREDO, A.M.F.; BENDER, A.A. Tectonics and stratigraphy of the East Brazil Rift system: an overview. *In:* Ziegler, P.A. (Editor), **Geodynamics of Rifting, Volume II. Case History Studies on Rifts: North and South America and Africa. Tectonophysics**, 1992. p. 97-138.

DANI, A. P. de O.; REMUS, M. V. D.; DANI, N.; LIMA, E. F. de. Magmatismo basáltico do Andar Alagoas (Bacia de Campos). **Geologia USP. Série Científica**, São Paulo, v.17, n.2, p.269-287, 2017.

DIAS, J. L.; OLIVEIRA, J. Q.; VIEIRA, J. C. Sedimentological and stratigraphyc analysis of the Lagoa Feia Formation, rift phase of Campos Basin, offshore Brazil. **Revista Brasileira de Geociências**, v.18, n.3, p.252-260, setembro.1988.

FRANK, Y. V. M.; VALENTE, S. C. Volcaniclastic rocks and reconstruction of a volcanosedimentary paleoenvironment in Campos Basin, SE Brazil. **Brazilian Journal of Geology**, v. 53, n. 2, 2023.

GORDON, A. C.; SANTOS, A. C.; CAITANO, G. R.; STANTON, N.; MOHRIAK, W. U. Magmatic cycles in Santos Basin (S.E. Brazil): Geochemical characterization and magmatic sources. **Journal of South American Earth Sciences**, v. 126, n. 104323, April 2023.

GORDON, A. C.; MOHRIAK, W. U.; STANTON, N.; SANTOS, A. C. Magmatic cycles in Santos Basin (S.E. Brazil): Tectonic control in the temporal-spatial distribution and geophysical signature. **Journal of South American Earth Sciences**, v. 121, n. 104111, Jan. 2023.

GUARDADO, L.R.; GAMBOA, L.A.P.; LUCCHESI, C.F. 1989. Petroleum geology of Campos Basin, Brazil: a model for producing Atlantic type basin. In: EDWARDS, J.D., SANTAGROSSI, P.A. (Eds). **Divergent/Passive Margins Basins**. AAPG Memoir, 1989. p. 3-36.

LOPES, M. F. B. V. **Caracterização Geológica da Província Petrolífera de Campos**. Dissertação de Mestrado. Universidade Federal do Rio de Janeiro, Rio de Janeiro, 196p. 2004.

MARINS, G. M.; PARIZEK-SILVA, Y.; MILLET, J. M.; JERRAM, D. A.; ROSSETII, L. M. M.; SOUSA, A. J.; PLANKE, S.; BEVILAQUA, L. A.; CARMO, I. O. Characterization of volcanic reservoirs; insights from the Badejo and Linguado oil field, Campos Basin, Brazil. **Marine and Petroleum Geology**, v, 146, Dec. 2022.

MIZUSAKI, A. M. P.; PETRINI, R.; BELLIENI, G.; COMIN-CHIARAMONI, P.; DIAS, J.; DE MIN, A.; PICCIRILLO, E. M. Basalt magmatism along the passive continental margin of SE Brazil (Campos basin). **Contributions to Mineralogy and Petrology**, v.111, p.143-160, jul./fev.1992.

MOHRIAK, W. U. Bacias Sedimentares da Margem Continental Brasileira. *In:* BIZZI, L. A.; SCHOBBENHAUS, C.; VIDOTTI, R. M.; GONÇALVES, J. H. **Geologia, Tectônica e Recursos Minerais do Brasil**. Brasília: CPRM, 2003. p.87-165.

MOREIRA, J. L. P.; ESTEVES, C. A.; RODRIGUES, J. J. G.; VASCONCELOS, C. S. Magmatismo, sedimentação e estratigrafia da porção norte da Bacia de Santos. **Boletim de Geociências da Petrobrás**, v. 14, n. 1, p. 161-170, 2006.

MOREIRA, J. L. P.; MADEIRA, C. V.; GIL, J. A.; MACHADO, M. A. P. Bacia de Santos. **Boletim de Geociências da Petrobrás**, Rio de Janeiro, v.15, n.2, p.531-549, maio/nov. 2007.

OREIRO, S. G. Magmatismo e sedimentação em uma área na Plataforma Continental de Cabo Frio, Rio de Janeiro, Brasil, no intervalo Cretáceo Superior–Terciário. **Boletim de Geociências da Petrobras**, v. 14, p. 95-112, maio 2006.

RANGEL, H. D. Manifestações magmáticas na parte sul da Bacia de Campos (Área de Cabo Frio) e na Bacia de Jequitinhonha. **Boletim de Geociências da Petrobras**, Rio de Janeiro, v.14, n. 1, p. 155-160, nov./maio 2006.

RICCOMINI, C.; SANT'ANNA, L. G.; TASSINARI, C. C. G. Pré-sal: geologia e exploração. **Revista USP**, São Paulo, n.95, p.33-42, set./out./nov.2012.

THOMAZ-FILHO, A.; MIZUSAKI, A. M. P.; ANTONIOLI, L. Magmatismo nas bacias sedimentares brasileiras e sua influência na geologia do petróleo. **Revista Brasileira de Geociências**, v. 38, n. 2, p. 128-13, junho 2008.

WINTER, W. R.; JAHNERT, R. J.; FRANÇA, A.B. Bacia de Campos. **Boletim de Geociências da Petrobrás**, Rio de Janeiro, v.15, n.2, p.511-529, maio/nov.2007.

* Estas referências são relacionadas aos trabalhos referenciados na parte do volume final que não é composta pelos artigos científicos.

ANEXOS

A – Dados litogeoquímicos das rochas dos poços EG1, EG2 e EG3.

B – Dados compilado do Alinhamento Poços de Caldas-Cabo Frio, Cadeia Vitória-Trindade, e reservatórios mantélicos (DM/MORB, HIMU, EMI e EMII).